A Riemann Solver for the Euler Equations with Non–Convex Equation of State

Siegfried Müller*, Alexander Voß†

Abstract

An algorithm is presented by which the Riemann problem in gas dynamics can be solved for a *non–convex* equation of state. The non–convexity causes non–standard wave patterns, e.g. *composite* waves and anomalous behavior of physical quantities along classical waves, e.g. *expansion* and *sonic* shocks, may occur. In contrast to standard Riemann solvers, these effects are taken into special account. The derivation of the algorithm is based on construction principles which are motivated by analytical investigations in the context of gas dynamics as well as general systems of hyperbolic conservation laws.

With the aid of the extended Riemann solver we compare an ideal gas and a real gas. The results show that the non–classical effects are significant and can not be treated as a perturbation of an ideal gas. This implies that existing flow solvers have to be appropriately adapted when performing numerical simulations of flows in fluids exhibiting non–classical effects such as retrograde fluids.

Key Words: Riemann problem, non–convex equation of state, composite wave, compression wave, expansion shock, sonic shock.

AMS Subject Classification: 35L65, 35L67, 35Q05, 70H35, 76N10

*The work of this author is partially supported by the SFB 401 of the Deutsche Forschungsgemeinschaft.

†The work of this author is supported by the Deutsche Forschungsgemeinschaft in the Priority Program "Analysis und Numerik von Erhaltungsgleichungen".

Contents

1 Introduction — The Riemann Problem in Fluid Dynamics

In continuum mechanics, the state of the fluid is characterized by several macroscopic variables, e.g. mass density ρ, specific internal energy e and particle velocity $\boldsymbol{u}$. The evolution of the fluid is governed by the balance equations of mass, momentum and energy

$$\begin{aligned} \rho_t &+ \operatorname{div}(\rho \boldsymbol{u}) = 0, \\ (\rho \boldsymbol{u})_t &+ \operatorname{div}(\rho \boldsymbol{u}\boldsymbol{u}^T + p\boldsymbol{I}) = \operatorname{div}\boldsymbol{\tau}, \\ (\rho E)_t &+ \operatorname{div}(\rho \boldsymbol{u}(E + p/\rho)) = \operatorname{div}(\boldsymbol{\tau}\boldsymbol{u} - \boldsymbol{q}) \end{aligned} \tag{1.1}$$

where $E = e + 0.5\boldsymbol{u}^2$ is the total specific energy, p is the pressure, $\boldsymbol{\tau}$ is the stress tensor and $\boldsymbol{q}$ is the heat flux. In the following, the effects of viscosity and heat conduction are neglected, i.e., $\boldsymbol{\tau} = \boldsymbol{0}$, $\boldsymbol{q} = \boldsymbol{0}$. Furthermore, p is assumed to be the equilibrium thermodynamic pressure. The resulting inviscid flow equations, in the following referred to as Euler equations, have to be supplemented by an additional equation, the so–called *equation of state* (EOS). The EOS characterizes the material properties of the fluid and has a strong influence on the structure and dynamics of waves. According to the fundamental identity of thermodynamics the pressure is related to specific volume $v = 1/\rho$ and specific entropy s. However, in view of computational fluid dynamics, it is preferable to write p in terms of the specific volume and the specific internal energy e.

In fluid dynamics, the propagation of waves is of special interest and has been the subject of numerous analytical and experimental investigations. These are inspired by the pioneering work of B. Riemann on wave propagation in air [Rie53]. An appropriate and simple experimental configuration that has been frequently considered is a shock tube where two states of a fluid are separated by a diaphragm. Instantly removing the diaphragm several waves, e.g. *shock waves*, *rarefaction waves* and *contact surfaces*, develop and propagate with increasing time as can be observed in shock tube experiments (see Fig. 1, 2).

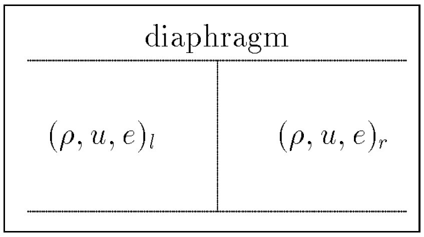

Figure 1: Initial configuration at $t = 0$

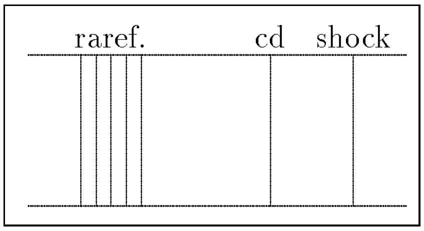

Figure 2: Wave propagation at $t > 0$

The Riemann problem is an initial value problem with scale–invariant initial data. Here, we always suppose the flow to exhibit planar symmetry, i.e., the problem is inherently onedimensional. It is of special interest in different research fields. For instance, it can be applied in (i) engineering as designing tool of shock tube experiments [Ess91], (ii) in numerical simulations as core ingredient of finite volume schemes [God59] and (iii) in physics for deriving constraints of the EOS [MP89].

By now, the Riemann problem is well understood for the Euler equations that model equilibrium hydrodynamics. Among other investigations, significant contributions with special emphasis on shock waves have been made by Bethe [Bet42], Weyl [Wey49], Courant and Friedrichs [CF48], Landau and Lifshitz [LL59], Wendroff [Wen72a, Wen72b]. These studies inspired the work of Gelfand [Gel59], Oleinik [Ole59], Lax [Lax57] and Liu [Liu75] who generalized the results from fluid dynamics to strictly hyperbolic conservation laws. A detailled review is given by Menikoff and Plohr [MP89].

The general construction principle is essentially based on the scale–invariance of the solution and the hyperbolicity of the governing equations of fluid motion. These properties require the solution to be composed of different waves in the time–space continuum which correspond to different characteristic velocities. Moreover, there exists a one–to–one correspondence between a single wave in the t–x plane and the states in the phase space which can be connected by this wave. All of these states are lying on a curve. Therefore, the solution of the Riemann problem can be calculated by determining the intersection points of the different curves in the phase space which connect the two initial states. To distinguish the respective settings in the course of discussion we will consistently refer to one parameter families of states in phase space as *curves* while speaking of *waves* in the t–x plane. The solution of the Riemann problem makes essential use of considerations in phase space. Hence, the most crucial point in solving the Riemann problem is the construction of the curves in phase space. These curves are composed of three kinds of elementary curves namely, *rarefaction curves, shock curves* and *contact discontinuities*. The composition of these curves significantly depends on the behavior of the corresponding characteristic field. These fields are linearly degenerated or genuinely nonlinear, i.e., the curve is just a contact discontinuity or it is composed of shock and rarefaction curves. In the context of gas dynamics, the characteristic field depends on the EOS for the pressure, in particular, on the behavior of the pressure along isentropes in the pressure–volume plane. In a wide range of the phase space, the isentropes are convex, frequently modelled by an ideal EOS which is used in many applications. However, near the vapor–liquid saturation boundary the isentropes are not strictly convex, e.g. modelled by the van der Waals EOS. Due to the non–convexity, the curves have to be modified which results in non–standard physical effects, e.g. sonic shocks, expansion shocks, compression waves or mixed waves. In general, existing Riemann solvers do not take these effects into account (see e.g. [Smo82, CG85]).

The main objective of the present work is the construction of an exact Riemann solver for the Euler equations in fluids with non–convex EOS. This solver may serve as a tool for validating numerical schemes applied to fluids which exhibit these non–standard phenomena. Furthermore, parameter studies can be performed by which the influence of the EOS (e.g. van der Waals, Redlich–Kwong, etc.) on the structure of the non–standard waves can be examined. Here, we follow a concept that has been originally derived by Wendroff for the Euler equations (see [Wen72a, Wen72b]). Later, Liu generalized the construction principles for systems of hyperbolic conservation laws (see [Liu75]). Although the construction principle is well–known, the analysis which is currently available has to be complemented by suitable constructive ingredients. In particular, this requires the identification of an appropriate curve parameter. To this end, we have to examine the monotonicity behavior of physical quantities such as pressure and velocity along the curves under consideration. Here, the thermodynamic pressure turns out to be an appropriate choice under certain thermodynamical constraints. The investigation of this problem is of special interest in the present work, since it strongly influences the algorithmic formulation of the Riemann solver.

We therefore reconsider to some extent the construction of the curves. With the aid of these curves, we explain how to solve the Riemann problem in the phase space by connecting the initial states in the p–u plane, i.e., we determine *one* intersection point of the *two* curves originating from the initial states. We emphasize that this procedure is specifically adapted to the Euler equations. In the context of general hyperbolic systems the construction principle is related to multiple shooting schemes which are applied to two–point boundary value problems. Finally, the Riemann solution is transferred from the phase space to the t–x plane. Here, the characteristic velocities and shock speeds corresponding to the intermediate states are of special interest. To this end, we discuss the behavior of these velocities along the curves in some detail.

In the course of deriving the Riemann solver, we consider the following three issues

- *constructive* analysis of the wave phenomena for the Riemann problem of the Euler equations with non–convex EOS,
- *identification* of the resulting mathematical problems and
- the *algorithmic* realization.

To this end, the paper is organized as follows. We start in Section 2 with a review on thermodynamical equilibrium which provides some physically meaningful constraints for the definition of the EOS. In Section 3 we summarize basic construction principles which hold for general systems of conservation laws. Here the proofs are omitted, instead we refer to the work of Liu [Liu74, Liu75, Liu76a, Liu76b]. These principles build the framework for deriving an algorithm presented in Section 4 by which the Riemann problem for the Euler equations with non–convex EOS can be exactly solved. This algorithm is essentially based on the parameterization of the curves with respect to the pressure. After computing the curves, the Riemann problem is solved by determining the intersection point of the curves in the velocity–pressure plane. By the profiles of the characteristic velocities and shock speeds the solution is mapped from the phase space to the t–x plane. In Section 6, we close with some applications and compare the Riemann solution where we apply a convex EOS and a non–convex EOS, respectively.

2 Some Remarks on the Equation of State

The material properties have a strong influence on the structure and dynamics of waves. These properties are characterized by the EOS. Therefore, we recall some basic principles of thermodynamics which impose certain constraints on the EOS. Here, we restrict to thermodynamical equilibrium, i.e., the internal specific energy e of an equilibrium state is related to the specific entropy s and the specific volume v

$$e = e(v, s). \tag{2.1}$$

In a wide range of the phase space, e is a smooth function. Therefore, we suppose that e is four times continuously differentiable throughout this work. However, at points along saturation boundaries the second derivatives may fail to exist. But they exhibit at most jump discontinuities.

Neglecting irreversible effects, e.g. viscosity and heat conduction, the first and second law of thermodynamics imply the *fundamental thermodynamic identity*

$$de = -pdv + Tds. \tag{2.2}$$

Consequently, the pressure p and the temperature T can be represented as partial derivatives of the internal specific energy

$$p(v,s) = -e_v(v,s), \quad T(v,s) = e_s(v,s) \tag{2.3}$$

which are supposed to be non–negative, i.e.,

$$p \geq 0, \quad T \geq 0. \tag{2.4}$$

In addition, the assumption of *thermodynamic stability* imposes some constraints on the second derivatives, namely, that e is jointly convex in (v, s). Since e is supposed to be sufficiently smooth this is equivalent to the fact that the Hessian of e is non–negative, i.e.,

$$e_{ss}(v,s) \geq 0, \quad e_{vv}(v,s) \geq 0, \quad e_{ss}(v,s)e_{vv}(v,s) \geq e_{sv}^2(v,s). \tag{2.5}$$

Finally, we need some assumptions concerning the *asymptotic behavior*, namely,

$$\lim_{T\to 0} s = 0, \quad \lim_{T\to\infty} s = \infty \tag{2.6}$$

where the first limit is given by the third law of thermodynamics. This implies that the domain of definition for the EOS is restricted to

$$v \geq 0, \quad s \geq 0. \tag{2.7}$$

Moreover, the limits

$$\lim_{v\to 0} p(v,s) = \infty, \quad \lim_{v\to\infty} p(v,s) = 0, \quad \lim_{s\to\infty} e(v,s) = \infty, \quad \lim_{s\to\infty} p(v,s) = \infty \tag{2.8}$$

hold.

In view of characterizing local properties of the EOS we introduce three dimensionless quantities based on the second derivatives of e (see [Dav85, MP89]). In particular, these are the *adiabatic exponent* γ, the *Grüneisen coefficient* Γ and the *dimensionless specific heat* g

$$\gamma \ := \ \frac{v}{p} e_{vv}(v,s) = -\frac{v}{p} p_v(v,s), \tag{2.9}$$

$$\Gamma \ := \ -\frac{v}{T} e_{sv}(v,s) = \frac{v}{T} p_s(v,s), \tag{2.10}$$

$$g \ := \ \frac{pv}{T^2} e_{ss}(v,s) = \frac{pv}{T^2} T_s(v,s). \tag{2.11}$$

The adiabatic exponent may also be interpreted as "dimensionless sound speed", see [MP89], since it is related to the sound speed c by

$$c^2 := -v^2 p_v(v,s) = \gamma p v > 0 \tag{2.12}$$

In view of the hyperbolicity of the fluid equations, this quantity is supposed to be strictly positive. This assumption is valid in the entire phase space except for the critical point.

In terms of the dimensionless quantities the stability assumptions (2.5) read

$$g \geq 0, \quad \gamma \geq 0, \quad \gamma g \geq \Gamma^2. \tag{2.13}$$

Menikoff and Plohr show in their investigation [MP89] that these conditions do not sufficiently characterize the material properties. To this end, they represent the shock curves with respect to the dimensionless quantities and deduce sufficient conditions for these quantities which guarantee the solution of the Riemann problem to exist.

Another dimensionless quantity defined by the third derivative of e is the *fundamental derivative of gas dynamics*

$$\mathcal{G} := -\frac{1}{2} \frac{e_{vvv}(v,s)}{e_{vv}(v,s)} = \frac{1}{2} \frac{v^2}{\gamma p} p_{vv}(v,s). \tag{2.14}$$

Obviously, the sign of $\mathcal{G}$ is related to the curvature of the isentropes in the p–v plane. For an *ideal gas*, the isentropes are convex, i.e., $\mathcal{G}$ is positive. However, close to the vapor–liquid saturation boundary materials are known to exhibit a region where the isentropes are concave, i.e., $\mathcal{G}$ is negative (see Fig. 3). Consequently, there need to exist points of inflection which are isolated zeros of $\mathcal{G}$ along isentropes. Therefore, we distinguish between *convex EOS* and *non–convex EOS* corresponding to the behavior of the isentropes. We will see later that $\mathcal{G}$ has significant influence on the structure of the Riemann problem.

Up to now, all relations have been derived from the EOS (2.1) in terms of v and s. However, in view of computational fluid dynamics it is more convenient to use an EOS in the form

$$p = p(v,e). \tag{2.15}$$

We will refer to (2.1) as the complete EOS and to (2.15) as the incomplete EOS following the notation in [MP89]. Whenever the pressure and the temperature are strictly positive, then e is a monotone function in v and s. Hence, we can change variables, i.e.,

$$s = s(v,e) \tag{2.16}$$

and substitute s in $p = p(v,s)$. This means that the incomplete EOS can be derived from the complete EOS. However, in general no incomplete EOS exists determining a complete EOS which is thermodynamically consistent (see [MP89], p. 83). Nevertheless,

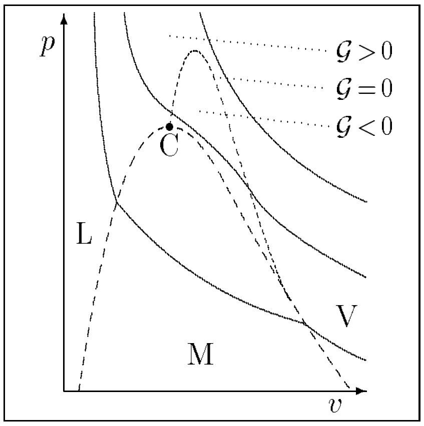

Figure 3: Isentropes in p–v plane, L=Liquid, V=Vapor, M=Mixture, C=Critical Point

we prefer to use the incomplete EOS as is usually done in computational fluid dynamics. Consequently, the incomplete EOS at hand may not be valid throughout the physically meaningful phase space. Hence, the range of validity is implicitly given by the demand of *thermodynamic consistency*, i.e., (i) $T \geq 0$ (change of variable), (ii) $\lim_{T\to 0} s = 0$ (3rd law of thermodynamics) and (iii) $s = s(v,e)$ is jointly concave (thermodynamic stability). Furthermore, the dimensionless quantities have to be written in terms of v and e. To this end, we notice that the first and second derivative of an arbitrary quantity $f = f(v,s) = f(v, e(v,s))$ along an isentrope are given by

$$f_v|_{(v,s)} = (f_v - pf_e)|_{(v,e)}, \tag{2.17}$$

$$f_{vv}|_{(v,s)} = (f_{vv} - p(2f_{ve} - f_e p_e - pp_{ee}) - f_e p_v)\,|_{(v,e)} \tag{2.18}$$

where the fundamental identity of thermodynamics implies $s_v(v,e) = p/T$ and $T = e_s(v,s) > 0$ for $s \neq 0$. From this we conclude $s_e(v,e) = 1/T$ and $p_e(v,e) = p_s(v,s)s_e(v,e) = p_s(v,s)/T$. For $f = p$ we obtain in particular

$$p_v(v,s) = p_v(v,e) - p(v,e)p_e(v,e) \tag{2.19}$$

We will close this section with some remarks on sufficient and necessary conditions on the first derivatives of p for thermodynamic stability (2.13), which, together with (2.4) and (2.7), imply

$$p_v(v,s) \leq 0. \tag{2.20}$$

Obviously, this condition is satisfied, if for the incomplete EOS

$$p_v(v,e) = -(\gamma - \Gamma)p/v \leq 0 \quad \text{and} \quad p_e(v,e) = \Gamma/v \geq 0 \tag{2.21}$$

hold along an isentrope. This is equivalent to

$$0 \leq \Gamma \leq \gamma. \tag{2.22}$$

In many applications and investigations the inequalities (2.21) and (2.22) are explicitly assumed to be true. However, these constraints might exclude physically admissible states, since they are only sufficient but not necessary for (2.20). For instance, there exist materials for which $\Gamma \geq 0$ is violated (e.g. water near 0^0 C and 1 bar). Nevertheless, there arise some constraints for γ and Γ not only induced by thermodynamics but from the existence of the Riemann solution as we will derive in the subsequent sections. At this point, we only assume (2.20) to be satisfied by the incomplete EOS instead of (2.22) in view of thermodynamic consistency.

Finally, we want to remark that in view of analytical investigations in the context of the Riemann solution we need the third derivatives of the EOS $p(v, s)$. These partial derivatives exist, since we assume that the energy function (2.1) is four times differentiable.

3 General Construction Principles

Before presenting a Riemann solver for the Euler equations, we summarize for the convenience of the reader some well–known characteristic construction principles for strictly hyperbolic systems of conservation laws, following essentially the work of Liu [Liu74, Liu75, Liu76a, Liu76b]. Since this part is primarily based on analytical arguments it is to offer a guide line for the subsequent discussion of the specific Euler equations mainly based on physical arguments.

3.1 The Riemann Problem for Systems of Conservation Laws

Systems of conservation laws in one spatial dimension can be written in the form

$$\boldsymbol{u}_t + \boldsymbol{f}(\boldsymbol{u})_x = \boldsymbol{0} \tag{3.1}$$

where $\boldsymbol{u} : \mathrm{IR}_+ \times \mathrm{IR} \to \mathcal{D} \subset \mathrm{IR}^n$ denotes the vector of n conservative quantities and $\boldsymbol{f} : \mathcal{D} \to \mathrm{IR}^n$ is the flux vector which is supposed to be sufficiently smooth, i.e., $f \in C^3(\mathcal{D})$. Here, $\mathcal{D} \subset \mathrm{IR}^n$ is the *admissible phase space*. Furthermore, the system is supposed to be *strictly hyperbolic*, i.e., there exists a complete set of eigenvalues $\lambda_k(\boldsymbol{u})$, $k = 1, \ldots, n$, of the Jacobian $\boldsymbol{A}(\boldsymbol{u}) := \partial \boldsymbol{f}(\boldsymbol{u})/\partial \boldsymbol{u}$ such that

$$\lambda_1(\boldsymbol{u}) < \ldots < \lambda_n(\boldsymbol{u}) \qquad \forall\, \boldsymbol{u} \in \mathcal{D} \tag{3.2}$$

and corresponding right eigenvectors $\boldsymbol{r}_k(\boldsymbol{u})$ and left eigenvectors $\boldsymbol{l}_k(\boldsymbol{u})$ of $\boldsymbol{A}(\boldsymbol{u})$ such that

$$\boldsymbol{l}_k^T(\boldsymbol{u})\ \boldsymbol{r}_j(\boldsymbol{u}) = \delta_{kj} \quad 1 \le k, j \le n, \quad \forall\, \boldsymbol{u} \in \mathcal{D}. \tag{3.3}$$

Hence, there exists an eigenvalue decomposition of $\boldsymbol{A}(\boldsymbol{u})$

$$\boldsymbol{L}(\boldsymbol{u})\boldsymbol{A}(\boldsymbol{u})\boldsymbol{R}(\boldsymbol{u}) = \boldsymbol{\Lambda}(\boldsymbol{u}) \quad \forall\, \boldsymbol{u} \in \mathcal{D} \tag{3.4}$$

where the rows of $\boldsymbol{L}$ are the left eigenvectors and the columns of $\boldsymbol{R}$ are the right eigenvectors.

In the literature, the eigenvalues λ_k are called *characteristic velocities* corresponding to the *characteristic k–field* which is characterized by the *nonlinearity factor*

$$\alpha_k(\boldsymbol{u}) := \nabla_{\boldsymbol{u}} \lambda_k(\boldsymbol{u})\, \boldsymbol{r}_k(\boldsymbol{u}) \qquad \forall\, \boldsymbol{u} \in \mathcal{D}. \tag{3.5}$$

Whenever α_k vanishes for all $\boldsymbol{u} \in \mathcal{D}$ then the k–field is called *linearly degenerated*. However, if α_k does not vanish throughout the admissible phase space, the k–field is called *genuinely nonlinear*. In general, the k–field is supposed to be either linearly degenerated or genuinely nonlinear. Here, we also consider the case of a *non–genuinely nonlinear field*, i.e., α_k locally vanishes at certain points of the phase space. To be more specific, we assume a $(n-1)$–dimensional hypersurface $\mathcal{M} \subset \mathcal{D}$ to exist where the nonlinearity factor vanishes, i.e., $\alpha_k|_{\mathcal{M}} = 0$, and, in addition, it separates regions $\mathcal{D}^+$, $\mathcal{D}^- \subset \mathcal{D}$ such that $\alpha_k|_{\mathcal{D}^+} > 0$ and $\alpha_k|_{\mathcal{D}^-} < 0$, respectively. Moreover, we demand that the trajectories defined by $\boldsymbol{u}'(\beta) = \boldsymbol{r}_k(\boldsymbol{u}(\beta))$ intersect $\mathcal{M}$ only at isolated points. Finally, we assume that the characteristic fields are *simply degenerated* on $\mathcal{M}$, i.e.,

$$\beta_k(\boldsymbol{u}) := \nabla_{\boldsymbol{u}} \alpha_k(\boldsymbol{u})\, \boldsymbol{r}_k(\boldsymbol{u}) \neq 0 \qquad \forall\, \boldsymbol{u} \in \mathcal{M}.$$

The Riemann problem to (3.1) is given by imposing the piecewise constant initial data

$$\boldsymbol{u}(0,x) = \begin{cases} \boldsymbol{u}_l & , \quad x < 0 \\ \boldsymbol{u}_r & , \quad x > 0 \end{cases} \tag{3.6}$$

for two states $\boldsymbol{u}_l,\ \boldsymbol{u}_r \in \mathcal{D}$. Obviously, the solution of this problem is in general not differentiable but only exists in the weak sense according to the hyperbolicity of the underlying equations. Because of the initial data it has to be scale–invariant, i.e., $u(t,x) = const$ along rays $x/t = const$. Therefore, the Riemann problem is inherently a onedimensional problem which can be parameterized by the ratio x/t. Moreover, there may exist up to n waves in the t–x plane which are propagating with different speeds, i.e., they are separated in the time–space continuum (see Fig. 4), since the system (3.1) is supposed to be strictly hyperbolic. These are referred to as k–waves since they correspond to the characteristic velocities λ_k.

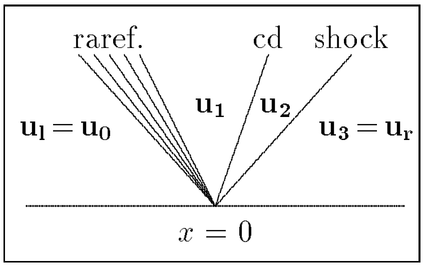

Figure 4: Waves in the t–x plane

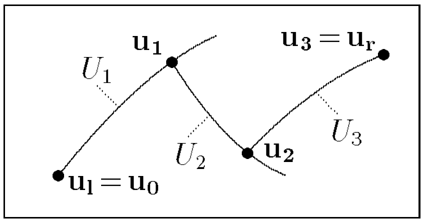

Figure 5: k–curves connected in the projected phase space

As is indicated by Fig. 4, solving the Riemann problem requires to find appropriate intermediate state $\boldsymbol{u}_k \in \mathcal{D}$, $k = 1,\dots,n-1$, by which the states $\boldsymbol{u}_l$ and $\boldsymbol{u}_r$ can be connected. Since the Riemann solution is scale–invariant, these states are lying on curves $\boldsymbol{U}_k = \boldsymbol{U}_k(\xi_k)$, $|\xi_k| < a$, $k = 1,\dots,n$ which are called k–curves. The basic idea is to connect the left state $\boldsymbol{u}_l$ and the right state $\boldsymbol{u}_r$ by a suitable combination of these curves in the admissible phase space. To this end, we move along the 1–curve starting in $\boldsymbol{U}_1(\xi_{1,0}) = \boldsymbol{u}_l$ up to a certain state $\boldsymbol{u}_1 = \boldsymbol{U}_1(\xi_1)$. There we switch to the 2–curve starting in $\boldsymbol{U}_2(\xi_{2,0}) = \boldsymbol{u}_1$ and continue along $\boldsymbol{U}_2$ up to another state $\boldsymbol{u}_2 = \boldsymbol{U}_2(\xi_2)$. This procedure is successively repeated for all k–curves, $k = 1,\dots,n$ (see Fig. 5). Hence, solving the Riemann problem reduces to determine a unique parameter vector $\boldsymbol{\xi} \in U := \{(\xi_1,\dots,\xi_n)^T \in \mathrm{IR}^n \ : \ |\xi_k| < a,\ k = 1,\dots,n\}$ such that $\boldsymbol{u}_n = \boldsymbol{u}_r$. In analogy to Smoller's proof in [Smo82], p. 335, for the standard case, i.e., the k–fields are either genuinely nonlinear or linearly degenerated, it can be shown that there uniquely exists an appropriate $\boldsymbol{\xi} \in U$, provided that $\boldsymbol{u}_r$ is sufficiently close to $\boldsymbol{u}_l$. The proof is based on a smooth mapping $\boldsymbol{T} : \mathcal{D} \times U \to \mathrm{IR}^n$ defined by $\boldsymbol{T}(\boldsymbol{u}_r, \boldsymbol{\xi}) := \boldsymbol{u}_n - \boldsymbol{u}_r$. Then the assertion follows by the implicit function theorem. Solving the nonlinear problem in order to determine the parameter values corresponding to the different curves can be interpreted as a multiple shooting scheme as it is frequently applied to two–point boundary value problems.

We will see that the construction of the k–curves strongly depends on the behavior of the k–field and the nonlinearity factor α_k, respectively. In general, the k–curve is composed of several types of elementary curves, namely, *rarefaction curves*, *shock curves* and *contact discontinuities*. In the non–genuinely nonlinear case, there, in addition, another type arises which is defined through a rarefaction curve and a family of shock curves. This curve is called *mixed* or *composite curve*. The composition of the k–curve by these elementary curves is determined by the propagation speeds of the corresponding states in the t–x plane. Here, the basic principle is connecting different elementary curves in such a way that the corresponding waves in the time–space continuum are separated and do not exhibit a multivalued solution.

3.2 Elementary Curves

In the following, we will describe the construction of the elementary curves and the composition of the k–curves. This investigation is independent of the initial states $\boldsymbol{u}_l$, $\boldsymbol{u}_r$ of the Riemann problem. We therefore denote the origin of every elementary curve by an arbitrary state $\boldsymbol{u}_0 \in \mathcal{D}$. After having described the composition of the k–curves, we finally present the corresponding k–waves in the t–x plane.

3.2.1 Rarefaction Curves

In the case of a scale–invariant smooth solution $\boldsymbol{u}$ of (3.1), the partial differential equation reduces to an ordinary differential equation for $\boldsymbol{u}_k(\xi) = \boldsymbol{u}(t,x)$ with $\xi = x/t$. In particular, if the k–field is genuinely nonlinear, then $\boldsymbol{u}_k$ is determined by the initial value problem (IVP)

$$\boldsymbol{u}_k'(\xi) = \frac{1}{\alpha_k(\boldsymbol{u}_k(\xi))}\boldsymbol{r}_k(\boldsymbol{u}_k(\xi)), \quad \xi \in U(\xi_0), \qquad \boldsymbol{u}_k(\xi_0) = \boldsymbol{u}_0 \tag{3.7}$$

in a neighborhood of $\boldsymbol{u}_0$, i.e., $\xi \in U(\xi_0) \subset \mathrm{IR}$ is sufficiently small. This curve is called *rarefaction curve*. Obviously, it is well–defined by (3.7) as long as the nonlinearity factor α_k does not vanish. This corresponds to the nonlinearity of the k–field.

For later use, we introduce the locus of all states $\boldsymbol{u} \in \mathcal{D}$ that can be connected to $\boldsymbol{u}_0$ by a rarefaction curve

$$\mathcal{R}_k(\boldsymbol{u}_0) := \text{clos}\,\{\boldsymbol{u} \in \mathcal{D} : \boldsymbol{u} = \boldsymbol{u}_k(\xi),\ \xi \in U(\xi_0),\ \boldsymbol{u}_k \text{ solution of (3.7)}\}$$

A characteristic feature of the rarefaction curve is the variation of the characteristic velocity λ_k which is monotonically increasing. In particular, it is determined by

$$\lambda_k(\boldsymbol{u}_k(\xi)) = \xi \quad \Longrightarrow \quad \lambda_k'(\boldsymbol{u}_k(\xi)) = \nabla_{\boldsymbol{u}}\lambda_k(\boldsymbol{u}_k(\xi))\boldsymbol{u}_k'(\xi) = 1. \tag{3.8}$$

Finally, we emphasize that the rarefaction curve must not be parametrized necessarily by the ratio x/t. In general, a regular parametrization is preferable in view of the algorithmic construction.

3.2.2 Shock Curves and Contact Discontinuities

A characteristic feature of hyperbolic conservation laws is the developing of jump discontinuities caused by the nonlinearity of the flux. However, these discontinuities have to satisfy certain constraints. A fundamental relation for two adjacent states $\boldsymbol{u}_0$, $\boldsymbol{u} \in \mathcal{D}$, $\boldsymbol{u}_0 \neq \boldsymbol{u}$, is named in honor of Rankine and Hugoniot, who derived it first in the context of gas dynamics. This jump condition, in the following referred to as *Rankine–Hugoniot jump condition* reads

$$\sigma(\boldsymbol{u} - \boldsymbol{u}_0) = \boldsymbol{f}(\boldsymbol{u}) - \boldsymbol{f}(\boldsymbol{u}_0) \tag{3.9}$$

where $\sigma = \sigma(\boldsymbol{u}_0, \boldsymbol{u})$ denotes the speed of the discontinuity.

In the sequel, we want to characterize the family of states that can be connected to $\boldsymbol{u}_0$ by a discontinuity satisfying the Rankine–Hugoniot jump conditions. For this purpose, we introduce the function $\boldsymbol{H}_{\boldsymbol{u}_0} : \mathcal{D} \times \mathrm{IR} \to \mathrm{IR}^n$ defined by

$$\boldsymbol{H}_{\boldsymbol{u}_0}(\boldsymbol{u}, \sigma) := -\sigma(\boldsymbol{u} - \boldsymbol{u}_0) + \boldsymbol{f}(\boldsymbol{u}) - \boldsymbol{f}(\boldsymbol{u}_0).$$

Then the Hugoniot locus $\mathcal{H}(\boldsymbol{u}_0)$ to a given initial state $\boldsymbol{u}_0$

$$\mathcal{H}(\boldsymbol{u}_0) := \text{clos}\ \{\boldsymbol{u} \in \mathcal{D} \subset \mathrm{IR}^n \ : \ \exists\, \sigma \in \mathrm{IR} \text{ s.t. } \boldsymbol{H}_{\boldsymbol{u}_0}(\boldsymbol{u}, \sigma) = \boldsymbol{0}\}$$

consists of all states $\boldsymbol{u} \in \mathcal{D}$ for which a shock speed $\sigma = \sigma(\boldsymbol{u}_0, \boldsymbol{u})$ exists such that $(\boldsymbol{u}, \sigma)$ is a root of the function $\boldsymbol{H}_{\boldsymbol{u}_0}$. Obviously, a one parameter family of states $(\boldsymbol{u}, \sigma)$ exists when rank $\boldsymbol{H}'_{\boldsymbol{u}_0}(\boldsymbol{u}, \sigma) = n$ or, equivalently, either of the two conditions holds

$$\sigma(\boldsymbol{u}_0, \boldsymbol{u}) \neq \lambda_i(\boldsymbol{u}), \quad \forall\, i = 1, \ldots, n \quad \text{or} \tag{3.10}$$
$$\sigma(\boldsymbol{u}_0, \boldsymbol{u}) = \lambda_i(\boldsymbol{u}), \quad \text{for one } i \in \{1, \ldots, n\} \quad \text{such that} \quad \boldsymbol{l}_i(\boldsymbol{u})(\boldsymbol{u} - \boldsymbol{u}_0) \neq 0. \tag{3.11}$$

In this case, the implicit function theorem implies that the zero set of $\boldsymbol{H}_{\boldsymbol{u}_0}$ is a one dimensional manifold in a neighborhood of $\boldsymbol{u} \neq \boldsymbol{u}_0,\ \sigma = \sigma(\boldsymbol{u}_0, \boldsymbol{u})$, whenever $(\boldsymbol{u}, \sigma)$ is a non–trivial zero of $\boldsymbol{H}_{\boldsymbol{u}_0}$, i.e., $\boldsymbol{H}_{\boldsymbol{u}_0}(\boldsymbol{u}, \sigma) = \boldsymbol{0},\ \boldsymbol{u} \neq \boldsymbol{u}_0$. However, there exist two kinds of bifurcation points

$$\text{a)} \quad \boldsymbol{u} = \boldsymbol{u}_0 \qquad \text{and} \qquad \text{b)} \quad \boldsymbol{u} \neq \boldsymbol{u}_0,\ \sigma(\boldsymbol{u}_0, \boldsymbol{u}) = \lambda_i(\boldsymbol{u}),\ \boldsymbol{l}_i(\boldsymbol{u})(\boldsymbol{u} - \boldsymbol{u}_0) = 0 \tag{3.12}$$

referred to as *primary* and *secondary bifurcation*. Primary bifurcation has been investigated by Lax in [Lax57] for strictly hyperbolic systems. He proved that there exist n smooth curves $\boldsymbol{u}_k = \boldsymbol{u}_k(\xi),\ k = 1, \ldots, n$ with $\boldsymbol{u}_k(\xi_0) = \boldsymbol{u}_0$ satisfying the jump conditions (3.9) and

$$\lim_{\boldsymbol{u} \to \boldsymbol{u}_0} \sigma_k(\boldsymbol{u}_0, \boldsymbol{u}) = \lambda_k(\boldsymbol{u}_0).$$

Since the system is supposed to be strictly hyperbolic, these curves can be enumerated with increasing velocity $\lambda_k(\boldsymbol{u}_0)$. The corresponding Hugoniot locus is denoted by $\mathcal{H}_k(\boldsymbol{u}_0)$. This curve is tangent to the rarefaction curve $\mathcal{R}_k(\boldsymbol{u}_0)$. In principle secondary bifurcation may occur. However, we will omit a discussion and refer to [Wen72b]. For the Euler equations these states are not known to exist. Therefore, we assume throughout this paper that

$$\boldsymbol{l}_i(\boldsymbol{u})(\boldsymbol{u} - \boldsymbol{u}_0) \neq 0 \qquad \forall\, \boldsymbol{u}, \boldsymbol{u}_0 \in \mathcal{D},\ \boldsymbol{u} \neq \boldsymbol{u}_0 \tag{3.13}$$

holds along discontinuity curves.

If the k–field is linearly degenerated, then the curve $\mathcal{H}_k(\boldsymbol{u}_0)$ is called a *contact discontinuity* which is characterized by

Proposition 3.1 *Assume that the k–field is linearly degenerated. Then the following properties hold along the discontinuity curve*

$$\boldsymbol{u}'_k(\xi) = \boldsymbol{r}_k(\boldsymbol{u}_k(\xi)), \quad \xi \in U(\xi_0), \quad \boldsymbol{u}_k(\xi_0) = \boldsymbol{u}_0, \tag{3.14}$$

$$\sigma = \lambda_k(\boldsymbol{u}_k(\xi)) = \lambda_k(\boldsymbol{u}_k(\xi_0)) = const. \qquad \forall\, \xi \tag{3.15}$$

In the case of a not necessarily genuinely nonlinear field, the curve corresponding to the Hugoniot locus is called a *shock curve*. Here a more thorough analysis is presented in the following. This is based on Liu's work [Liu75]. First of all, we specify the orientation of the shock curve by the condition

$$\left.\frac{d\boldsymbol{u}}{d\xi}\right|_{\xi=\xi_0} = \boldsymbol{u}'(\xi_0) = \boldsymbol{r}_k(\boldsymbol{u}_0). \tag{3.16}$$

We emphasize that this parametrization is chosen here purely for the purpose of analysis. A different parametrization may be preferable when deriving a constructive algorithm for a concrete system, e.g., the Euler equations. We now consider shock curves in some detail with special emphasise on the following issues: (i) admissibility of shock curves and (ii) existence of sonic shocks.

Admissibility of Shock Curves

Besides the Rankine–Hugoniot relations we need an additional condition characterizing the physically meaningful states, since not all states of the Hugoniot locus are admissible. In the literature, there exist several admissibility criteria. In view of the composition of the k–curves, a criterion is preferable by which the shock speed σ_k and the characteristic velocity λ_k are related. Here the *Lax jump conditions* are adequate

$$\text{a)}\quad \lambda_k(\boldsymbol{u}) < \sigma_k(\boldsymbol{u}_0, \boldsymbol{u}) < \lambda_k(\boldsymbol{u}_0), \quad \text{b)}\quad \lambda_{k-1}(\boldsymbol{u}_0) < \sigma_k(\boldsymbol{u}_0, \boldsymbol{u}) < \lambda_{k+1}(\boldsymbol{u}) \tag{3.17}$$

which have been derived by Lax [Lax57]. If the k–field is genuinely nonlinear, then the Lax criterion is sufficient. However, for a non–genuinely nonlinear field it has to be replaced by Liu's *extended admissibility relation*

$$\sigma_k(\boldsymbol{u}_0, \boldsymbol{u}) \le \sigma_k(\boldsymbol{u}_0, \tilde{\boldsymbol{u}}) \qquad \forall\, \tilde{\boldsymbol{u}} \in [\boldsymbol{u}_0, \boldsymbol{u}] \subset \mathcal{H}_k(\boldsymbol{u}_0). \tag{3.18}$$

This relation implies that the shock speed is non–increasing along the admissible branch of the shock curve. It relaxes the Lax condition in the sense that we can conclude

$$\lambda_k(\boldsymbol{u}) \le \sigma_k(\boldsymbol{u}_0, \boldsymbol{u}) \le \lambda_k(\boldsymbol{u}_0). \tag{3.19}$$

If the k–field is genuinely nonlinear, then the two conditions (3.17) and (3.18) are equivalent, because equality cannot occur in (3.19).

Comparing (3.19) and (3.17), we notice that for non–genuinely nonlinear fields there also may occur contact discontinuities where the characteristic velocity and the shock speed coincide. These states are characterized by the following result from [Liu75].

Proposition 3.2 *Assume that there exists no point of secondary bifurcation, i.e., (3.13) holds, and let be $\boldsymbol{u} \in \mathcal{H}_k(\boldsymbol{u}_0)$ such that (3.17b) is satisfied. The parametrization of the shock curve is chosen such that (3.16) holds. Then the following assertions are valid*

a) If $\boldsymbol{u}_k(\xi) \neq \boldsymbol{u}_0$, then the two conditions are equivalent

$$\textit{i)}\quad \sigma_k'(\boldsymbol{u}_0, \boldsymbol{u}_k(\xi)) = 0 \qquad \textit{ii)}\quad \sigma_k(\boldsymbol{u}_0, \boldsymbol{u}_k(\xi)) = \lambda_k(\boldsymbol{u}_k(\xi)) \tag{3.20}$$

where the prime denotes the derivative with respect to the convention (3.16) of the shock curves;

b) For $\boldsymbol{u} \in \mathcal{H}_k(\boldsymbol{u}_0)$, $\boldsymbol{u} \neq \boldsymbol{u}_0$, there exist coefficients a_i such that $\boldsymbol{u} - \boldsymbol{u}_0 = \sum_{i=1}^n a_i \boldsymbol{r}_i(\boldsymbol{u})$ and, in particular, $a_k \neq 0$;

c) The shock curve $\mathcal{H}_k(\boldsymbol{u}_0)$ is tangent to the rarefaction curve $\mathcal{R}_k(\boldsymbol{u})$ at $\boldsymbol{u}$.

The details of the proofs are omitted. The interested reader is referred to [Liu75].

Furthermore, the admissible branch of the shock curve can be characterized with the aid of the extended admissibility relation.

Proposition 3.3 *Let be $\mathcal{H}_k^{\pm}(\boldsymbol{u}_0) := \{\boldsymbol{u} \in \mathcal{H}_k(\boldsymbol{u}_0) \ : \ sign\, a_k = \pm 1\}$ where a_k denotes the coefficient in the expansion shown in Prop. 3.2. Assume that no point of secondary bifurcation exists, i.e., (3.13) holds. Then the admissible branches are $\mathcal{H}_k^{-}(\boldsymbol{u}_0)$ for $\sigma_k'(\boldsymbol{u}_0, \boldsymbol{u}_0) > 0$ and $\mathcal{H}_k^{+}(\boldsymbol{u}_0)$ for $\sigma_k'(\boldsymbol{u}_0, \boldsymbol{u}_0) < 0$.*

This result is essential in the algorithmic construction of the Riemann solution. Therefore we sketch the relation between the shock speed and the characteristic velocity at $\boldsymbol{u}_0$. First of all, we notice that $\mathcal{H}_k^{+}(\boldsymbol{u}_0) \cap \mathcal{H}_k^{-}(\boldsymbol{u}_0) = \{\boldsymbol{u}_0\}$, since $a_k \neq 0$, $\boldsymbol{u} \neq \boldsymbol{u}_0$. This means that the shock curve is split up into branches connected in the origin $\boldsymbol{u}_0$. For $\boldsymbol{u} = \boldsymbol{u}_0$ we then obtain

$$\sigma_k(\boldsymbol{u}_0, \boldsymbol{u}_0) = \lambda_k(\boldsymbol{u}_0) \quad \text{and} \quad \sigma_k'(\boldsymbol{u}_0, \boldsymbol{u}_0) = 0.5\, \lambda_k'(\boldsymbol{u}_0) \neq 0.$$

Therefore, the inequalities

$$\begin{array}{ll} \text{a) } \sigma_k'(\boldsymbol{u}_0, \boldsymbol{u}_0) > 0 \ \Rightarrow \ \lambda_k'(\boldsymbol{u}) > \sigma_k'(\boldsymbol{u}_0, \boldsymbol{u}) > 0 & \text{or} \\ \text{b) } \sigma_k'(\boldsymbol{u}_0, \boldsymbol{u}_0) < 0 \ \Rightarrow \ \lambda_k'(\boldsymbol{u}) < \sigma_k'(\boldsymbol{u}_0, \boldsymbol{u}) < 0 & \end{array}$$

hold in a small neighborhood of $\boldsymbol{u}_0$. The two cases are sketched in Figs. 6 and 7.

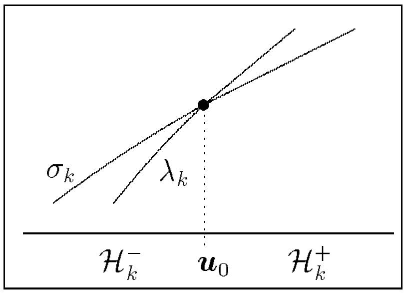

Figure 6: Velocity profile

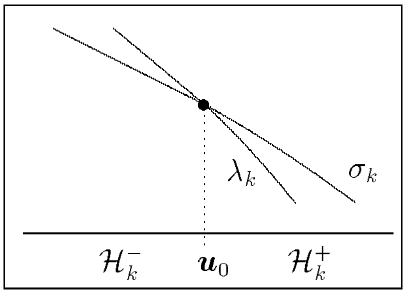

Figure 7: Velocity profile

Then the Prop. 3.3 characterizes the admissible branch:
$\boldsymbol{u} \in \mathcal{H}_k^{+}(\boldsymbol{u}_0)$ is admissible, if and only if

$$\sigma_k'(\boldsymbol{u}_0, \boldsymbol{u}) < 0 \Leftrightarrow \sigma_k(\boldsymbol{u}_0, \boldsymbol{u}) > \lambda_k(\boldsymbol{u}),$$

whereas $\boldsymbol{u} \in \mathcal{H}_k^{-}(\boldsymbol{u}_0)$ is admissible, if and only if

$$\sigma_k'(\boldsymbol{u}_0, \boldsymbol{u}) > 0 \Leftrightarrow \sigma_k(\boldsymbol{u}_0, \boldsymbol{u}) < \lambda_k(\boldsymbol{u}).$$

For a different parametrization of the shock curve, we have to consider the relation between the derivative of σ_k with respect to the parametrization (3.16) and the new parametrization, in order to determine the admissible branch of the shock curve with respect to the new parametrization.

Another admissibility concept is based on mimicing the behavior of the thermodynamic entropy across a shock which has to increase according to the second law of thermodynamics. This *entropy concept* was introduced by Lax [Lax71]. It turned out to be equivalent to the Lax jump conditions provided that the k–field is genuinely nonlinear.

The most general approach is based on the limit of the *viscous shock profile* (see e.g. [Wey49, Gil51, Liu76a, Liu76b, Peg86]) which results in equivalent admissibility conditions. Here, the shock profile is considered in the limiting case of vanishing viscosity and heat conduction in the context of fluid dynamics.

Existence of Sonic Shocks

Finally, we present the influence of a non–genuinely nonlinear field. This is quite obvious for rarefaction curves. However, for shock curves a more thorough analysis is necessary. From the following proposition we conclude that there exists no sonic shock if the k–field is genuinely nonlinear.

Proposition 3.4 *Let be $\boldsymbol{u} \in \mathcal{H}_k(\boldsymbol{u}_0)$ where the shock speed is sonic and choose the parametrization of the shock curve such that (3.16) holds. Then there exists a state $\tilde{\boldsymbol{u}} \in \mathcal{H}_k(\boldsymbol{u}_0)$ where the nonlinear field degenerates, i.e., $\alpha_k(\tilde{\boldsymbol{u}}) = 0$ and this state lies on $\mathcal{H}_k(\boldsymbol{u}_0)$ between the origin $\boldsymbol{u}_0$ of the shock curve and the sonic state $\boldsymbol{u}$.*

Proof: Since this result is not derived explicitly in [Liu74], we will sketch the principal ideas how to prove this conclusion. First of all, we know by the Lax jump conditions (3.17) that the characteristic velocity λ_k has to be less than the shock speed σ_k along the admissible shock curve and, in addition, both have to be less than $\lambda_k(\boldsymbol{u}_0)$ From this we conclude that both velocities decrease monotonically in a neighborhood of $\boldsymbol{u}_0$.

Next, we have to derive the relation between the derivative of λ_k and the nonlinearity factor α_k. To this end, we will make use of the analysis which is presented in [Liu74]. First of all, we expand the derivative of the conservative quantities along the shock curve with respect to the right eigenvectors $\boldsymbol{r}_i(\boldsymbol{u}_k)$, i.e.,

$$\boldsymbol{u}_k' = \sum_{i=1}^{n} b_i \, \boldsymbol{r}_i(\boldsymbol{u}_k).$$

Then the derivative of the characteristic velocity is given by

$$\lambda_k'(\boldsymbol{u}_k) = \nabla_{\boldsymbol{u}} \lambda_k(\boldsymbol{u}_k) \, \boldsymbol{u}_k' = \sum_{i=1}^{n} b_i \, \nabla_{\boldsymbol{u}} \lambda_k(\boldsymbol{u}_k) \, \boldsymbol{r}_i(\boldsymbol{u}_k), \tag{3.21}$$

where the coefficient b_k is known to be positive. Moreover, we know that the shock curve $\mathcal{H}_k(\boldsymbol{u}_0)$ is tangent to the rarefaction curve $\mathcal{R}_k(\boldsymbol{u})$ in the state $\boldsymbol{u} = \boldsymbol{u}_k$ where the shock becomes sonic, i.e., there exists some scalar factor $\tilde{c} \in \mathrm{I\!R}$ such that $\boldsymbol{u}_k' = \tilde{c} \, \boldsymbol{r}_k(\boldsymbol{u})$ and therefore $b_k = \tilde{c}, \; b_i = 0, \; i \neq k$. For $\boldsymbol{u}_k = \boldsymbol{u}$ we conclude from (3.21)

$$\lambda_k'(\boldsymbol{u}) = \tilde{c} \, \alpha_k(\boldsymbol{u}). \tag{3.22}$$

On the other hand we obtain from standard analysis for genuinely nonlinear fields

$$\lambda_k'(\boldsymbol{u}_0) = 0.5 \, \alpha_k(\boldsymbol{u}_0). \tag{3.23}$$

One of the two possible situations is sketched in Fig. 8. Since $\operatorname{sign} \lambda_k'(\boldsymbol{u}) \neq \operatorname{sign} \lambda_k'(\boldsymbol{u}_0)$

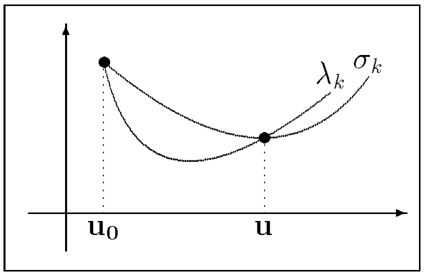

Figure 8: Characteristic velocity and shock speed along $\mathcal{H}_k(\boldsymbol{u}_0)$

and Liu's extended admissibility relation (3.18) hold and, in addition, the coefficients in (3.22), (3.23) are positive, we conclude $\operatorname{sign}\alpha_k(\boldsymbol{u}) \neq \operatorname{sign}\alpha_k(\boldsymbol{u}_0)$. Therefore α_k changes its sign, since α_k is a continuous function along the shock curve. Hence there exists a state $\tilde{\boldsymbol{u}} \in \mathcal{H}_k(\boldsymbol{u}_0)$ where the nonlinearity factor α_k vanishes. □

3.2.3 Mixed Curves

Up to now, we have considered the genuinely nonlinear or the linearly degenerated k–field. However, the rarefaction curve is no longer defined by (3.7) if it approaches a state $\overline{\boldsymbol{u}} = \lim_{\xi\to\overline{\xi}} \boldsymbol{u}_k(\xi) \in \mathcal{D}$ with $\alpha_k(\overline{\boldsymbol{u}}) = 0$, i.e., the k–field degenerates. In order to continue the k–curve construction, another curve in the phase space has to be derived which can be connected to $\mathcal{R}_k(\boldsymbol{u}_0)$ in $\overline{\boldsymbol{u}}$. For this purpose, we introduce the function $\boldsymbol{C} : [\xi_0, \overline{\xi}] \times \mathcal{D} \to \mathrm{IR}^n$ defined by

$$\boldsymbol{C}(\xi, \boldsymbol{u}) := -\lambda_k(\boldsymbol{u}_k(\xi))(\boldsymbol{u} - \boldsymbol{u}_k(\xi)) + \boldsymbol{f}(\boldsymbol{u}) - \boldsymbol{f}(\boldsymbol{u}_k(\xi)). \tag{3.24}$$

Then the *composite locus* (see [Liu75]) is composed of all roots $\boldsymbol{u}$ of the function $\boldsymbol{C}$ and, in addition, $\boldsymbol{u} \neq \boldsymbol{u}_k(\xi)$ is the first point on $\mathcal{H}_k(\boldsymbol{u}_k(\xi))$ satisfying

$$\sigma(\boldsymbol{u}_k(\xi), \boldsymbol{u}) = \lambda_k(\boldsymbol{u}_k(\xi)), \tag{3.25}$$

i.e.,

$$\mathcal{C}(\mathcal{R}_k, \boldsymbol{u}_0) := \operatorname{clos}\{\boldsymbol{u} \in \mathcal{D} : \begin{array}{ll} 1.) & \exists\, \xi \in [\xi_0, \overline{\xi}] \text{ s.t. } \boldsymbol{C}(\xi, \boldsymbol{u}) = \boldsymbol{0} \\ 2.) & \boldsymbol{u} \neq \boldsymbol{u}_k(\xi) \text{ first on } \mathcal{H}_k(\boldsymbol{u}_k(\xi)) \text{ with (3.25)}\} \end{array} \tag{3.26}$$

The composite locus can be interpreted as the union of all states $\boldsymbol{u} \in \mathcal{D}$ where a state $\boldsymbol{u}^* \in \mathcal{R}_k(\boldsymbol{u}_0)$ exists on the rarefaction curve, i.e., $\boldsymbol{u}^* = \boldsymbol{u}_k(\xi^*),\ \xi^* \in [\xi_0, \overline{\xi}]$, such that (3.25) holds for $\xi = \xi^*$. Moreover, the Hugoniot curve $\mathcal{H}_k(\boldsymbol{u}^*)$ is tangent to the composite locus $\mathcal{C}(\mathcal{R}_k, \boldsymbol{u}_0)$ in $\boldsymbol{u}$. This situation is sketched in Figure 9.

As to the analysis of the composite locus, we can proceed analogously to the Hugoniot locus. For this purpose, we first determine the derivatives of $\boldsymbol{C}$. A straightforward calculus where we apply (3.4) and (3.25) yields

$$\boldsymbol{C}_\xi = \boldsymbol{u}_k(\xi) - \boldsymbol{u}, \quad \boldsymbol{C}_{\boldsymbol{u}} = \boldsymbol{R}(\boldsymbol{u})\,(\boldsymbol{\Lambda}(\boldsymbol{u}) - \lambda_k(\boldsymbol{u}_k(\xi))\boldsymbol{I})\,\boldsymbol{L}(\boldsymbol{u}).$$

Once again, a one parameter family of solutions of $\boldsymbol{C}(\xi, \boldsymbol{u}) = \boldsymbol{0}$ exists in a neighborhood of $\boldsymbol{u} \neq \boldsymbol{u}_k(\xi)$, if $\operatorname{rank} \boldsymbol{C}'(\xi, \boldsymbol{u}) = n$. This is equivalent to

$$\sigma(\boldsymbol{u}, \boldsymbol{u}_k(\xi)) = \lambda_k(\boldsymbol{u}_k(\xi)) \neq \lambda_k(\boldsymbol{u}) \quad \text{or} \tag{3.27}$$

$$\sigma(\boldsymbol{u}, \boldsymbol{u}_k(\xi)) = \lambda_k(\boldsymbol{u}_k(\xi)) = \lambda_k(\boldsymbol{u}) \quad \text{and} \quad \boldsymbol{l}_k(\boldsymbol{u})(\boldsymbol{u} - \boldsymbol{u}_k(\xi)) \neq 0. \tag{3.28}$$

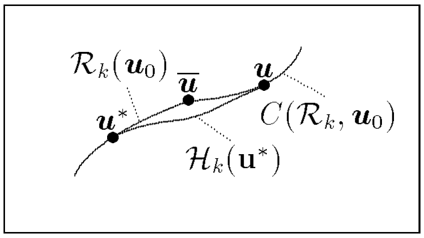

Figure 9: Composite curve

The implicit function theorem implies that the zero set of $\boldsymbol{C}$ is a one dimensional manifold close to $\boldsymbol{u}$. In particular, we can choose the same parameter as for the rarefaction wave. Hence, the derivative reads

$$\boldsymbol{u}'(\xi) = \boldsymbol{R}(\boldsymbol{u}(\xi))\,(\boldsymbol{\Lambda}(\boldsymbol{u}(\xi)) - \lambda_k(\boldsymbol{u}_k(\xi))\boldsymbol{I})^{-1}\,\boldsymbol{L}(\boldsymbol{u}(\xi))(\boldsymbol{u}(\xi) - \boldsymbol{u}_k(\xi)). \tag{3.29}$$

Similar to the Hugoniot locus, there also occur primary and secondary bifurcations, if either one of the two conditions holds

$$\text{a) } \boldsymbol{u} = \boldsymbol{u}_k(\xi), \quad \text{b) } \boldsymbol{u} \neq \boldsymbol{u}_k(\xi),\ \sigma(\boldsymbol{u}, \boldsymbol{u}_k(\xi)) = \lambda_k(\boldsymbol{u}_k(\xi)) = \lambda_k(\boldsymbol{u}),\ \boldsymbol{l}_k(\boldsymbol{u})(\boldsymbol{u} - \boldsymbol{u}_k(\xi)) = 0. \tag{3.30}$$

The composite locus has been investigated by Liu to some extent. Here we summarize some characteristic features in the following proposition.

Proposition 3.5 *Let be $\boldsymbol{u}^* = \boldsymbol{u}_k(\xi^*) \in \mathcal{R}_k(\boldsymbol{u}_0)$ a state on the rarefaction curve and $\boldsymbol{u} \in \mathcal{H}_k(\boldsymbol{u}^*)$ the corresponding state on the mixed curve such that (3.25) holds. Then we obtain*

a) The shock curve $\mathcal{H}_k(\boldsymbol{u}^*)$ is tangent to the mixed curve $\mathcal{C}(\mathcal{R}_k, \boldsymbol{u}_0)$ at $\boldsymbol{u}$;

b) If the shock speed is sonic, then the mixed curve $\mathcal{C}(\mathcal{R}_k, \boldsymbol{u}_0)$ is tangent to the rarefaction curve $\mathcal{R}_k(\boldsymbol{u})$ at $\boldsymbol{u}$.

The details of the proofs are omitted. The interested reader is referred to [Liu75]. However, there remains an open question in Liu's investigations which can be verified for a two by two system provided certain assumptions hold (see [Liu74], Theorem 2.1). In the context of a general hyperbolic system no proof is given in [Liu75].

Conjecture 3.1 *We conjecture that if we approach locally $\overline{\boldsymbol{u}}$ on the rarefaction curve, then the existing corresponding state on the mixed curve approaches $\overline{\boldsymbol{u}}$ as well.*

From this we can conclude that the mixed curve is tangent to the rarefaction curve $\mathcal{R}_k(\boldsymbol{u}_0)$ at $\boldsymbol{u} = \overline{\boldsymbol{u}}$. Moreover, if we choose the same parametrization for the two curves, then we run backward along the mixed curve when proceeding forward along the rarefaction curve. Since our numerical investigations in the context of the Euler equations confirm this conjecture, we believe it to hold provided certain assumptions hold. A detailled analysis will be given in [FFMV].

3.3 Composition of k–Curves

We now describe how to construct a *smooth* curve in the admissible phase space $\mathcal{D}$ by an appropriate composition of the elementary curves. There will be one curve for each of the k–fields which is referred to as k–curve. We emphasize that the subsequent proceeding is restricted to a possibly small neighborhood of a state $\boldsymbol{u}_0 \in \mathcal{D}$, since the elementary curves only exist locally. The construction principle is strongly related to the characteristic velocities λ_k and the shock speeds σ_k corresponding to the rarefaction curves and the shock curves, respectively. Therefore, we have to change the type of the elementary curve in states where the derivative of λ_k vanishes or coincides with the shock speed, respectively.

If the k–field is linearly degenerated, then the k–curve coincides with the contact discontinuity which is determined by (3.14). According to (3.15), the speed of the contact discontinuity remains constant throughout the curve.

However, the k–curve construction becomes more difficult if the k–field is nonlinear. In the following we describe one possible composition where we start the construction at a state $\boldsymbol{u}_0 \in \mathcal{D}$ with $\alpha_k(\boldsymbol{u}_0) \neq 0$. The construction is graphically presented in the context of the Euler equations in Sec. 4.3. From standard results in the genuinely nonlinear case we know that in $\boldsymbol{u}_0$ the shock curve $\mathcal{H}_k(\boldsymbol{u}_0)$ is tangent to the rarefaction curve $\mathcal{R}_k(\boldsymbol{u}_0)$. Furthermore, we know by Prop. 3.3 in which parameter direction $\mathcal{H}_k(\boldsymbol{u}_0)$ is admissible. Here we first proceed along the admissible shock curve $\mathcal{H}_k(\boldsymbol{u}_0)$ originating at $\boldsymbol{u}_0$. Moving along $\mathcal{H}_k(\boldsymbol{u}_0)$ is admissible as long as Liu's extended admissibility relation (3.18) holds. Whenever we arrive at a state $\boldsymbol{u}_1 \neq \boldsymbol{u}_0$ where these conditions are violated, i.e., either of the relations in (3.20) are satisfied, then we have to continue with the rarefaction curve $\mathcal{R}_k(\boldsymbol{u}_1)$ which is tangent to $\mathcal{H}_k(\boldsymbol{u}_0)$ in $\boldsymbol{u}_1$. Here again, the sonic point is no point of secondary bifurcation, since $\boldsymbol{l}_k(\boldsymbol{u}_1)(\boldsymbol{u}_1 - \boldsymbol{u}_0) \neq 0$ is assumed. Starting in $\boldsymbol{u}_1$, we now move along the rarefaction curve $\mathcal{R}_k(\boldsymbol{u}_1)$. This is admissible as long as the characteristic speed increases, i.e. until we reach a state where

$$\boldsymbol{u}_2 = \lim_{\xi \to \overline{\xi}} \boldsymbol{u}_k(\xi) \in \mathcal{D}, \quad \alpha_k(\boldsymbol{u}_2) = 0.$$

If the rarefaction curve is tangent to the hypersurface $\mathcal{M}$ at $\boldsymbol{u}_2$ but does not intersect $\mathcal{M}$, we proceed on the rarefaction curve. Whenever the rarefaction curve intersects $\mathcal{M}$, then we have to continue the k–curve construction by a different kind of elementary curve, since the characteristic velocity becomes extremal. If we proceeded on the rarefaction curve beyond $\boldsymbol{u}_2$ then the characteristic velocity is no longer increasing. This, however, would cause a multivalued solution in the t–x plane. Instead, we continue with a mixed curve, i.e., we connect a state of $\mathcal{R}_k(\boldsymbol{u}_1)$ with a state on the mixed curve by a shock. Besides bifurcation points (3.30), the mixed curve $\mathcal{C}(\mathcal{R}_k, \boldsymbol{u}_1)$ is smooth and can be determined by computing the roots of (3.24) in an appropriate way. For a two by two system of equations, Liu proved that $\mathcal{C}(\mathcal{R}_k, \boldsymbol{u}_1)$ joins $\mathcal{R}_k(\boldsymbol{u}_1)$ tangentially in the state $\boldsymbol{u}_2$. We emphasize that for $n \times n$ systems there is no explicit proof given by Liu. In [Liu75] he only refers to the two by two case described in [Liu74].

Proceeding on the mixed curve, there may exist a state $\boldsymbol{u}_3 \in \mathcal{D}$ where this curve is no longer admissible. Here we distinguish two cases

$$\text{a) } \exists\, \xi \in (\xi_0, \overline{\xi}) \text{ such that } \lambda_k(\boldsymbol{u}_3) = \lambda_k(\boldsymbol{u}_k(\xi)),\ \boldsymbol{u}_3 \neq \boldsymbol{u}_k(\xi), \qquad \text{b) } \boldsymbol{u}_3 = \boldsymbol{u}_1.$$

In the first case, the shock becomes sonic. Since $\boldsymbol{l}_k(\boldsymbol{u}_3)(\boldsymbol{u}_3 - \boldsymbol{u}_k(\xi)) \neq \boldsymbol{0}$ holds, this state does not correspond to a point of secondary bifurcation. Then we can continue with a rarefaction curve $\mathcal{R}_k(\boldsymbol{u}_3)$ which is justified by (3.20). This procedure is in complete analogy to the situation where we change from the shock curve to the rarefaction curve $\mathcal{R}_k(\boldsymbol{u}_0)$. The second case occurs when we approach the state $\boldsymbol{u}_3$ which is connected to $\boldsymbol{u}_1 = \boldsymbol{u}_k(\xi_0) \in \mathcal{R}_k(\boldsymbol{u}_1)$ by a shock. Then we have to continue the k–curve by the shock curve $\mathcal{H}_k(\boldsymbol{u}_0)$, because $\boldsymbol{u}_3 \in \mathcal{H}_k(\boldsymbol{u}_0)$.

In principle, the k–curve construction is completed by the above procedure which might have to be repeated. All possible combinations of connections have been described.

3.4 Wave Construction

By now we only derived the Riemann solution in the admissible phase space. Finally we need to explain how to transfer it to the time–space continuum. Since the solution of (3.1), (3.6) is scale–invariant, the k–curves in the phase space can be transferred to the t–x plane identifying the parameter ξ with the ratio x/t. Here, we only consider the elementary waves. This suffices, since the k–waves are separated in the t–x plane according to the strict hyperbolicity of the underlying equations. The overall solution can be determined by composing the solutions of *all* k–waves. For the Euler equations we graphically present the different configurations in Sec. 4.3.

First we consider the case where the state $\boldsymbol{u}_0$ is connected to another state $\boldsymbol{u} \in \mathcal{H}_k(\boldsymbol{u}_0)$ on either a shock curve or a contact discontinuity. The corresponding solution in the t–x plane reads

$$\boldsymbol{u}(t,x) = \begin{cases} \boldsymbol{u}_0 & , \quad x/t < \sigma_k(\boldsymbol{u}_0, \boldsymbol{u}) \\ \boldsymbol{u} & , \quad \sigma_k(\boldsymbol{u}_0, \boldsymbol{u}) < x/t \end{cases} \tag{3.31}$$

where the speed of the discontinuity $\sigma_k(\boldsymbol{u}_0, \boldsymbol{u})$ satisfies (3.15) or (3.17), respectively. If $\boldsymbol{u}_0$ is connected to $\boldsymbol{u} \in \mathcal{R}_k(\boldsymbol{u}_0)$ by a rarefaction curve, then the solution is given by

$$\boldsymbol{u}(t,x) = \begin{cases} \boldsymbol{u}_0 & , \quad x/t < \lambda_k(\boldsymbol{u}_0) \\ \boldsymbol{u}_k(x/t) & , \quad \lambda_k(\boldsymbol{u}_0) < x/t < \lambda_k(\boldsymbol{u}) \\ \boldsymbol{u} & , \quad \lambda_k(\boldsymbol{u}) < x/t \end{cases} \tag{3.32}$$

where, in particular,

$$\boldsymbol{u}_0 = \lim_{x/t \to \lambda_k(\boldsymbol{u}_0)} \boldsymbol{u}_k(x/t), \quad \boldsymbol{u} = \lim_{x/t \to \lambda_k(\boldsymbol{u})} \boldsymbol{u}_k(x/t).$$

If the k–field is genuinely nonlinear then the k–wave is given by either the shock wave (3.31) or the rarefaction wave (3.32). However, if the nonlinear k–field degenerates, then the wave structure becomes more complicate. First we consider the case where $\boldsymbol{u}_0$ is connected to $\boldsymbol{u} \in \mathcal{C}(\mathcal{R}_k, \boldsymbol{u}_0)$ by a mixed curve. Then we have to determine $\boldsymbol{u}^* \in \mathcal{R}_k(\boldsymbol{u}_0)$ such that (3.25) holds. The solution now reads

$$\boldsymbol{u}(t,x) = \begin{cases} \boldsymbol{u}_0 & , \quad x/t < \lambda_k(\boldsymbol{u}_0) \\ \boldsymbol{u}_k(x/t) & , \quad \lambda_k(\boldsymbol{u}_0) < x/t < \lambda_k(\boldsymbol{u}^*) \\ \boldsymbol{u} & , \quad \lambda_k(\boldsymbol{u}^*) < x/t \end{cases} . \tag{3.33}$$

In contrast to (3.32), the solution is no longer continuous in $x/t = \lambda_k(\boldsymbol{u}^*)$, i.e.,

$$\boldsymbol{u}^* = \lim_{x/t \to \lambda_k(\boldsymbol{u}^*)} \boldsymbol{u}_k(x/t) \neq \boldsymbol{u}.$$

As discussed in Sec. 3.3, there exist two different cases where the mixed curve $\mathcal{C}(\mathcal{R}_k, \boldsymbol{u}_0)$ stops and is to be continued by a rarefaction curve $\mathcal{R}_k(\overline{\boldsymbol{u}}_0)$ or a shock curve $\mathcal{H}_k(\overline{\boldsymbol{u}}_0)$, respectively. For the first case, the corresponding wave reads

$$\boldsymbol{u}(t,x) = \begin{cases} \boldsymbol{u}_0 & , \quad x/t < \lambda_k(\boldsymbol{u}_0) \\ \boldsymbol{u}_k(x/t) & , \quad \lambda_k(\boldsymbol{u}_0) < x/t < \lambda_k(\overline{\boldsymbol{u}}) \\ \overline{\boldsymbol{u}}_k(x/t) & , \quad \lambda_k(\overline{\boldsymbol{u}}) < x/t < \lambda_k(\boldsymbol{u}) \\ \boldsymbol{u} & , \quad \lambda_k(\boldsymbol{u}) < x/t \end{cases} \tag{3.34}$$

with $\boldsymbol{u}_k \in \mathcal{R}_k(\boldsymbol{u}_0)$ and $\overline{\boldsymbol{u}}_k \in \mathcal{R}_k(\overline{\boldsymbol{u}}_0)$. In the second case, i.e., $\boldsymbol{u} \in \mathcal{H}_k(\overline{\boldsymbol{u}}_0)$, the wave is given by

$$\boldsymbol{u}(t,x) = \begin{cases} \boldsymbol{u}_0 & , \quad x/t < \sigma_k(\overline{\boldsymbol{u}}_0, \boldsymbol{u}) \\ \boldsymbol{u} & , \quad \sigma_k(\overline{\boldsymbol{u}}_0, \boldsymbol{u}) < x/t \end{cases} . \tag{3.35}$$

Since the k–curve may be composed of several parts of shock curves, rarefaction curves and mixed curves the above procedure might be repeated where we start from the state $\boldsymbol{u}$. We are allowed to do this, since the corresponding characteristic velocities are non–decreasing and the shock speeds are non–increasing. This implies that the different parts of the wave do not overlap which is related to the uniqueness of the Riemann problem.

4 The Riemann Problem for the Euler Equations

Based on the general construction principles, we now present a Riemann solver for the Euler equations for fluids with non–convex EOS. This is based on general techniques that also fit to strictly hyperbolic systems of conservation laws which we have summarized in the previous section. Here we proceed analogously.

4.1 Governing Equations

Whenever the flow exhibits planar symmetry it is one dimensional. Then the fluid equations (1.1) — neglecting viscosity and heat conduction — reduce to

$$\begin{aligned} \rho_t \quad &+ \quad (\rho u)_x = 0, \\ (\rho u)_t \quad &+ \quad (\rho u^2 + p)_x = 0, \\ (\rho E)_t \quad &+ \quad (\rho u(E + p/\rho))_x = 0, \end{aligned} \tag{4.1}$$

provided that the symmetry plane is perpendicular to the x axis and u is the corresponding velocity component. Moreover, the equilibrium pressure is defined by the EOS $p = p(v, e)$ which is supposed to be thermodynamically consistent (see Sec. 2).

Obviously, the resulting equations can be written in the form (3.1) with the conservative quantities $\boldsymbol{u} = (\rho, \rho u, \rho E)^T$ and the flux $\boldsymbol{f}(\boldsymbol{u}) = (\rho u, \rho u^2 + p, \rho u(E + p/\rho))^T$. The characteristic velocities, i.e., the eigenvalues of the Jacobian of $\boldsymbol{f}$, are given by

$$\lambda_k(\boldsymbol{u}) = u + \varepsilon_k c \quad \text{with} \quad \varepsilon_k := k - 2, \qquad k = 1, 2, 3$$

and the corresponding nonlinearity factors read

$$\alpha_k(\boldsymbol{u}) = \nabla_{\boldsymbol{u}} \lambda_k(\boldsymbol{u})\, \boldsymbol{r}_k(\boldsymbol{u}) = \varepsilon_k \mathcal{G} c / v, \qquad k = 1, 2, 3 \tag{4.2}$$

where $\boldsymbol{r}_k$ denotes the right eigenvector to λ_k. The structure of the associated k–field is determined by α_k. Here, the 2–field is linearly degenerated, whereas the k–fields, $k = 1, 3$, are nonlinear. In particular, the nonlinear fields are essentially influenced by the fundamental derivative of gas dynamics $\mathcal{G}$, since it may degenerate in zeros of $\mathcal{G}$. These states are known to exist in the phase space and arise in non–convex EOS (see Sec. 2). According to Fig. 3 we suppose that $\mathcal{G}$ only vanishes at isolated states of an isentrope. These states build a twodimensional hypersurface $\mathcal{M} \subset \mathcal{D}$ which is composed of all inflection points of the isentropes in the p–v plane, i.e., $p_{vv}(v, s) = 0$, $p_{vvv}(v, s) \neq 0$. This hypersurface separates subdomains $\mathcal{D}^-$, $\mathcal{D}^+ \subset \mathcal{D}$, $\mathcal{D}^+ \cap \mathcal{D}^- = \emptyset$ such that $\alpha_k|_{\mathcal{D}^-} < 0$, $\alpha_k|_{\mathcal{D}^+} > 0$ and $\alpha_k|_{\mathcal{M}} = 0$. In addition, we know that the nonlinear fields are simply degenerated at states of $\mathcal{M}$, since

$$\beta_k(\boldsymbol{u}) = \nabla_{\boldsymbol{u}} \alpha_k(\boldsymbol{u})\, \boldsymbol{r}_k(\boldsymbol{u}) = -\alpha_k(\boldsymbol{u}) - \frac{v^2}{2\,c} p_{vvv}(v, s) \neq 0 \quad \forall\, \boldsymbol{u} \in \mathcal{M}.$$

Numerous investigations have been performed in the standard case of an ideal gas. There $\mathcal{G}$ is strictly positive and consequently the nonlinear fields do not degenerate. Deriving the Riemann solver, we will therefore focus on the construction of the mixed curves which come into play when $\mathcal{G}$ vanishes along a rarefaction curve. For completion we summarize the construction of rarefaction curves and shock curves. Moreover, we present and discuss to some extent the algorithmic realization. Here, the choice of parameterization will be of special interest. The pressure turns out to be appropriate. Finally, we determine the intermediate states in the phase space. This simplifies for the Euler equations, since the pressure and the velocity do not jump across a contact discontinuity. Therefore, it suffices to look for the intersection point of the nonlinear curves in the p–u plane.

4.2 Elementary Curves

In the following we derive the underlying equations by which the elementary curves are determined. In particular, we discuss the choice of an appropriate parameterization. Moreover, we present useful representations of the nonlinear problems by which the curves are defined. These are helpful for their discretization.

4.2.1 Rarefaction Curves

In principal, the rarefaction curve is determined by the IVP (3.7). To this end, the right eigenvectors of the Jacobian of the flux $\boldsymbol{f}$ have to be calculated. However, this is too cumbersome for the Euler equations (4.1). Instead, it is more convenient to rewrite these equations in terms of the primitive variables v, u, and e (see Sec. 7)

$$\begin{aligned} v_t + uv_x - vu_x &= 0, \\ u_t + vp_v(v,e)v_x + uu_x + vp_e(v,e)e_x &= 0, \\ e_t + vpu_x + ue_x &= 0. \end{aligned} \tag{4.3}$$

These equations are equivalent to the Euler equations in the smooth part of the solution. In particular, for inverting this transformation no assumptions concerning the sign of the partial derivatives $p_v(v,e)$ and $p_e(v,e)$ are necessary. We mention this since in many investigations equations for p and s, respectively, are used instead of e. However, the corresponding transformations impose some assumptions on these derivatives with regard to inverting the transformation.

In terms of the primitive variables, the ODEs (3.7) read

$$\frac{dv}{d\xi} = -\varepsilon_k \mathcal{G}^{-1}\frac{v}{c}, \quad \frac{du}{d\xi} = \mathcal{G}^{-1}, \quad \frac{de}{d\xi} = \varepsilon_k \mathcal{G}^{-1}\frac{vp}{c} \tag{4.4}$$

which can be derived multiplying (3.7) with the Jacobian of the parameter transformation. Here, we use the parametrization $\xi = x/t$. By the fundamental derivative of gas dynamics (2.2), we furthermore conclude

$$T\frac{ds}{d\xi} = \frac{de}{d\xi} + p\frac{dv}{d\xi} = 0,$$

i.e., the entropy remains constant. This means that the rarefaction curve coincides with an isentrope in the p–v plane (see Fig. 3). Since $\mathcal{G}$ is supposed to vanish only at isolated zeros of an isentrope, the rarefaction curve can be continuously extended in these states.

In view of the Riemann solver, we are interested in the variation of characteristic velocities λ_k. These are related to the Lagrangian characteristic velocities $\overline{\lambda}_k$ by $\overline{\lambda}_k = (\lambda_k - u)/v = \varepsilon_k c/v$ and there derivatives are given by

$$\frac{d\overline{\lambda}_k}{d\xi} = \varepsilon_k^2 \frac{1}{v},$$

i.e., $\overline{\lambda}_k,\ k = 1, 3$, is strictly monotonically decreasing.

In order to remove the singularities in (4.4), we want to change the parameterization. For this purpose, we consider the variation of the pressure which is determined by

$$\frac{dp}{d\xi} = \varepsilon_k \mathcal{G}^{-1} \frac{c}{v} = \frac{\overline{\lambda}_k}{\mathcal{G}} \tag{4.5}$$

according to the EOS. Obviously, p is strictly monotone as long as the fundamental derivative does not vanish. We will see later that the rarefaction curve is not admissible throughout the whole range of definition (see Sec. 4.3). Starting from a state $\boldsymbol{u}_0 \in \mathcal{D}$ with $\mathcal{G}_0 \neq 0$, only the branch of the rarefaction curve with increasing parameter $\xi = x/t$ is admissible. This branch on the isentrope is bounded by the first zero of $\mathcal{G}$ in this direction. Therefore, we can use p or a reparametrization of p as integration parameter instead of ξ along the admissible branch. Then the derivatives with respect to an arbitrary parameter β read

$$\frac{dv}{d\beta} = -\frac{1}{\overline{\lambda}_k^2}\frac{dp}{d\beta}, \quad \frac{du}{d\beta} = \frac{1}{\overline{\lambda}_k}\frac{dp}{d\beta}, \quad \frac{de}{d\beta} = \frac{p}{\overline{\lambda}_k^2}\frac{dp}{d\beta}, \quad \frac{d\overline{\lambda}_k}{d\beta} = \frac{\mathcal{G}}{v\,\overline{\lambda}_k}\frac{dp}{d\beta}. \tag{4.6}$$

Finally, we summarize the basic results in

Proposition 4.1 *Along the rarefaction curve the following statements hold:*

a) The entropy is constant, i.e., an isentrope in the p–v plane coincides with a rarefaction curve;

b) the following quantities are strictly monotone except at states where the nonlinear field degenerates: the pressure p, the specific volume v, the velocity u, the specific internal energy e and the characteristic velocity $\overline{\lambda}_k$.

We want to point out that the notion *rarefaction* might be confusing in the context of the Euler equations with non–convex EOS. In the standard case of convex isentropes, the admissible branch corresponds to the *expansive* part where the specific volume increases and the pressure decreases. In the non–convex case, this is reversed, i.e., the *compressive* branch is only admissible. In order to avoid misunderstandings we therefore specify the *admissible* branch of the rarefaction curve by *expansive* or *compressive*.

4.2.2 Shock Curves and Contact Discontinuities

Discontinuities are characterized by the *Rankine–Hugoniot (RH) jump conditions*

$$\sigma\Delta\rho = \Delta(\rho u), \quad \sigma\Delta(\rho u) = \Delta(\rho u^2 + p), \quad \sigma\Delta(\rho E) = \Delta(\rho u(E + p/\rho)),$$

where we use the notation $\Delta A = A - A_0$ for an arbitrary quantity A. The Eulerian shock speed is denoted by σ. Introducing the relative velocity $\tilde{u} := u - \sigma$ the RH conditions can be written as

$$\Delta(\rho\tilde{u}) = 0, \quad \Delta(\rho\tilde{u}^2 + p) = 0, \quad \Delta(\rho\tilde{u}(e + p/\rho + \tilde{u}^2/2)) = 0.$$

Applying the Leibnitz rule $\Delta(AB) = \hat{A}\Delta B + \hat{B}\Delta A$ with the average $\hat{A} := (A + A_0)/2$, these equations can be transformed into the *Lagrangian jump conditions*

$$-\overline{\sigma}\Delta v - \Delta u = 0, \quad -\overline{\sigma}\Delta u + \Delta p = 0, \quad -\overline{\sigma}\Delta E + \Delta(up) = 0, \tag{4.7}$$

where $\overline{\sigma}$ is the Lagrangian shock speed. These relations correspond to the Lagrangian equations formally determined by the vector $\overline{\boldsymbol{u}} = (v, u, E)^T$ and the flux $\overline{\boldsymbol{f}}(\overline{\boldsymbol{u}}) = (-u, p, u)^T$ which result when rewriting the Euler equations in Lagrangian coordinates (see Sec. 7). In order to distinguish between quantities such as eigenvalues, shock speed and eigenvectors corresponding to the Eulerian and the Lagrangian formulation, respectively, we label the latter by a bar. For the Laplacian fluid equations the characteristic velocities read

$$\overline{\lambda}_k(\overline{\boldsymbol{u}}) = \varepsilon_k c/v, \ k = 1, 2, 3. \tag{4.8}$$

Obviously, the Eulerian shock speed σ, the Lagrangian shock speed $\overline{\sigma}$ and the relative velocity $\tilde{u}$ are related by

$$\overline{\sigma} = -\rho\tilde{u} = -\rho(u - \sigma) = -\rho(u_0 - \sigma).$$

In the following we distinguish between two cases. If $\overline{\sigma} = 0 = \overline{\lambda}_2$, then the discontinuity is a contact discontinuity. This is characterized by

$$\overline{\sigma} = 0 \Longleftrightarrow \rho\tilde{u} = 0 \Longleftrightarrow \rho(u - \sigma) = 0 \Longleftrightarrow \sigma = u = \lambda_2$$

from which we conclude

$$\Delta u = 0, \ \Delta p = 0.$$

These relations will simplify the solution of the Riemann problem, since we can project the phase space to the p–u plane.

The second case is related to $\overline{\sigma} \neq 0$ which is supposed to hold for the remaining part of this subsection. Then the Lagrangian conditions can be written in the form

$$\overline{\sigma}^2 = -\frac{\Delta p}{\Delta v}, \quad \Delta u = \frac{1}{\overline{\sigma}}\Delta p, \quad \Delta e + \hat{p}\Delta v = 0. \tag{4.9}$$

The convexity of the energy $e = e(v, s)$ implies $\Delta p \Delta v \leq 0$ where " $=$ " holds if and only if $p = p_0$ or $v = v_0$ or $\gamma = 0$, i.e., the state $\boldsymbol{u}_0$ coincides with the critical point (see [MP89], p. 91). Therefore $\overline{\sigma}^2$ is positive and there exist two shock curves $\mathcal{H}_k(\boldsymbol{u}_0)$ corresponding to $\overline{\sigma}_k = \varepsilon_k\sqrt{-\Delta p/\Delta v}, \ k = 1, 3$.

The implicit function theorem implies the existence of a smooth shock curve in a neighborhood of a zero $\overline{\boldsymbol{u}} \in \mathcal{D}$ of (4.9) except for points of primary and secondary bifurcation corresponding to (3.12). In the case of primary bifurcation two branches are known to exist [Lax57]. Whereas secondary bifurcation only occurs if (3.12 b) holds. These relations are equivalent to

$$1 + \gamma\frac{\Delta v}{\Delta p}\frac{p}{v} = 0, \quad 1 + \frac{\Gamma}{2}\frac{\Delta v}{v} = 0 \tag{4.10}$$

which have been derived in [Wen72b]. They imply

$$\overline{\sigma}_k^2 = \gamma p/v = c^2/v^2 = \overline{\lambda}_k^2, \quad \gamma = 0.5\Gamma\Delta p/p,$$

from which we conclude that secondary bifurcation can only occur in the case of sonic shocks. However, in fluids flow of real materials this never seems to be satisfied (see [MP89], p. 122) and we therefore exclude states satisfying (4.10). This is in agreement with condition (3.13).

In order to determine the shock curve, it is useful to introduce the shock adiabatic or Hugoniot curve of states (v, e) such that

$$h(v, e) := e - e_0 + 0.5(p + p_0)(v - v_0) = 0. \tag{4.11}$$

The zero–set is a projection of the shock curve in the v–u–e space into the v–e plane. It is characterized by

Proposition 4.2 *Let be (v, e) a zero of (4.11). Then there exists a neighborhood of (v, e) where the Hugoniot locus is a one parameter family of states which can be parametrized by v or e, respectively, provided that*

$$1 + \frac{\Gamma}{2}\frac{\Delta v}{v} \neq 0 \quad or \quad 1 + \frac{\Gamma}{2}\frac{\Delta v}{v} \neq \frac{\Delta p}{p}\left(1 + \gamma \frac{\Delta v}{\Delta p}\frac{p}{v}\right)$$

hold. Furthermore, there exists no point of bifurcation, if we exclude points satisfying (4.10).

Proof: The starting point are the partial derivatives of (4.11) given by

$$h_e = k_p \quad \text{and} \quad h_v = p\, k_p - \frac{1}{2}\Delta v \left(\overline{\lambda}_k^2 - \overline{\sigma}_k^2\right) = \frac{p}{\gamma}\left(k_v - \frac{1}{2}\frac{\Delta v}{p}\left(\overline{\lambda}_k^2 - \overline{\sigma}_k^2\right)(\gamma - \Gamma)\right), \quad (4.12)$$

where the coefficients k_v and k_p are defined by

$$k_p := 1 + \frac{\Gamma}{2}\frac{\Delta v}{v}, \qquad k_v := \gamma - \frac{\Gamma}{2}\frac{\Delta p}{p}. \quad (4.13)$$

Here we make use of the equations (2.21) and incorporate the relations $\overline{\lambda}_k^2 = \gamma p/v = pp_e - p_v$ as well as $\overline{\sigma}_k^2 = -\Delta p/\Delta v$. Then the assertion follows by the implicit function theorem. □

In the subsequent investigation, those states are of special interest for which the shock speed $\overline{\sigma}_k$ and the characteristic velocity $\overline{\lambda}_k$ coincide. For the Hugoniot curve the following results hold.

Proposition 4.3 *Let be (v, e) a zero of (4.11) such that $\overline{\lambda}_k(\overline{\boldsymbol{u}}) = \overline{\sigma}_k(\overline{\boldsymbol{u}}_0, \overline{\boldsymbol{u}})$ and $\gamma \neq 0.5\,\Gamma\Delta p/p$. Then we conclude*

a) $h_v = \frac{p}{\gamma}\left(\gamma - \frac{\Gamma}{2}\frac{\Delta p}{p}\right) = p\, h_e \neq 0,$

b) $\frac{dp}{dv} = -\overline{\lambda}_k^2(\overline{\boldsymbol{u}}) \neq 0, \quad \frac{dp}{de} = \frac{\overline{\lambda}_k^2(\overline{\boldsymbol{u}})}{p} \neq 0.$

Proof: Incorporating the assumptions into (4.12) we immediately obtain a). In order to verify b), we take the derivatives of the EOS (2.21) and the Hugoniot curve (4.11) with respect to v and e, respectively. From these derivatives we determine

$$\frac{dp}{dv} = p_v + p_e\frac{de}{dv} = -\frac{k_v}{\gamma\, k_p}\overline{\lambda}_k^2 \quad \text{and} \quad \frac{dp}{de} = p_v\frac{de}{dv} + p_e = \frac{\overline{\lambda}_k^2 k_p - \frac{\Gamma}{2}\frac{\Delta v}{v}\left(\overline{\lambda}_k^2 - \overline{\sigma}_k^2\right)}{p\, k_p - \frac{1}{2}\Delta v\left(\overline{\lambda}_k^2 - \overline{\sigma}_k^2\right)},$$

respectively. Obviously, these relations imply assertion b). □

Except for the bifurcation points, the Hugoniot curve is a smooth curve which we will examine in some detail. Here we are particularly interested in aspects with regard to the algorithmic realization. To this end, we recall some well–known analytical results for the convenience of the reader. These are partially derived in [Bet42, Wey49, Wen72b, Liu75, MP89] among others. In the sequel, we consider the following items more carefully

1.) derivatives of certain physical quantities with respect to the shock curve parameter,

2.) the correlation between shock speed and characteristic velocity,

3.) the existence of a sonic shock,

4.) local and global admissibility criteria,

5.) physical constraints to be imposed on the EOS.

Derivatives of Physical Quantities

In order to determine an appropriate parameterization as well as to characterize the admissible branch of the shock curve we need to know how certain physical quantities vary along the shock curve. To this end, we determine the derivatives with respect to an *arbitrary shock curve parameter* α. We emphasize that this parameter is not necessarily the time–space ration t/x as is chosen for the rarefaction curve. First of all, we conclude from the Hugoniot curve (4.11) and the EOS (2.15) the relation

$$k_p \frac{dp}{d\alpha} = -k_v \frac{p}{v} \frac{dv}{d\alpha}, \tag{4.14}$$

where we make use of the equations (2.21) which correlate the partial derivatives p_e and p_v with the dimensionless quantities γ and Γ. Moreover, we have to incorporate the relations $\overline{\lambda}_k^2 = c^2/v^2 = \gamma p/v = pp_e - p_v$ for the characteristic velocity and $\overline{\sigma}_k^2 = -\Delta p/\Delta v$ for the Langrangian shock speed. In all of the subsequent derivatives we will always make use of these relations.

In the sequel, we assume that k_v is positive. For a perfect gas it is known to hold. We will discuss later the constraints for a real gas arising from this assumption. Then we can resolve (4.14)

$$\frac{dv}{d\alpha} = -\frac{v}{p}\frac{k_p}{k_v}\frac{dp}{d\alpha} = -\frac{k_p}{\overline{\lambda}_k^2 k_p + \frac{\Gamma}{2}\frac{\Delta v}{v}(\overline{\sigma}_k^2 - \overline{\lambda}_k^2)}\frac{dp}{d\alpha}. \tag{4.15}$$

From the fundamental identity of gas dynamics (2.2) we furthermore derive

$$\frac{ds}{d\alpha} = \frac{1}{2T}\frac{v}{p}\frac{1}{k_v}\left(\overline{\lambda}_k^2 - \overline{\sigma}_k^2\right)\frac{\Delta p}{\overline{\sigma}_k^2}\frac{dp}{d\alpha}. \tag{4.16}$$

where we apply (4.11) and (4.15) and, in addition, make use of the definitions for the Lagrangian shock speed (4.9) and the characteristic velocity (4.8), respectively. With the aid of (4.15) and (4.16), we then conclude from the fundamental thermodynamic identity (2.2)

$$\frac{de}{d\alpha} = \frac{v}{p}\frac{1}{k_v}\left(pk_p - 0.5\,\Delta v(\overline{\lambda}_k^2 - \overline{\sigma}_k^2)\right)\frac{dp}{d\alpha}. \tag{4.17}$$

Alternatively, this can be obtained from (4.15) and the Hugoniot relation (4.11). Next, we determine the variation of the shock speed $\overline{\sigma}_k$ defined by (4.9)

$$\frac{d\overline{\sigma}_k}{d\alpha} = -\frac{1}{2}\frac{v}{p}\frac{\overline{\lambda}_k^2 - \overline{\sigma}_k^2}{\Delta v\, k_v}\frac{1}{\overline{\sigma}_k}\frac{dp}{d\alpha} = \frac{T}{(\Delta v)^2}\frac{1}{\overline{\sigma}_k}\frac{ds}{d\alpha} \tag{4.18}$$

where we apply (4.15) in the first part. The second representation immediately follows from (4.16). With the aid of (4.18) we conclude after some lengthy calculations

$$\frac{du}{d\alpha} = \frac{1}{2}\left(1 + \gamma\frac{k_p}{k_v}\frac{\overline{\sigma}_k^2}{\overline{\lambda}_k^2}\right)\frac{1}{\overline{\sigma}_k}\frac{dp}{d\alpha} = \frac{\gamma}{2\,k_v\overline{\lambda}_k^2}\left(\frac{(\gamma-\Gamma)p}{v} + \Gamma\frac{p_0}{v} + \overline{\sigma}_k^2\right)\frac{1}{\overline{\sigma}_k}\frac{dp}{d\alpha}. \tag{4.19}$$

Finally, we present the derivative of the characteristic velocity $\overline{\lambda}_k$ along the shock curve. To this end, we derive the relation $\overline{\lambda}_k^2 = pp_e - p_v$ with respect to the shock curve parameter α. Incorporating the fundamental thermodynamic identity (2.2) as well as (2.17) with $f = p$, we end up with

$$\frac{d\overline{\lambda}_k}{d\alpha} = -\frac{1}{2\,\overline{\lambda}_k}\left(p_{vv}(v,s)\frac{dv}{d\alpha} + p_{vs}(v,s)\frac{ds}{d\alpha}\right) = -\mathcal{G}\frac{\overline{\lambda}_k}{v}\frac{dv}{d\alpha} - \frac{p_{vs}(v,s)}{2\,\overline{\lambda}_k}\frac{ds}{d\alpha} \tag{4.20}$$

with

$$p_{vs}(v,s) = -\left(p_e^2(v,e) + pp_{ee}(v,e) - p_{ve}(v,e)\right)T.$$

The derivatives which have just been derived are of particular interest at states $\boldsymbol{u}$ of the shock curve $\mathcal{H}_k(\boldsymbol{u}_0)$ where the shock speed and the characteristic velocity coincide.

Proposition 4.4 *Assume that k_v is positive. Let be $\boldsymbol{u} \in \mathcal{H}_k(\boldsymbol{u}_0)$ such that $\overline{\lambda}_k(\overline{\boldsymbol{u}}) = \overline{\sigma}_k(\overline{\boldsymbol{u}}_0, \overline{\boldsymbol{u}})$. Then the following statements hold:*

a) The derivatives at $\boldsymbol{u}$ are given by

$$\frac{dv}{d\alpha} = -\frac{1}{\overline{\lambda}_k^2}\frac{dp}{d\alpha}, \quad \frac{du}{d\alpha} = \frac{1}{\overline{\lambda}_k}\frac{dp}{d\alpha}, \quad \frac{de}{d\alpha} = \frac{p}{\overline{\lambda}_k^2}\frac{dp}{d\alpha}, \quad \frac{ds}{d\alpha} = 0 \qquad \textit{and}$$

$$\frac{d\overline{\lambda}_k}{d\alpha} = \frac{\mathcal{G}}{v\,\overline{\lambda}_k}\frac{dp}{d\alpha} = \overline{\alpha}_k(\overline{\boldsymbol{u}})\frac{1}{\overline{\lambda}_k^2}\frac{dp}{d\alpha};$$

b) the shock curve $\mathcal{H}_k(\boldsymbol{u})$ is tangent to the rarefaction curve $\mathcal{R}_k(\boldsymbol{u})$ at $\boldsymbol{u}$. In particular, we obtain for the Euler equations in Lagrangian coordinates

$$\frac{d\overline{\boldsymbol{u}}}{d\alpha} = \overline{\boldsymbol{r}}_k(\overline{\boldsymbol{u}})\frac{1}{\overline{\lambda}_k^2}\frac{dp}{d\alpha}. \tag{4.21}$$

The relations in a) immediately result from (4.15), (4.19), (4.17), (4.16) and (4.20). In the latter case, we also apply (4.2). Then assertion b) can obviously be concluded comparing the relations in a) with those in (4.6). We want to remark that (4.21) even holds for general systems if we choose the parametrization $dp/d\alpha = \overline{\lambda}_k^2$ at $\boldsymbol{u}_0$ (cf. Prop. 3.2, (3.16)), for instance $\alpha = -e$.

Shock Speed and Characteristic Velocity

The connection between the characteristic velocity $\overline{\lambda}_k$ and the shock speed $\overline{\sigma}_k$ is of special interest in the construction of the Riemann solver. With the aid of the previous discussion concerning the derivatives along the shock curve we are now able to prove

Proposition 4.5 *Assume that k_v is positive. Let be $\boldsymbol{u} \in \mathcal{H}_k(\boldsymbol{u}_0)$ such that $\overline{\lambda}_k(\overline{\boldsymbol{u}}) = \overline{\sigma}_k(\overline{\boldsymbol{u}}_0, \overline{\boldsymbol{u}})$. Then the following statements hold:*

a) $\overline{\sigma}_k(\overline{\boldsymbol{u}}_0, \overline{\boldsymbol{u}}_0) = \overline{\lambda}_k(\overline{\boldsymbol{u}}_0)$;

b) *If* $\boldsymbol{u} = \boldsymbol{u}_0$, *then the derivative of the shock speed at this state is given by*

$$\frac{d\overline{\sigma}_k}{d\alpha} = \frac{1}{2\,\overline{\lambda}_k^2(\overline{\boldsymbol{u}}_0)}\overline{\alpha}_k(\overline{\boldsymbol{u}}_0)\frac{dp}{d\alpha} = \frac{1}{2}\frac{d\overline{\lambda}_k}{d\alpha} \quad \textit{and elsewhere by} \quad \frac{d\overline{\sigma}_k}{d\alpha} = 0;$$

In addition, one has $d\overline{\sigma}_k/d\alpha \neq 0$ *provided that* $\mathcal{G}_0 \neq 0$;

c) *If* $\boldsymbol{u} \neq \boldsymbol{u}_0$, *then* $d\overline{\sigma}_k/d\alpha = 0$ *if and only if* $\overline{\sigma}_k(\overline{\boldsymbol{u}}_0, \overline{\boldsymbol{u}}) = \overline{\lambda}_k(\overline{\boldsymbol{u}})$;

d) *If* $\boldsymbol{u} \neq \boldsymbol{u}_0$, *then the entropy* s *becomes extremal, if and only if the shock speed* $\overline{\sigma}_k$ *becomes extremal.*

Proof: For simplicity of notation we denote the derivative with respect to the shock curve parameter α by a prime. Furthermore, the origin $\boldsymbol{u}_0$ of the shock curve corresponds to the parameter value α_0. In order to prove assertion a) and b), respectively, we need to consider the limit $\alpha \to \alpha_0$ of certain ratios where the nominator as well as the denominator tend to zero.

a) The shock speed $\overline{\sigma}_k$ can be written as

$$\overline{\sigma}_k = \varepsilon_k \left(-\frac{p(\alpha) - p(\alpha_0)}{v(\alpha) - v(\alpha_0)}\right)^{1/2} = \varepsilon_k \left(-\frac{p'(\alpha_p)(\alpha - \alpha_0)}{v'(\alpha_v)(\alpha - \alpha_0)}\right)^{1/2}$$

where $\alpha_p,\ \alpha_v \in (\alpha_0, \alpha)$ denote certain intermediate parameter values. For $\alpha \to \alpha_0$ the derivatives tend to $p'(\alpha_0)$ and $v'(\alpha_0) = -p'(\alpha_0)/\overline{\lambda}_k^2(\overline{\boldsymbol{u}}_0)$, respectively, where we apply (4.14) and (4.15). This immediately implies the assertion.

b) Using the notation $\overline{\lambda}_k(\alpha) := \overline{\lambda}_k(\overline{\boldsymbol{u}}(\alpha))$, $\overline{\sigma}_k(\alpha) := \overline{\sigma}_k(\overline{\boldsymbol{u}}_0, \overline{\boldsymbol{u}}(\alpha))$, we notice that

$$\overline{\lambda}_k(\alpha) - \overline{\sigma}_k(\alpha) = \overline{\lambda}_k(\alpha) - \overline{\lambda}_k(\alpha_0) + \overline{\sigma}_k(\alpha_0) - \overline{\sigma}_k(\alpha),$$

since a) holds. Next, we observe that the limits

$$\begin{aligned}
\lim_{\alpha\to\alpha_0} \frac{\overline{\lambda}_k(\alpha) - \overline{\lambda}_k(\alpha_0)}{v(\alpha) - v_k(\alpha_0)} &= \lim_{\alpha\to\alpha_0} \frac{\overline{\lambda}'_k(\alpha_{\overline{\lambda}})(\alpha - \alpha_0)}{v'(\alpha_v)(\alpha - \alpha_0)} = -\frac{p_{vv}(v_0, s_0)}{2\,\overline{\lambda}_k(\alpha_0)}, \\
\lim_{\alpha\to\alpha_0} \frac{\overline{\sigma}_k(\alpha) - \overline{\sigma}_k(\alpha_0)}{v(\alpha) - v_k(\alpha_0)} &= \lim_{\alpha\to\alpha_0} \frac{\overline{\sigma}'_k(\alpha_{\overline{\sigma}})(\alpha - \alpha_0)}{v'(\alpha_v)(\alpha - \alpha_0)} = -\frac{\overline{\sigma}'_k(\alpha_{\overline{\sigma}})}{p'(\alpha_0)}\overline{\lambda}_k^2(\alpha_0)
\end{aligned}$$

hold. We now incorporate these limits as well as assertion a) when performing the limiting process in the first relation of (4.18):

$$\begin{aligned}
\overline{\sigma}'_k(\alpha_0) &= \frac{1}{2\,\overline{\lambda}_k^2(\alpha_0)}\left(\frac{p_{vv}(v_0, s_0)}{2\,\overline{\lambda}_k(\alpha_0)} - \frac{\overline{\sigma}'_k(\alpha_0)}{p'(\alpha_0)}\overline{\lambda}_k^2(\alpha_0)\right)\frac{\overline{\lambda}_k(\alpha_0) + \overline{\sigma}_k(\alpha_0)}{\overline{\sigma}_k(\alpha_0)}p'(\alpha_0) \\
&= \frac{p_{vv}(v_0, s_0)}{2\,\overline{\lambda}_k(\alpha_0)}\frac{p'(\alpha_0)}{\overline{\lambda}_k^2(\alpha_0)} - \overline{\sigma}'_k(\alpha_0).
\end{aligned}$$

From this relation the assertion immediately follows upon using (2.14) and (4.2). Moreover, $d\overline{\sigma}_k/d\alpha \neq 0$ since $\mathcal{G}_0 \neq 0$ is assumed to hold and $dp/d\alpha \neq 0$ because of Prop. 4.3.

c), d) These assertions can be concluded from (4.18) and (4.16), respectively. Here, the assumption of thermodynamic stability is essential. This requires the entropy to be a concave function of the specific volume v and the specific internal energy e. □

Finally, we want to remark that the relations $\overline{\sigma}_k(\alpha_0) = \overline{\lambda}_k(\alpha_0)$ and $\overline{\sigma}'_k(\alpha_0) = 0.5\,\overline{\lambda}'_k(\alpha_0)$ even hold for general systems (cf. [Liu75]).

Existence of Sonic Shocks

Up to now, we have characterized shocks where the shock speed becomes sonic. We now want to investigate under which circumstances there exists a sonic shock. The following proposition states that a necessary condition is that the nonlinear field degenerates along the shock curve.

Proposition 4.6 *Let be $\boldsymbol{u} \in \mathcal{H}_k(\boldsymbol{u}_0)$, $\boldsymbol{u} \neq \boldsymbol{u}_0$, such that $\overline{\lambda}_k(\overline{\boldsymbol{u}}) = \overline{\sigma}_k(\overline{\boldsymbol{u}}_0, \overline{\boldsymbol{u}})$. Then there exists a state $\tilde{\boldsymbol{u}} \in \mathcal{H}_k(\boldsymbol{u}_0)$ between $\boldsymbol{u}_0$ and $\boldsymbol{u}$ where the nonlinear field degenerates.*

This proposition implies that there exists no sonic shock for a genuinely nonlinear field, which also holds for general systems. The proof is similar to that sketched for Prop. 3.4. Since we are dealing with a special system the proof simplifies and can be given in full.
Proof: For simplicity we assume that $\boldsymbol{u}$ is the first state on the shock curve $\mathcal{H}_k(\boldsymbol{u}_0)$ where the shock becomes sonic. Then we conclude from (4.16) and (4.18) that the shock speed $\overline{\sigma}_k$ varies monotonically between $\boldsymbol{u}_0$ and $\boldsymbol{u}$. Furthermore, we know from Prop. 4.5 b) that the derivative of $\overline{\sigma}_k$ is only half of the derivative of $\overline{\lambda}_k$ at $\boldsymbol{u}_0$ where, in addition, $\overline{\lambda}_k$ and $\overline{\sigma}_k$ coincide. Then there exist two possible situations depending on the sign of the derivatives at $\boldsymbol{u}_0$. One of the two situations is sketched in Fig. 8. From this we conclude that the sign of $\overline{\lambda}_k'(\overline{\boldsymbol{u}}_0)$ is different from that of $\overline{\lambda}_k'(\overline{\boldsymbol{u}})$. Together with Prop. 4.4 a) this implies that also $\overline{\alpha}_k(\overline{\boldsymbol{u}}_0)$ and $\overline{\alpha}_k(\overline{\boldsymbol{u}})$ differ in sign. Hence, there exists a state $\tilde{\boldsymbol{u}} \in \mathcal{H}_k(\boldsymbol{u}_0)$ between $\boldsymbol{u}_0$ and $\boldsymbol{u}$ where α_k changes its sign, i.e., $\overline{\alpha}_k(\tilde{\boldsymbol{u}}) = 0$. □

Admissibility of Shock Curves

Although (4.14) holds along the whole Hugoniot curve, we are only interested in the admissible part. In order to determine the admissible branch, we consider the jump in entropy in terms of the pressure jump. This is locally given by

$$\Delta s = \frac{1}{12} T_0 p_{vv}(v_0, s_0)(\Delta p)^3 + \mathcal{O}\left((\Delta p)^4\right)$$

(see [Tho72], p. 318). Since the second law of thermodynamics has to be satisfied, the pressure needs to increase when the isentrope is convex. Moreover, density also increases because of (4.9). This is the standard case of a *compression shock*. In the non–convex part of the isentrope, however, the signs change and pressure as well as density decrease. Then the admissible Hugoniot curve corresponds to an *expansion shock*. Both cases can occur when applying a non–convex EOS. Hence, the admissible branch can be determined by the pressure variation in a neighborhood of the initial state $\boldsymbol{u}_0$.

According to the second law of thermodynamics, the entropy increases across the shock. Hence, the admissible part of the Hugoniot curve is characterized by $ds/d\alpha$ is greater or less than zero. Here we emphasize that the sign depends on the parameter choice. Since α is arbitrarily chosen, we cannot specify the sign. This implies that the pressure has to be monotone along the admissible branch. Moreover, Δp does not change sign, since otherwise the pressure would have become extremal before. Consequently, we can choose p as parameter of the admissible branch. This is the key result of the previous discussion.

In addition, the variation of the shock speed $\overline{\sigma}_k$ and the entropy s along a shock curve are directly related by (4.18). In analogy to the entropy, the shock speed varies monotonically along the admissible branch as is predicted by Liu's extended admissibility relations (3.19). It is extremal, if the shock becomes sonic. This coincides with the state where the second law of thermodynamics is violated marking the end of the admissible branch. Hence, we can use the variation of the shock speed as admissibility criterion of the shock. This is in agreement with the Lax jump conditions (3.17).

The main results of the previous discussion are summarized below.

Proposition 4.7 *Assume that k_v is positive. Then the following statements hold:*

a) The admissible branch of the shock curve $\mathcal{H}_k(\boldsymbol{u}_0)$ is characterized by

$$\begin{array}{lll} i)\ \mathcal{G}_0 > 0 & \Longrightarrow & \Delta p > 0,\ \Delta v < 0 \ \textit{(compression branch)}, \\ ii)\ \mathcal{G}_0 < 0 & \Longrightarrow & \Delta p < 0,\ \Delta v > 0 \ \textit{(expansive branch)}. \end{array}$$

b) Along the admissible branch of the shock curve $\mathcal{H}_k(\boldsymbol{u}_0)$ the pressure p, the entropy s and the shock speed $\overline{\sigma}_k$ are monotone; the velocity u is monotone provided that $0 \le \Gamma \le \gamma$.

Physical Constraints

Up to now, we have made the assumption that k_v is strictly positive. We will now derive sufficient conditions for the EOS. These lead to physical constraints with respect to the material for which the Riemann problem can be solved.

First of all, we notice that k_p and k_v are positive close to the initial state $\boldsymbol{u}_0$. Moreover, they do not vanish at the same state. This is only possible in states where secondary bifurcation occurs which are excluded in our investigations. Furthermore, these coefficients are related by

$$k_v = \gamma \left(1 + \frac{\Gamma}{2} \frac{\Delta v}{v} \frac{\overline{\sigma}_k^2}{\overline{\lambda}_k^2} \right) = \gamma \left(k_p + \frac{\Gamma}{2} \frac{\Delta v}{v} \left(\frac{\overline{\sigma}_k^2}{\overline{\lambda}_k^2} - 1 \right) \right). \tag{4.22}$$

If the shock is sonic, then this simplifies to $k_v = \gamma k_p$.

From the local behavior of the pressure we furthermore conclude that k_v is positive along the admissible branch provided that

$$0 < \Gamma \le 2\gamma. \tag{4.23}$$

This can be verified with the aid of Prop. 4.7 b). We emphasize that $\Gamma > 0$ is only required for the non–convex case. In the convex case $\Gamma \le 2\gamma$ is sufficient. This condition seems to be satisfied for all known materials. Moreover, it excludes secondary bifurcation (see [MP89], p. 97). For $p_v(v, e) < 0$ it can be proven to hold.

4.2.3 Mixed Curves

The rarefaction curve $\mathcal{R}_k(\boldsymbol{u}_0)$ is no longer admissible when it approaches a state $\hat{\boldsymbol{u}} \in \mathcal{D}$ where the nonlinear field degenerates, i.e., $\hat{\mathcal{G}} = 0$ (cf. (3.7), (4.4)). At this point we have to switch to the mixed curve. This curve is determined by the rarefaction curve and a family of shock curves, since it is composed of all states $\boldsymbol{u} \in \mathcal{H}_k(\boldsymbol{u}^*)$ where a state $\boldsymbol{u}^* \in \mathcal{R}_k(\boldsymbol{u}_0)$ exists such that $\sigma_k(\boldsymbol{u}, \boldsymbol{u}^*) = \lambda_k(\boldsymbol{u}^*)$. Moreover, $\boldsymbol{u} \ne \boldsymbol{u}^*$ is the first point on $\mathcal{H}_k(\boldsymbol{u}^*)$ where this equality holds. In Lagrangian coordinates these conditions are equivalent to

$$\begin{aligned} \overline{\boldsymbol{u}} \in \mathcal{H}_k(\overline{\boldsymbol{u}}^*) \Longleftrightarrow h(v, e) = 0 \quad &\Longleftrightarrow \quad e - e^* = -\frac{1}{2}(p + p^*)(v - v^*) \\ \overline{\sigma}_k^2(\overline{\boldsymbol{u}}^*, \overline{\boldsymbol{u}}) = \overline{\lambda}_k^2(\overline{\boldsymbol{u}}^*) \quad &\Longleftrightarrow \quad v - v^* = -(p - p^*)/\overline{\lambda}_k^2(\overline{\boldsymbol{u}}^*). \end{aligned} \tag{4.24}$$

In view of an algorithmic construction the definition which follows Liu's concept of the composite locus is not suitable. Instead, we derive a different construction based on solving an IVP. For this purpose, we consider the following items in some detail:

1.) characterization of the composite locus by a one parameter manifold,

2.) derivatives of certain physical quantities with respect to an arbitrary parametrization of the mixed curve and

3.) tangential connection of the rarefaction curve and mixed curve at $\boldsymbol{u} = \hat{\boldsymbol{u}}$.

Characterization of Composite Locus

The starting point are the conditions (4.24). Assuming that the rarefaction curve is parametrized by an arbitrary parameter β then these conditions can be rewritten as

$$h_1(v,e,\beta) := e - e_k - \frac{1}{2}\frac{p^2 - p_k^2}{\overline{\lambda}_k^2(\overline{\boldsymbol{u}}_k)} = 0, \qquad h_2(v,e,\beta) := v - v_k + \frac{p - p_k}{\overline{\lambda}_k^2(\overline{\boldsymbol{u}}_k)} = 0, \tag{4.25}$$

where the states $\overline{\boldsymbol{u}}^* = \overline{\boldsymbol{u}}_k = \overline{\boldsymbol{u}}_k(\beta)$ on the rarefaction curve are uniquely determined by the parameter β indicated by the index k. The states without a label correspond to the composite locus which, in particular, lie on the shock curve $\mathcal{H}_k(\overline{\boldsymbol{u}}_k)$. This holds except for the characteristic velocity $\overline{\lambda}_k$. Here, we have to be more precise, i.e., we need to specify the state where this quantity is evaluated. Then the composite locus is characterized in a neighborhood of a zero of $\boldsymbol{h} = (h_1, h_2)^T$ by the following proposition.

Proposition 4.8 *Let (v,e,β), $v \neq v_k(\beta)$, $e \neq e_k(\beta)$ be a zero of (4.25). Then there exists a neighborhood of (v,e,β) where the composite locus is a one parameter family of states provided that $\overline{\lambda}_k(\overline{\boldsymbol{u}}) \neq \overline{\lambda}_k(\overline{\boldsymbol{u}}_k(\beta)) = \overline{\sigma}_k(\overline{\boldsymbol{u}}_k(\beta), \overline{\boldsymbol{u}})$.*

Proof: First of all, we determine the partial derivatives of $\boldsymbol{h}$ given by

$$\begin{aligned}
h_{1,v} &= -\frac{pp_v}{\overline{\lambda}_k^2(\overline{\boldsymbol{u}}_k)}, \quad h_{1,e} = 1 - \frac{pp_e}{\overline{\lambda}_k^2(\overline{\boldsymbol{u}}_k)}, \quad h_{1,\beta} = -\frac{p + p_k}{2} h_{2,\beta}, \\
h_{2,v} &= 1 + \frac{p_v}{\overline{\lambda}_k^2(\overline{\boldsymbol{u}}_k)}, \quad h_{2,e} = \frac{p_e}{\overline{\lambda}_k^2(\overline{\boldsymbol{u}}_k)}, \quad h_{2,\beta} = -2\frac{(p - p_k)\,\mathcal{G}_k}{v_k \overline{\lambda}_k^4(\overline{\boldsymbol{u}}_k)}\frac{dp_k}{d\beta},
\end{aligned} \tag{4.26}$$

where we apply the derivatives (4.6) along the rarefaction curve. From these we determine the determinants

$$\det(\partial\boldsymbol{h}/\partial(e,v)) = \frac{\overline{\lambda}_k^2(\overline{\boldsymbol{u}}) - \overline{\lambda}_k^2(\overline{\boldsymbol{u}}_k)}{\overline{\lambda}_k^2(\overline{\boldsymbol{u}}_k)}, \quad \det(\partial\boldsymbol{h}/\partial(e,\beta)) = -2\,k_p\,\frac{(p - p_k)\,\mathcal{G}_k}{v_k \overline{\lambda}_k^4(\overline{\boldsymbol{u}}_k)}\frac{dp_k}{d\beta},$$

$$\det(\partial\boldsymbol{h}/\partial(v,\beta)) = -\frac{(p - p_k)\,\mathcal{G}_k}{v_k \overline{\lambda}_k^4(\overline{\boldsymbol{u}}_k)}\frac{dp_k}{d\beta}\left(2pk_p - (v - v_k)\left(\overline{\lambda}_k^2(\overline{\boldsymbol{u}}) - \overline{\lambda}_k^2(\overline{\boldsymbol{u}}_k)\right)\right).$$

Here we apply (2.21) and (4.24). The quantity k_p is defined by (4.13) where we replace $\overline{\boldsymbol{u}}_0$ by $\overline{\boldsymbol{u}}_k(\beta)$. Then the assertion immediately follows by the implicit function theorem and (4.22). □

If $\overline{\lambda}_k(\overline{\boldsymbol{u}}) \neq \overline{\lambda}_k(\overline{\boldsymbol{u}}_k(\beta)) = \overline{\sigma}_k(\overline{\boldsymbol{u}}_k(\beta), \overline{\boldsymbol{u}})$ holds, then this curve can be locally parametrized by β. Provided that there exists no state satisfying (4.10), it can be locally parametrized by e or v, respectively, if $\overline{\lambda}_k(\overline{\boldsymbol{u}}) = \overline{\lambda}_k(\overline{\boldsymbol{u}}_k(\beta))$, $\overline{\boldsymbol{u}} \neq \overline{\boldsymbol{u}}_k$.

With the aid of Prop. 4.8 we can now characterize the states where the characteristic velocity $\overline{\lambda}_k(\overline{\boldsymbol{u}})$ and the shock speed $\overline{\sigma}_k(\overline{\boldsymbol{u}}_k, \overline{\boldsymbol{u}})$ coincide. Here the derivative of the pressure is of special interest with regard to the algorithmic construction of the mixed curve.

Proposition 4.9 *Let (v, e, β), $v \neq v_k(\beta)$, $e \neq e_k(\beta)$ be a zero of (4.24) such that $\overline{\lambda}_k(\overline{\boldsymbol{u}}) = \overline{\lambda}_k(\overline{\boldsymbol{u}}_k(\beta))$ and $k_p \neq 0$. Then we obtain*

$$\frac{dp}{de} = \frac{\overline{\lambda}_k^2(\overline{\boldsymbol{u}}_k)}{p_k} \qquad \textit{and} \qquad \frac{dp}{dv} = -\overline{\lambda}_k^2(\overline{\boldsymbol{u}}_k).$$

Proof: According to Prop. 4.8 we can locally parametrize the mixed curve at (v, e, β) by v or e, respectively. Differentiating (4.25) with respect to v and e we obtain

$$\begin{aligned}
\frac{de}{dv} &= -\frac{1}{2}\frac{1}{k_p}\left(2pk_p - (v - v_k)\left(\overline{\lambda}_k^2(\overline{\boldsymbol{u}}) - \overline{\lambda}_k^2(\overline{\boldsymbol{u}}_k)\right)\right) = \left(\frac{dv}{de}\right)^{-1}, \\
\frac{d\beta}{dv} &= \frac{1}{2}\frac{\overline{\lambda}_k^2(\overline{\boldsymbol{u}}_k) - \overline{\lambda}_k^2(\overline{\boldsymbol{u}})}{p - p_k}\frac{\overline{\lambda}_k^2(\overline{\boldsymbol{u}}_k)\, v_k}{\mathcal{G}_k k_p}\left(\frac{dp_k}{d\beta}\right)^{-1} = \frac{d\beta}{de}\left(\frac{dv}{de}\right)^{-1}.
\end{aligned}$$

These relations are used when differentiating the EOS (2.15) which yields

$$\frac{dp}{de} = \overline{\lambda}_k^2(\overline{\boldsymbol{u}}_k)\left(\frac{\overline{\lambda}_k^2(\overline{\boldsymbol{u}})}{\overline{\lambda}_k^2(\overline{\boldsymbol{u}}_k)} - 1 + k_p\right)\left(pk_p - \frac{1}{2}(v - v_k)\left(\overline{\lambda}_k^2(\overline{\boldsymbol{u}}) - \overline{\lambda}_k^2(\overline{\boldsymbol{u}}_k)\right)\right)^{-1}$$

and

$$\frac{dp}{dv} = -\frac{\overline{\lambda}_k^2(\overline{\boldsymbol{u}}_k)}{k_p}\left(\frac{\overline{\lambda}_k^2(\overline{\boldsymbol{u}})}{\overline{\lambda}_k^2(\overline{\boldsymbol{u}}_k)} - 1 + k_p\right),$$

respectively. From this we conclude the assertion. □

Derivatives of Physical Quantities

Since we want to characterize the mixed curve by a system of ordinary differential equations, we need to know the derivatives of certain physical quantities along the mixed curve. Here we only consider states on the mixed curve where $\overline{\lambda}_k(\overline{\boldsymbol{u}}) \neq \overline{\lambda}_k(\overline{\boldsymbol{u}}_k(\beta))$ holds. The derivation is quite similar to that in the context of the shock curve in Sec. 4.2.2. Again, we incorporate the relations $\overline{\lambda}_k^2(\overline{\boldsymbol{u}}) = c^2/v^2 = \gamma p/v = pp_e - p_v$ for the characteristic velocity and $\overline{\sigma}_k^2 = -(p - p_k)/(v - v_k)$ for the shock speed where we have $\overline{\sigma}_k^2 = \overline{\lambda}_k^2(\overline{\boldsymbol{u}}_k)$. Moreover, we will make use of the equations (2.21). In the following we assume that the mixed curve is parametrized by an arbitrary parameter α. Here we would like to emphasize that now the parameter β of the rarefaction curve depends on the parametrization of the mixed curve by the definition (4.24), i.e., $\beta = \beta(\alpha)$ and, hence, $\overline{\boldsymbol{u}}_k(\beta) = \overline{\boldsymbol{u}}_k(\beta(\alpha))$. In contrast to Sec. 4.2.2, we first determine the derivatives of e and v along the mixed curve from (4.25)

$$\begin{aligned}
\frac{de}{d\alpha} &= 2\frac{p - p_k}{\overline{\lambda}_k^2(\overline{\boldsymbol{u}}) - \overline{\lambda}_k^2(\overline{\boldsymbol{u}}_k)}\frac{1}{\overline{\lambda}_k(\overline{\boldsymbol{u}}_k)}\left(pk_p - \frac{1}{2}(v - v_k)\left(\overline{\lambda}_k^2(\overline{\boldsymbol{u}}) - \overline{\lambda}_k^2(\overline{\boldsymbol{u}}_k)\right)\right)\frac{d\overline{\lambda}_k(\overline{\boldsymbol{u}}_k)}{d\beta}\frac{d\beta}{d\alpha}, \\
\frac{dv}{d\alpha} &= -2k_p\,\frac{p - p_k}{\overline{\lambda}_k^2(\overline{\boldsymbol{u}}) - \overline{\lambda}_k^2(\overline{\boldsymbol{u}}_k)}\frac{1}{\overline{\lambda}_k(\overline{\boldsymbol{u}}_k)}\frac{d\overline{\lambda}_k(\overline{\boldsymbol{u}}_k)}{d\beta}\frac{d\beta}{d\alpha}.
\end{aligned}$$

The above equations are now applied when differentiating the EOS (2.21)

$$\frac{dp}{d\alpha} = 2\frac{p-p_k}{\overline{\lambda}_k^2(\overline{\boldsymbol{u}}) - \overline{\lambda}_k^2(\overline{\boldsymbol{u}}_k)} \frac{k_v}{\gamma} \frac{\overline{\lambda}_k^2(\overline{\boldsymbol{u}})}{\overline{\lambda}_k(\overline{\boldsymbol{u}}_k)} \frac{d\overline{\lambda}_k(\overline{\boldsymbol{u}}_k)}{d\beta} \frac{d\beta}{d\alpha}. \tag{4.27}$$

Then we can rewrite the derivatives of e and v as

$$\frac{dv}{d\alpha} = -\frac{v}{p}\frac{k_p}{k_v}\frac{dp}{d\alpha}, \quad \frac{de}{d\alpha} = \frac{v}{p}\frac{1}{k_v}\left(pk_p - \frac{1}{2}(v-v_k)(\overline{\lambda}_k^2(\overline{\boldsymbol{u}}) - \overline{\lambda}_k^2(\overline{\boldsymbol{u}}_k))\right)\frac{dp}{d\alpha}. \tag{4.28}$$

From the fundamental identity of gas dynamics (2.2) we furthermore obtain

$$\frac{ds}{d\alpha} = \frac{1}{2T}\frac{v}{p}\frac{1}{k_v}\left(\overline{\lambda}_k^2(\overline{\boldsymbol{u}}) - \overline{\lambda}_k^2(\overline{\boldsymbol{u}}_k)\right)\frac{p-p_k}{\overline{\lambda}_k^2(\overline{\boldsymbol{u}}_k)}\frac{dp}{d\alpha}. \tag{4.29}$$

Next we determine from the relation $\overline{\sigma}_k^2 = -(p-p_k)/(v-v_k)$ the variation of the shock speed

$$\frac{d\overline{\sigma}_k}{d\alpha} = -\frac{1}{2}\frac{v}{p}\frac{\overline{\lambda}_k^2(\overline{\boldsymbol{u}}) - \overline{\lambda}_k^2(\overline{\boldsymbol{u}}_k)}{(v-v_k)\,k_v}\frac{1}{\overline{\sigma}_k}\frac{dp}{d\alpha} = \frac{1}{2}\frac{v}{p}\frac{1}{k_v}\frac{\overline{\lambda}_k^2(\overline{\boldsymbol{u}}) - \overline{\lambda}_k^2(\overline{\boldsymbol{u}}_k)}{(p-p_k)}\overline{\sigma}_k\frac{dp}{d\alpha} = \frac{T}{(v-v_k)^2}\frac{1}{\overline{\sigma}_k}\frac{ds}{d\alpha}. \tag{4.30}$$

This relation is applied when calculating the velocity variation from $u = u_k + (p-p_k)/\overline{\sigma}_k$

$$\frac{du}{d\alpha} = \frac{\gamma}{2\,k_v\overline{\lambda}_k^2(\overline{\boldsymbol{u}})}\left(\frac{(\gamma-\Gamma)p}{v} + \Gamma\frac{p_k}{v} + \overline{\lambda}_k^2(\overline{\boldsymbol{u}}_k)\right)\frac{1}{\overline{\sigma}_k}\frac{dp}{d\alpha}. \tag{4.31}$$

Later on, we also need the variation of the characteristic velocity

$$\frac{d\overline{\lambda}_k(\overline{\boldsymbol{u}})}{d\alpha} = -\mathcal{G}\frac{\overline{\lambda}_k(\overline{\boldsymbol{u}})}{v}\frac{dv}{d\alpha} - \frac{p_{vs}(v,s)}{2\,\overline{\lambda}_k(\overline{\boldsymbol{u}})}\frac{ds}{d\alpha}, \tag{4.32}$$

which immediately follows by (2.12) and (2.14).

Comparing the above derivatives with those derived for the shock curve in Sec. 4.2.2 and taking into account that $\overline{\lambda}_k(\overline{\boldsymbol{u}}_k) = \overline{\sigma}_k(\overline{\boldsymbol{u}}_k, \overline{\boldsymbol{u}})$, we immediately obtain the following proposition.

Proposition 4.10 *Assume that k_v is positive. Let be $\boldsymbol{u} \in \mathcal{C}(\mathcal{R}_k, \boldsymbol{u}_0)$ a state on the mixed curve and $\boldsymbol{u}^* \in \mathcal{R}_k(\boldsymbol{u}_0)$ such that $\boldsymbol{u} \in \mathcal{H}_k(\boldsymbol{u}^*)$. Then the shock curve $\mathcal{H}_k(\boldsymbol{u}^*)$ is tangent to the mixed curve $\mathcal{C}(\mathcal{R}_k, \boldsymbol{u}_0)$ at $\boldsymbol{u}$.*

In analogy to Prop. 4.4 we also can characterize the mixed curve at states $\boldsymbol{u} \in \mathcal{C}(\mathcal{R}_k, \boldsymbol{u}_0)$ where the shock speed and the characteristic velocity coincide.

Proposition 4.11 *Assume that k_v is positive. Let be $\boldsymbol{u} \in \mathcal{C}(\mathcal{R}_k, \boldsymbol{u}_0)$ and $\boldsymbol{u}_k \in \mathcal{R}_k(\boldsymbol{u}_0)$ such that $\boldsymbol{u} \in \mathcal{H}_k(\boldsymbol{u}^*)$ and $\overline{\sigma}_k(\overline{\boldsymbol{u}}^*, \overline{\boldsymbol{u}}) = \overline{\lambda}_k(\overline{\boldsymbol{u}}^*) = \overline{\lambda}_k(\overline{\boldsymbol{u}})$. Then the following statements hold:*

a) The derivatives of the mixed curve at $\boldsymbol{u}$ are given by

$$\frac{dv}{d\alpha} = -\frac{1}{\overline{\lambda}_k^2}\frac{dp}{d\alpha}, \quad \frac{du}{d\alpha} = \frac{1}{\overline{\lambda}_k}\frac{dp}{d\alpha}, \quad \frac{de}{d\alpha} = \frac{p}{\overline{\lambda}_k^2}\frac{dp}{d\alpha}, \quad \frac{ds}{d\alpha} = 0 \qquad \textit{and}$$

$$\frac{d\overline{\lambda}_k}{d\alpha} = \frac{\mathcal{G}}{v\,\overline{\lambda}_k}\frac{dp}{d\alpha} = \overline{\alpha}_k(\overline{\boldsymbol{u}})\frac{1}{\overline{\lambda}_k^2}\frac{dp}{d\alpha};$$

In particular, we obtain for the Euler equations in Lagrangian coordinates

$$\frac{d\overline{\boldsymbol{u}}}{d\alpha} = \overline{\boldsymbol{r}}_k(\overline{\boldsymbol{u}})\frac{1}{\overline{\lambda}_k^2}\frac{dp}{d\alpha}. \tag{4.33}$$

b) *If $\boldsymbol{u} \neq \boldsymbol{u}^*$, then the composite curve $\mathcal{C}(\mathcal{R}_k, \boldsymbol{u}_0)$ is tangent to the rarefaction curve $\mathcal{R}_k(\boldsymbol{u})$ at $\boldsymbol{u}$.*

c) *If the composite curve $\mathcal{C}(\mathcal{R}_k, \boldsymbol{u}_0)$ is attached to the rarefaction curve $\mathcal{R}_k(\boldsymbol{u}_0)$ at $\hat{\boldsymbol{u}}$, then the tangent directions of both curves coincide.*

The relations in a) immediately result from (4.28), (4.29), (4.30) and (4.31). The assertion b) and c) can obviously be concluded by comparing (4.33) with the derivatives (4.6).

Finally, we summarize some characteristic features of certain physical quantities along the mixed curve which are similar to those derived for the shock curve in Sec. 4.2.2.

Proposition 4.12 *Assume that k_v is positive. Let be $\boldsymbol{u} \in \mathcal{C}(\mathcal{R}_k, \boldsymbol{u}_0)$ and $\boldsymbol{u}^* \in \mathcal{R}_k(\boldsymbol{u}_0)$ such that $\boldsymbol{u} \in \mathcal{H}_k(\boldsymbol{u}^*)$. Then the following statements hold:*

a) *If $\boldsymbol{u} \neq \hat{\boldsymbol{u}}$, then the entropy s becomes extremal if and only if the shock speed $\overline{\sigma}_k$ becomes extremal, i.e., $\overline{\sigma}_k(\overline{\boldsymbol{u}}^*, \overline{\boldsymbol{u}}) = \overline{\lambda}_k(\overline{\boldsymbol{u}})$.*

b) *The pressure p is monotone as long as $\overline{\sigma}_k(\overline{\boldsymbol{u}}^*, \overline{\boldsymbol{u}}) \neq \overline{\lambda}_k(\overline{\boldsymbol{u}})$.*

c) *If $0 \leq \Gamma \leq \gamma$, then the velocity u is monotone as long as $\overline{\sigma}_k(\overline{\boldsymbol{u}}^*, \overline{\boldsymbol{u}}) \neq \overline{\lambda}_k(\overline{\boldsymbol{u}})$.*

These properties follow from (4.29), (4.27) and (4.31).

Connection of Rarefaction Curve and Mixed Curve

So far, we have characterized the composite locus by a curve and have derived the derivatives of certain physical quantities along the mixed curve. But it is not obvious that the mixed curve $\mathcal{C}(\mathcal{R}_k, \boldsymbol{u}_0)$ and the rarefaction curve $\mathcal{R}_k(\boldsymbol{u}_0)$ are attached at $\hat{\boldsymbol{u}}$. For a two–by–two system Liu verified this property imposing certain constraints on the derivatives of the fluxes (see [Liu74]). However, there exists no explicit proof for the general case (see [Liu75]). Recall that at this point we assume that the curves are attached. We will identify next necessary conditions on the parametrizations arising in this case. The starting point for this investigation is the connection between the parametrizations of the two curves. These are related by the condition $\boldsymbol{u}(\alpha) \in \mathcal{H}_k(\boldsymbol{u}_k(\beta))$ according to Liu's definition of the mixed curve. By this relation the parametrization β of the rarefaction curve depends on the parametrization α of the mixed curve, i.e., $\beta = \beta(\alpha)$, by which the two curves are glued. From (4.27) we conclude

$$\frac{d\beta}{d\alpha} = \frac{1}{2}\frac{\overline{\lambda}_k^2(\overline{\boldsymbol{u}}) - \overline{\lambda}_k^2(\overline{\boldsymbol{u}}_k)}{p - p_k}\frac{\gamma}{k_v}\frac{\overline{\lambda}_k(\overline{\boldsymbol{u}}_k)}{\overline{\lambda}_k^2(\overline{\boldsymbol{u}})}\left(\frac{d\overline{\lambda}_k(\overline{\boldsymbol{u}}_k)}{d\beta}\right)^{-1}\frac{dp}{d\alpha} \tag{4.34}$$

which is well–defined for $\overline{\boldsymbol{u}} \neq \overline{\boldsymbol{u}}_k$ and $\overline{\alpha}_k(\overline{\boldsymbol{u}}) \neq 0$. In the case of $\overline{\boldsymbol{u}} = \overline{\boldsymbol{u}}_k = \hat{\boldsymbol{u}}$ with $\overline{\alpha}_k(\hat{\boldsymbol{u}}) = 0$, see (A1) below, we now will derive the limit of the derivative (4.34) at the state $\hat{\boldsymbol{u}}$. For this purpose, we consider the following setting

(S1) $\overline{\boldsymbol{u}}_k = \overline{\boldsymbol{u}}_k(\beta),\ \beta \in [\beta_0, \hat{\beta}]$ and $\overline{\boldsymbol{u}} = \overline{\boldsymbol{u}}(\alpha),\ \alpha \in [\hat{\alpha}, \overline{\alpha}]$ with $\beta_0 < \hat{\beta} = \hat{\alpha} < \overline{\alpha}$,

(S2) $\frac{d^i p}{d\alpha^i},\ \frac{d^i p_k}{d\beta^i},\ i = 1, 2$, exist for $\alpha \in [\hat{\alpha}, \overline{\alpha}]$ and $\beta \in [\beta_0, \hat{\beta}]$, respectively,

(S3) $\left.\frac{dp}{d\alpha}\right|_{\alpha=\hat{\alpha}} \neq 0,\ \left.\frac{dp_k}{d\beta}\right|_{\beta=\hat{\beta}} \neq 0,$

(S4) $\left.\frac{dp}{d\alpha}\right|_{\alpha=\hat{\alpha}} \left.\frac{dp_k}{d\beta}\right|_{\beta=\hat{\beta}} > 0.$

Condition (S1) means that we independently parametrize the mixed curve $\overline{\boldsymbol{u}} = \overline{\boldsymbol{u}}(\alpha)$ and the rarefaction curve $\overline{\boldsymbol{u}}_k = \overline{\boldsymbol{u}}_k(\beta)$. Without loss of generality we shift the two parameter domains such that they are attached at $\hat{\beta} = \hat{\alpha}$. Moreover, we choose the parametrization on each of the two curves under consideration such that they are twice differentiable according to (S2) which, in particular, implies

(C1) $\left.\frac{dp}{d\alpha}\right|_{\alpha=\hat{\alpha}},\ \left.\frac{d^2 p}{d\alpha^2}\right|_{\alpha=\hat{\alpha}},\ \left.\frac{dp_k}{d\beta}\right|_{\beta=\hat{\beta}},\ \left.\frac{d^2 p_k}{d\beta^2}\right|_{\beta=\hat{\beta}}$ bounded.

We emphasize that in the proceeding investigations we only considered the first derivative of the physical quantities along the different types of curves. However, we assume the specific energy e to be four times differentiable which implies that the third derivatives of the EOS exist (see Sec. 2). Incorporating this knowledge into the above discussion of the curves, we conclude that the second derivatives also exist. Finally, we assume that the parametrizations are regular which implies (S3) and, in addition, we choose the orientation of the parametrizations such that (S4) holds.

By the definition of the mixed curve, the two parametrizations are implicitly linked to each other according to

(S5) $\overline{\boldsymbol{u}}(\alpha) \in \mathcal{H}_k(\overline{\boldsymbol{u}}_k(\beta))$, i.e., $\beta = \beta(\alpha)$.

For the subsequent discussion we therefore have to keep in mind that the parametrization of the rarefaction curve is no longer independent but depends on the parametrization of the mixed curve, i.e., $\overline{\boldsymbol{u}}_k(\beta) = \overline{\boldsymbol{u}}_k(\beta(\alpha))$. Hence, we have to apply the chain rule when taking the derivative of a quantity on the rarefaction curve with respect to α.

Next, we assume that the rarefaction curve and the mixed curve are attached at the state $\hat{\boldsymbol{u}}$ and, moreover, if we are approaching $\hat{\boldsymbol{u}}$ on the mixed curve the corresponding states of the rarefaction curve are also approaching $\hat{\boldsymbol{u}}$. In terms of the above setting this assumption reads

(A1) $\overline{\boldsymbol{u}}_k(\hat{\beta}) = \hat{\boldsymbol{u}} = \overline{\boldsymbol{u}}(\hat{\alpha})$, i.e., $\lim_{\alpha\to\hat{\alpha}} \beta(\alpha) = \hat{\beta}$

which is in agreement with Liu's results for a two–by–two system of equations (see [Liu74]).

From the settings (S1) – (S5) as well as assumption (A1) we now conclude by the chain rule

$$\frac{dp_k}{d\alpha} = \frac{dp_k}{d\beta}\frac{d\beta}{d\alpha}, \quad \frac{d^2 p_k}{d\alpha^2} = \frac{d^2 p_k}{d\beta^2}\frac{d\beta}{d\alpha} + \frac{dp_k}{d\beta}\frac{d^2\beta}{d\alpha^2}$$

and the regularity of the parametrization

(C2) $\left.\frac{d\beta}{d\alpha}\right|_{\alpha=\hat{\alpha}},\ \left.\frac{d^2\beta}{d\alpha}\right|_{\alpha=\hat{\alpha}^2}$ bounded,

(C3) $\lim\limits_{\alpha\to\hat{\alpha}} \overline{\alpha}_k(\boldsymbol{u}_k(\beta))\frac{d^2\beta}{d\alpha^2} = 0.$

Finally, we have to make one more assumption in order to perform the subsequent analysis

(A2) $\frac{dp}{d\alpha}\big|_{\alpha=\hat\alpha} \pm \frac{dp_k}{d\alpha}\big|_{\alpha=\hat\alpha} \neq 0,\ \neq \pm\infty.$

which has to be checked once we have determined the limit of (4.34) at the state $\hat{\boldsymbol{u}}$. Then we can prove the following limit which will be essential for Lemma 4.2.

Lemma 4.1 *Let be $\hat{\boldsymbol{u}} \in \mathcal{M}$, i.e., $\overline{\alpha}_k(\hat{\boldsymbol{u}}) = 0$, $\overline{\beta}_k(\hat{\boldsymbol{u}}) \neq 0$ or $p_{vv}(\hat v, \hat s) = 0$, $p_{vvv}(\hat v, \hat s) \neq 0$, respectively. Then the limit*

$$\lim_{\alpha\to\hat\alpha} \frac{d\overline{\lambda}_k(\overline{\boldsymbol{u}}_k)}{d\alpha} \frac{p - p_k}{\overline{\lambda}_k(\overline{\boldsymbol{u}}) - \overline{\lambda}_k(\overline{\boldsymbol{u}}_k)} = 2\left(\left.\frac{dp_k}{d\alpha}\right|_{\alpha=\hat\alpha}\right)^2 \left(\left.\frac{d(p+p_k)}{d\alpha}\right|_{\alpha=\hat\alpha}\right)^{-1} \tag{4.35}$$

holds under the assumptions (A1) – (A2) provided that the parametrizations of the mixed curve and the rarefaction curve are chosen according to (S1) – (S5).

Proof: The basic tool we apply for deriving the limit (4.35) is the theorem by l'Hospital that we make use of several times. In order to avoid too much confusion in the presentation of the proof, we do not proceed in a generic way but prefer a reversed strategy, i.e., we first derive certain limits which occur in the limiting process (4.35).

First of all, we consider the limits on the rarefaction curve. From (4.6) we immediately obtain

$$\frac{d\overline{\boldsymbol{u}}_k}{d\alpha} = \frac{1}{\overline{\lambda}_k^2(\overline{\boldsymbol{u}}_k)} \overline{\boldsymbol{r}}_k(\overline{\boldsymbol{u}}_k) \frac{dp_k}{d\alpha} \qquad \text{and} \qquad \lim_{\alpha\to\hat\alpha} \frac{d\overline{\boldsymbol{u}}_k}{d\alpha} = \frac{1}{\overline{\lambda}_k^2(\hat{\boldsymbol{u}})} \overline{\boldsymbol{r}}_k(\hat{\boldsymbol{u}}) \left.\frac{dp_k}{d\alpha}\right|_{\alpha=\hat\alpha}.$$

The variation of the corresponding characteristic velocity is given by

$$\frac{d\overline{\lambda}_k(\overline{\boldsymbol{u}}_k)}{d\alpha} = \frac{\overline{\alpha}_k(\overline{\boldsymbol{u}}_k)}{\overline{\lambda}_k^2(\overline{\boldsymbol{u}}_k)} \frac{dp_k}{d\alpha} \qquad \text{and} \qquad \lim_{\alpha\to\hat\alpha} \frac{d\overline{\lambda}_k(\overline{\boldsymbol{u}}_k)}{d\alpha} = \frac{\overline{\alpha}_k(\hat{\boldsymbol{u}})}{\overline{\lambda}_k^2(\hat{\boldsymbol{u}})} \left.\frac{dp_k}{d\alpha}\right|_{\alpha=\hat\alpha} = 0.$$

In addition, we also need the second derivative

$$\frac{d^2\overline{\lambda}_k(\overline{\boldsymbol{u}}_k)}{d\alpha^2} = -\frac{6\overline{\alpha}_k^2(\overline{\boldsymbol{u}}_k) + p_{vvv}(v_k, s_k)}{2\overline{\lambda}_k^5(\overline{\boldsymbol{u}}_k)} \left(\frac{dp_k}{d\alpha}\right)^2 + \frac{\overline{\alpha}_k(\overline{\boldsymbol{u}}_k)}{\overline{\lambda}_k^2(\overline{\boldsymbol{u}}_k)} \frac{d^2p_k}{d\alpha^2}$$

and

$$\lim_{\alpha\to\hat\alpha} \frac{d^2\overline{\lambda}_k(\overline{\boldsymbol{u}}_k)}{d\alpha^2} = -\frac{p_{vvv}(\hat v, \hat s)}{2\overline{\lambda}_k^5(\hat{\boldsymbol{u}})} \left(\left.\frac{dp_k}{d\alpha}\right|_{\alpha=\hat\alpha}\right)^2 \neq 0,$$

where we apply

$$\overline{\beta}_k(\overline{\boldsymbol{u}}_k) = \nabla_{\overline{\boldsymbol{u}}} \overline{\alpha}_k(\overline{\boldsymbol{u}}_k) \overline{\boldsymbol{r}}_k(\overline{\boldsymbol{u}}_k) = -\frac{2\overline{\alpha}_k^2(\overline{\boldsymbol{u}}_k) + p_{vvv}(v_k, s_k)}{2\overline{\lambda}_k(\overline{\boldsymbol{u}}_k)},$$

which due to the assumptions does not vanish at $\overline{\boldsymbol{u}}_k = \hat{\boldsymbol{u}}$. Finally, we also need the variation of the nonlinearity factor

$$\frac{d\overline{\alpha}_k(\overline{\boldsymbol{u}}_k)}{d\alpha} = \overline{\beta}_k(\overline{\boldsymbol{u}}_k) \frac{dp_k}{d\alpha} \qquad \text{and} \qquad \lim_{\alpha\to\hat\alpha} \frac{d\overline{\alpha}_k(\overline{\boldsymbol{u}}_k)}{d\alpha} = -\frac{p_{vvv}(\hat v, \hat s)}{2\overline{\lambda}_k^3(\hat{\boldsymbol{u}})} \left.\frac{dp_k}{d\alpha}\right|_{\alpha=\hat\alpha} \neq 0.$$

From this we conclude

$$\lim_{\alpha\to\hat\alpha}\frac{\overline{\alpha}_k(\overline{\boldsymbol{u}}_k)}{p-p_k}=\frac{\lim\limits_{\alpha\to\hat\alpha}\frac{d\overline{\alpha}_k(\overline{\boldsymbol{u}}_k)}{d\alpha}}{\lim\limits_{\alpha\to\hat\alpha}\left(\frac{d(p-p_k)}{d\alpha}\right)}=\frac{-\frac{p_{vvv}(\hat v,\hat s)}{2\overline{\lambda}_k^3(\hat{\boldsymbol{u}})}\left.\frac{dp_k}{d\alpha}\right|_{\alpha=\hat\alpha}}{\left.\frac{d(p-p_k)}{d\alpha}\right|_{\alpha=\hat\alpha}}.$$

The same limits are to be considered for the mixed curve. First, we conclude from the derivatives (4.28) and (4.31) in the previous subsection

$$\lim_{\alpha\to\hat\alpha}\frac{d\overline{\boldsymbol{u}}}{d\alpha}=\frac{1}{\overline{\lambda}_k^2(\hat{\boldsymbol{u}})}\overline{\boldsymbol{r}}_k(\hat{\boldsymbol{u}})\left.\frac{dp}{d\alpha}\right|_{\alpha=\hat\alpha}.$$

This result is incorporated in

$$\lim_{\alpha\to\hat\alpha}\frac{d\overline{\lambda}_k(\overline{\boldsymbol{u}})}{d\alpha}=\frac{\overline{\alpha}_k(\hat{\boldsymbol{u}})}{\overline{\lambda}_k^2(\hat{\boldsymbol{u}})}\left.\frac{dp}{d\alpha}\right|_{\alpha=\hat\alpha}=0\qquad\text{and}\qquad\lim_{\alpha\to\hat\alpha}\frac{d^2\overline{\lambda}_k(\overline{\boldsymbol{u}})}{d\alpha^2}=-\frac{p_{vvv}(\hat v,\hat s)}{2\overline{\lambda}_k^5(\hat{\boldsymbol{u}})}\left(\left.\frac{dp}{d\alpha}\right|_{\alpha=\hat\alpha}\right)^2\neq 0.$$

Furthermore, we have to determine the derivative of the nonlinearity factor

$$\lim_{\alpha\to\hat\alpha}\frac{d\overline{\alpha}_k(\overline{\boldsymbol{u}})}{d\alpha}=-\frac{p_{vvv}(\hat v,\hat s)}{2\overline{\lambda}_k^3(\hat{\boldsymbol{u}})}\left.\frac{dp}{d\alpha}\right|_{\alpha=\hat\alpha}\neq 0,$$

from which we derive

$$\lim_{\alpha\to\hat\alpha}\frac{\overline{\alpha}(\overline{\boldsymbol{u}})}{p-p_k}=\frac{\lim\limits_{\alpha\to\hat\alpha}\frac{d\overline{\alpha}_k(\overline{\boldsymbol{u}})}{d\alpha}}{\left(\frac{d(p-p_k)}{d\alpha}\right)}=\frac{-\frac{p_{vvv}(\hat v,\hat s)}{2\overline{\lambda}_k^3(\hat{\boldsymbol{u}})}\left.\frac{dp}{d\alpha}\right|_{\alpha=\hat\alpha}}{\left.\frac{d(p-p_k)}{d\alpha}\right|_{\alpha=\hat\alpha}}.$$

Up to now, we independently considered the limits for the rarefaction curve and the mixed curve. In the following, we combine these results. Firstly, we observe that

$$\lim_{\alpha\to\hat\alpha}\frac{d}{d\alpha}\left(\overline{\lambda}_k(\overline{\boldsymbol{u}})-\overline{\lambda}_k(\overline{\boldsymbol{u}}_k)\right)=-\frac{\overline{\alpha}_k(\hat{\boldsymbol{u}})}{\overline{\lambda}_k^2(\hat{\boldsymbol{u}})}\left.\frac{d(p-p_k)}{d\alpha}\right|_{\alpha=\hat\alpha}=0,$$

and

$$\lim_{\alpha\to\hat\alpha}\frac{d^2}{d\alpha^2}\left(\overline{\lambda}_k(\overline{\boldsymbol{u}})-\overline{\lambda}_k(\overline{\boldsymbol{u}}_k)\right)=-\frac{p_{vvv}(\hat v,\hat s)}{2\overline{\lambda}_k^5(\hat{\boldsymbol{u}})}\left(\left.\frac{d(p-p_k)}{d\alpha}\right|_{\alpha=\hat\alpha}\right)\left(\left.\frac{d(p+p_k)}{d\alpha}\right|_{\alpha=\hat\alpha}\right)\neq 0.$$

These limits imply

$$\lim_{\alpha\to\hat\alpha}\frac{\overline{\lambda}_k(\overline{\boldsymbol{u}})-\overline{\lambda}_k(\overline{\boldsymbol{u}}_k)}{p-p_k}=\frac{\lim\limits_{\alpha\to\hat\alpha}\frac{d\left(\overline{\lambda}_k(\overline{\boldsymbol{u}})-\overline{\lambda}_k(\overline{\boldsymbol{u}}_k)\right)}{d\alpha}}{\lim\limits_{\alpha\to\hat\alpha}\frac{d(p-p_k)}{d\alpha}}=\frac{\overline{\alpha}_k(\hat{\boldsymbol{u}})}{\overline{\lambda}_k^2(\hat{\boldsymbol{u}})}=0\tag{4.36}$$

and

$$\lim_{\alpha\to\hat\alpha}\frac{\overline{\lambda}_k(\overline{\boldsymbol{u}})-\overline{\lambda}_k(\overline{\boldsymbol{u}}_k)}{(p-p_k)^2}=\frac{\lim\limits_{\alpha\to\hat\alpha}\frac{d\left(\overline{\lambda}_k(\overline{\boldsymbol{u}})-\overline{\lambda}_k(\overline{\boldsymbol{u}}_k)\right)}{d\alpha}}{\lim\limits_{\alpha\to\hat\alpha}\frac{d(p-p_k)^2}{d\alpha}}=\frac{\lim\limits_{\alpha\to\hat\alpha}\frac{d^2\left(\overline{\lambda}_k(\overline{\boldsymbol{u}})-\overline{\lambda}_k(\overline{\boldsymbol{u}}_k)\right)}{d\alpha^2}}{\lim\limits_{\alpha\to\hat\alpha}\frac{d^2(p-p_k)^2}{d\alpha^2}}=-\frac{p_{vvv}(\hat v,\hat s)}{4\overline{\lambda}_k^5(\hat{\boldsymbol{u}})}\frac{\left.\frac{d(p+p_k)}{d\alpha}\right|_{\alpha=\hat\alpha}}{\left.\frac{d(p-p_k)}{d\alpha}\right|_{\alpha=\hat\alpha}}.$$

Furthermore, we calculate by the above results

$$
\begin{aligned}
I_1 \quad &:= \quad \lim_{\alpha\to\hat\alpha} \frac{\frac{d\left(\overline{\lambda}_k(\overline{\boldsymbol{u}})-\overline{\lambda}_k(\overline{\boldsymbol{u}}_k)\right)}{d\alpha}}{p-p_k} = \frac{1}{\overline{\lambda}_k^2)\hat{\boldsymbol{u}})} \left(\lim_{\alpha\to\hat\alpha} \frac{\overline{\alpha}_k(\overline{\boldsymbol{u}})}{p-p_k}\frac{dp}{d\alpha} - \lim_{\alpha\to\hat\alpha} \frac{\overline{\alpha}_k(\overline{\boldsymbol{u}}_k)}{p-p_k}\frac{dp_k}{d\alpha} \right) \\
&= \quad -\frac{p_{vvv}(\hat v,\hat s)}{2\overline{\lambda}_k^5(\hat{\boldsymbol{u}})} \left.\frac{d(p+p_k)}{d\alpha}\right|_{\alpha=\hat\alpha} \neq 0,
\end{aligned}
$$

and

$$
I_2 := \lim_{\alpha\to\hat\alpha} \frac{\overline{\lambda}_k(\overline{\boldsymbol{u}})-\overline{\lambda}_k(\overline{\boldsymbol{u}}_k)}{(p-p_k)^2}\frac{d(p-p_k)}{d\alpha} = -\frac{p_{vvv}(\hat v,\hat s)}{4\overline{\lambda}_k^5(\hat{\boldsymbol{u}})} \left.\frac{d(p+p_k)}{d\alpha}\right|_{\alpha=\hat\alpha} \neq 0.
$$

Combining these results we obtain

$$
\lim_{\alpha\to\hat\alpha} \frac{d}{d\alpha}\left(\frac{\overline{\lambda}_k(\overline{\boldsymbol{u}})-\overline{\lambda}_k(\overline{\boldsymbol{u}}_k)}{p-p_k}\right) = I_1 - I_2 = -\frac{p_{vvv}(\hat v,\hat s)}{4\overline{\lambda}_k^5(\hat{\boldsymbol{u}})} \left.\frac{d(p+p_k)}{d\alpha}\right|_{\alpha=\hat\alpha} \neq 0
$$

and finally

$$
\lim_{\alpha\to\hat\alpha} \frac{d\overline{\lambda}_k(\overline{\boldsymbol{u}}_k)}{d\alpha}\frac{p-p_k}{\overline{\lambda}_k(\overline{\boldsymbol{u}})-\overline{\lambda}_k(\overline{\boldsymbol{u}}_k)} = \lim_{\alpha\to\hat\alpha} \frac{d^2\overline{\lambda}_k(\overline{\boldsymbol{u}}_k)}{d\alpha^2}\left(\lim_{\alpha\to\hat\alpha}\frac{d}{d\alpha}\left(\frac{\overline{\lambda}_k(\overline{\boldsymbol{u}})-\overline{\lambda}_k(\overline{\boldsymbol{u}}_k)}{p-p_k}\right)\right)^{-1},
$$

from which the assertion follows. □

With the aid of Lemma 4.1 we are now able to determine the derivative of $d\beta/d\alpha|_{\alpha=\hat\alpha}$

Lemma 4.2 *If the assumptions in Lemma 4.1 are fulfilled, then the limits*

$$
\left.\frac{d\beta}{d\alpha}\right|_{\alpha=\hat\alpha} = -\frac{1}{2}\left.\frac{dp}{d\alpha}\right|_{\alpha=\hat\alpha}\left(\left.\frac{dp_k}{d\beta}\right|_{\beta=\hat\beta}\right)^{-1} \tag{4.37}
$$

or equivalently

$$
\left.\frac{dp_k}{d\alpha}\right|_{\alpha=\hat\alpha} = -\frac{1}{2}\left.\frac{dp}{d\alpha}\right|_{\alpha=\hat\alpha}
$$

exist provided that the parametrizations of the mixed and the rarefaction curve are chosen according to (S1) – (S5) and the assumptions (A1) – (A2) hold.

Proof: By Lemma 4.1 and (4.27) we know

$$
\left.\frac{dp}{d\alpha}\right|_{\alpha=\hat\alpha} = 2\left(\left.\frac{dp_k}{d\alpha}\right|_{\alpha=\hat\alpha}\right)^2\left(\left.\frac{d(p+p_k)}{d\alpha}\right|_{\alpha=\hat\alpha}\right)^{-1}.
$$

This is a quadratic equation for $dp_k/d\alpha|_{\alpha=\hat\alpha}$ which reads

$$
\left(\left.\frac{dp_k}{d\alpha}\right|_{\alpha=\hat\alpha}\right)^2 - \frac{1}{2}\left.\frac{dp}{d\alpha}\right|_{\alpha=\hat\alpha}\left.\frac{dp_k}{d\alpha}\right|_{\alpha=\hat\alpha} - \frac{1}{2}\left(\left.\frac{dp}{d\alpha}\right|_{\alpha=\hat\alpha}\right)^2 = 0.
$$

There exist two solutions, namely,

$$
\left.\frac{dp_k}{d\alpha}\right|_{\alpha=\hat\alpha} = \left.\frac{dp}{d\alpha}\right|_{\alpha=\hat\alpha} \qquad \text{and} \qquad \left.\frac{dp_k}{d\alpha}\right|_{\alpha=\hat\alpha} = -\frac{1}{2}\left.\frac{dp}{d\alpha}\right|_{\alpha=\hat\alpha}
$$

or equivalently

$$\left.\frac{d\beta}{d\alpha}\right|_{\alpha=\hat{\alpha}} = \left.\frac{dp}{d\alpha}\right|_{\alpha=\hat{\alpha}} \left(\left.\frac{dp_k}{d\beta}\right|_{\beta=\hat{\beta}} \right)^{-1} =: q \qquad \text{and} \qquad \left.\frac{d\beta}{d\alpha}\right|_{\alpha=\hat{\alpha}} = -\frac{q}{2}.$$

In order to determine the admissible solution, we have to check the validity of the assumption (A2). First of all, we notice that

$$\left.\frac{d\beta}{d\alpha}\right|_{\alpha=\hat{\alpha}} < 0$$

is implied by (S1) and (A1). From this we conclude

$$\left.\frac{d\beta}{d\alpha}\right|_{\alpha=\hat{\alpha}} = \begin{cases} q & , \quad q < 0 \\ -q/2 & , \quad q > 0 \end{cases} .$$

Furthermore, we obtain

$$\left.\frac{d(p-p_k)}{d\alpha}\right|_{\alpha=\hat{\alpha}} = \left(q - \left.\frac{d\beta}{d\alpha}\right|_{\alpha=\hat{\alpha}}\right) \left.\frac{dp_k}{d\beta}\right|_{\beta=\hat{\beta}} = \left.\frac{dp_k}{d\beta}\right|_{\beta=\hat{\beta}} \begin{cases} 0 & , \quad q < 0 \\ 3\,q/2 & , \quad q > 0 \end{cases}$$

and

$$\left.\frac{d(p+p_k)}{d\alpha}\right|_{\alpha=\hat{\alpha}} = \left(q + \left.\frac{d\beta}{d\alpha}\right|_{\alpha=\hat{\alpha}}\right) \left.\frac{dp_k}{d\beta}\right|_{\beta=\hat{\beta}} = \left.\frac{dp_k}{d\beta}\right|_{\beta=\hat{\beta}} \begin{cases} 2\,q & , \quad q < 0 \\ q/2 & , \quad q > 0 \end{cases} .$$

Obviously, assumption (A2) is valid, if and only if the parametrization of the mixed curve and rarefaction curve are chosen such that $q > 0$. This is always possible, since the parametrizations are independent. We therefore have chosen the parametrization accordingly, see (S3) and (S4). Thus, only one of the two solutions is admissible which proves the assertion. □

Finally, we want to remark that the characteristic velocity and the shock speed behave differently at $\boldsymbol{u} = \boldsymbol{u}_k = \hat{\boldsymbol{u}}$ than they do in the case of the shock curve $\mathcal{H}_k(\boldsymbol{u}_0)$ at $\boldsymbol{u} = \boldsymbol{u}_0$.

Proposition 4.13 *Choose the parametrizations of the mixed and the rarefaction curve according to (S1) – (S5) and assume the assumptions (A1) – (A2) to hold. Furthermore, let $\boldsymbol{u} \in \mathcal{C}(\mathcal{R}_k, \boldsymbol{u}_0)$ and $\boldsymbol{u}^* \in \mathcal{R}_k(\boldsymbol{u}_0)$ such that $\boldsymbol{u} \in \mathcal{H}_k(\boldsymbol{u}^*)$. If $\overline{\sigma}_k(\overline{\boldsymbol{u}}^*, \overline{\boldsymbol{u}}) = \overline{\lambda}_k(\overline{\boldsymbol{u}}^*) = \overline{\lambda}_k(\overline{\boldsymbol{u}})$, then the variation of the characteristic velocity and the shock speed are related by*

$$\frac{d\overline{\sigma}_k}{d\alpha} = \frac{d\overline{\lambda}_k}{d\alpha} = 0$$

provided that $k_v \neq 0$.

Proof: In the case of $\boldsymbol{u} \neq \boldsymbol{u}^*$, the assertion can be immediately concluded from (4.30) and (4.32). Here we have to assume that k_v is positive. Otherwise, we already verified for $\boldsymbol{u} = \boldsymbol{u}^* = \hat{\boldsymbol{u}}$ the limit (4.36). Together with (4.30) and (4.32) this implies

$$\left.\frac{d\overline{\sigma}_k}{d\alpha}\right|_{\alpha=\hat{\alpha}} = \frac{\overline{\alpha}_k(\hat{\boldsymbol{u}})}{\overline{\lambda}_k(\hat{\boldsymbol{u}})} \left.\frac{dp}{d\alpha}\right|_{\alpha=\hat{\alpha}} = \left.\frac{d\overline{\lambda}_k}{d\alpha}\right|_{\alpha=\hat{\alpha}} = 0.$$

Here the positivity of k_v has not to be assumed, since $\boldsymbol{u} = \boldsymbol{u}^* = \hat{\boldsymbol{u}}$ and, consequently, $k_v = \gamma > 0$. □

Alternative Construction of Mixed Curve

By the previous investigations we are now able to characterize the mixed curve by an IVP for the states $\boldsymbol{u} = \boldsymbol{u}(\alpha)$ on the mixed curve and the relation $\beta = \beta(\alpha)$ by which the mixed curve $\mathcal{C}(\mathcal{R}_k, \boldsymbol{u}_0)$ is glued to the rarefaction curve $\mathcal{R}_k(\boldsymbol{u}_0)$:

$$\begin{aligned} \frac{d\overline{\boldsymbol{u}}(\alpha)}{d\alpha} &= \boldsymbol{g}(\overline{\boldsymbol{u}}(\alpha), \beta(\alpha)),\ \alpha \in (\hat{\alpha}, \tilde{\alpha}), \qquad \overline{\boldsymbol{u}}(\hat{\alpha}) = \hat{\boldsymbol{u}}, \\ \frac{d\beta(\alpha)}{d\alpha} &= f(\overline{\boldsymbol{u}}(\alpha), \beta(\alpha)),\ \alpha \in (\hat{\alpha}, \tilde{\alpha}), \qquad \beta(\hat{\alpha}) = \hat{\beta} = \hat{\alpha} \end{aligned} \tag{4.38}$$

where $\boldsymbol{g}$ is defined by the representation of derivatives for v, u, E according to (4.28) and (4.31) and f by (4.34) and (4.37). This IVP has to be satisfied by any smooth curve that coincides with the composite locus composed of a one parameter family of states satisfying (4.24) and which is attached to the rarefaction curve $\mathcal{R}_k(\boldsymbol{u}_0)$ at $\hat{\boldsymbol{u}}$. By Prop. 4.11 c), we immediately conclude that the mixed curve is tangent to the rarefaction curve at $\hat{\boldsymbol{u}}$. However, these statements only hold provided that the assumption (A1) is valid and $\hat{\boldsymbol{u}}$ is a simple degeneration point of the nonlinear characteristic field, i.e., $\beta_k(\hat{\boldsymbol{u}}) \neq 0$ if $\alpha_k(\hat{\boldsymbol{u}}) = 0$. For a two–by–two system Liu explicitly verified the validity of (A1) (see [Liu74]). For a general system Liu also claims that the mixed curve satisfies this condition but without presenting an explicit proof (see [Liu75]). We want to emphasize that Liu makes no assumption with respect to the second derivative of the characteristic field in case of states where the nonlinear field degenerates. However, in our investigations the demand for a *simple degeneration* seems to be *necessary*. Therefore, we believe that it is worthwhile to consider the case of a general system more carefully with special emphasize on the characterization of the degeneration points. For more details see [FFMV].

Finally, we want to remark that the mixed curve is not uniquely characterized by (4.38). For this purpose one has to check that the state $\overline{\boldsymbol{u}} = \overline{\boldsymbol{u}}(\alpha) \in \mathcal{H}_k(\overline{\boldsymbol{u}}_k(\beta))$ is the first state on the shock curve where the condition $\overline{\lambda}_k(\overline{\boldsymbol{u}}_k) = \overline{\sigma}_k(\overline{\boldsymbol{u}}_k, \overline{\boldsymbol{u}})$ and $\overline{\boldsymbol{u}} \neq \overline{\boldsymbol{u}}_k$ holds. In principle, there are at least two possibilities. Excluding bifurcation at $\boldsymbol{u} = \hat{\boldsymbol{u}} = \boldsymbol{u}_k$ is one possibility (see [FFMV]). Alternatively, one could verify that the right–hand side of (4.38) is a Lipschitz–continuous function of $\boldsymbol{u}$ and β. Then standard results from ODE theory guarantee the existence of a unique solution. However, this is beyond the scope of the present work. We are therefore convinced that the following conjecture is true.

Conjecture 4.1 *The curve defined by the IVP (4.38) coincides with the mixed curve defined by (3.26) provided that the degeneration point of the nonlinear field is simple.*

4.3 Composition of k–Curves and k–Waves

The basic principles how to construct the k–curves by composing the elementary curves in an appropriate manner has already been described in Sec. 3.3. We therefore do not recall them here in detail, but we summarize the curve composition for a nonlinear field.

Here we present in particular the evolution of the curve in the p–u plane as well as the corresponding waves and characteristics in the t–x plane. The corresponding curves and waves are sketched in Figs. 25 — 29 which are attached in the Appendix 7.2. We start at a state $\boldsymbol{u}_0 \in \mathcal{D}$ with $\mathcal{G}_0 \neq 0$ and proceed along the admissible branch of the shock curve. How to determine the admissible branch with the help of the characteristic velocities and the shock speed is discussed in Sec. 3.3. The situation of a single shock is sketched in Fig. 25. If the shock becomes sonic in a state $\boldsymbol{u}_1 \in \mathcal{D}$, then the curve is continued by the rarefaction curve $\mathcal{R}_k(\boldsymbol{u}_1)$ (see Fig. 26). We can proceed along the rarefaction curve as long as we arrive at a state $\boldsymbol{u}_2 \in \mathcal{D}$ where the nonlinear field degenerates, i.e., $\mathcal{G}_2 = 0$. There we continue with the mixed curve $\mathcal{C}(\mathcal{R}_k, \boldsymbol{u}_1)$. In the t–x plane this means that we connect a state $\boldsymbol{u} \in \mathcal{C}(\mathcal{R}_k, \boldsymbol{u}_1)$ with an appropriate state on the rarefaction curve $\boldsymbol{u}^* \in \mathcal{R}_k(\boldsymbol{u}_1)$ by a shock (see Fig. 27). If this shock becomes sonic in $\boldsymbol{u}_3 \in \mathcal{C}(\mathcal{R}_k, \boldsymbol{u}_1)$, then the curve is continued by a rarefaction curve $\mathcal{R}_k(\boldsymbol{u}_3)$ (see Fig. 28). Before we arrive at such a state, there might occur the case $\boldsymbol{u}_3^* = \boldsymbol{u}_1$. Then we alternatively proceed with the shock curve $\mathcal{H}_k(\boldsymbol{u}_3) = \mathcal{H}_k(\boldsymbol{u}_0)$ (see Fig. 29). In principle, all possible cases have been considered. Proceeding furthermore on the curve, the above cases may occur repeatedly.

4.4 Solving the Riemann Problem

We are now able to determine the Riemann solution for the Euler equations in complete analogy to the treatment of the general hyperbolic systems. This procedure requires the solution of a nonlinear system of equations for the parameters of the different k–curves (see Sec. 3.1). It can be solved iteratively. We emphasize that in each iteration step the k–curves have to be determined again, since the intermediate states are changing depending on the parameter values. This procedure stops, if we find intermediate states such that $\boldsymbol{u}_r$ is connected to $\boldsymbol{u}_l$, i.e., there exists a path in the admissible phase space composed of the different k–curves. Hence the algorithm can be interpreted as a *multiple shooting* procedure as is used for solving boundary value problems for ODEs. For the Euler equations, this algorithm can be significantly simplified. The starting point is the observation that the 2–field is linearly degenerate and pressure as well as velocity do not change across the corresponding contact discontinuity. Therefore, we do not have to determine the intersection points of the *three* curves in the phase space. Instead, we project this problem to the p–u plane where we only search for *one* intersection point of the *two* nonlinear fields (see Fig. 10). In the previous sections we have already analyzed

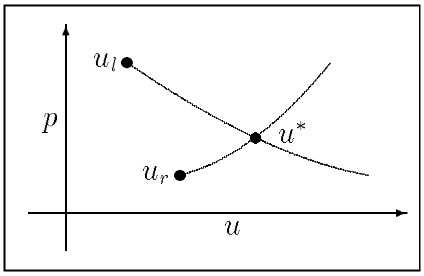

Figure 10: Intersection of curves

the behavior of the pressure and the velocity along the elementary curves. In any case we observe that the pressure is monotone along the admissible branches according to Prop. 4.1 b), 4.7 b) and 4.12 b). Therefore, we use the pressure as parameter. In order to determine a unique solution of the Riemann problem, there may be exactly one intersection point in the p–u plane. This is only guaranteed when the velocity u is monotone along the admissible branches. Provided that the EOS is chosen such that the conditions (2.22) hold and k_v is positive along the admissible part of the mixed curve, then the monotonicity is again ensured by Prop. 4.1 b), 4.7 b) and 4.12 b). By the monotonicity of u, more than one intersection point of the two curves as sketched in Fig. 11 are excluded. However, it might happen that there exists no intersection point at all. This is the case when the parameter p is approaching zero before the curves intersect as is shown in Fig. 12. Then

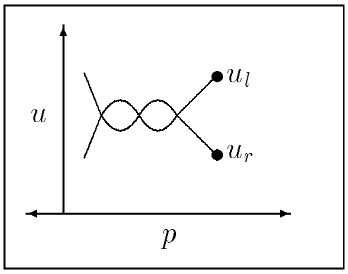

Figure 11: Multiple intersection points

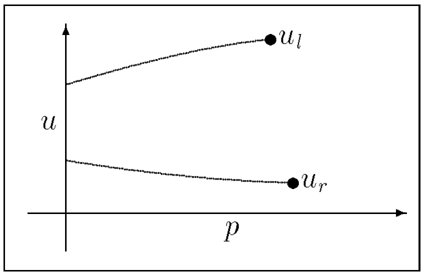

Figure 12: Vacuum

the specific volume v tends to infinity according to thermodynamic consistency (2.8). In this case we have to admit vacuum as a Riemann solution. In our investigations it will be of no interest. We therefore omit the details.

4.5 How to compute the Riemann Solution

In the sequel we outline the main ideas how to compute the Riemann solution for the Euler equations. This is based on determining the intersection points of the two curves corresponding to the nonlinear fields originating in the initial states $\boldsymbol{u}_l$ and $\boldsymbol{u}_r$, respectively. For this purpose, we need three types of algorithms by which we can determine

- a state of the elementary curves for a given parameter value p;
- the admissible branch of the elementary curves which originates from either one of the initial states depending on the parameter p;
- the intersection point in the p–u plane where we compute the two curves with varying parameter p.

4.5.1 Computation of the Elementary Curves

The k–curves, $k = 1, 3$, are determined in the p–u plane with respect to the pressure p. To this end, we need algorithms by which we can determine a *single* state of an elementary curve. The structure for all of these routines is the same. In any case we prescribe a parameter value $\tilde{p}$ and determine a state $\boldsymbol{u} = \boldsymbol{u}(\tilde{p})$ on the elementary curve such that

$$\tilde{p} = p(v(\tilde{p}), e(\tilde{p})).$$

In addition, we need the initial state $\boldsymbol{u}_0$ where the elementary curve starts, e.g., $\mathcal{H}_k(\boldsymbol{u}_0)$, $\mathcal{R}_k(\boldsymbol{u}_0)$, $\mathcal{C}(\mathcal{R}_k, \boldsymbol{u}_0)$. For the iteration process itself, we have to specify an initial guess $\boldsymbol{u}^{(0)}$. If we already have determined a state $\hat{\boldsymbol{u}}$ of the elementary curve in a previous step, then we choose $\boldsymbol{u}^{(0)} = \hat{\boldsymbol{u}}$ and $\tilde{p} = \hat{p} + \Delta\tilde{p}$ where $\Delta\tilde{p}$ denotes an arbitrary but fixed parameter increment. The iteration process for $\boldsymbol{u}$ stops, if the error

$$|\tilde{p} - p(v, e)| \leq \varepsilon \tag{4.39}$$

is less than a tolerance $\varepsilon > 0$. If the tolerance is not met within an upper bound k_{max} of iteration steps, then the algorithm fails to converge and, moreover, we stop the computation of the curve. When proceeding forward on the elementary curve then we might arrive at a state where the curves become non–admissible, i.e.,

a) the shock becomes sonic on $\mathcal{H}_k(\boldsymbol{u}_0)$ if $\lambda_k(\boldsymbol{u}) = \sigma_k(\boldsymbol{u}_0, \boldsymbol{u})$;

b) the rarefaction curve $\mathcal{R}_k(\boldsymbol{u}_0)$ ends at $\mathcal{G}(\boldsymbol{u}) = 0$;

c) the mixed curve $\mathcal{C}(\mathcal{R}_k, \boldsymbol{u}_0)$ corresponds to either

   i) a sonic shock on $\mathcal{H}_k(\boldsymbol{u}^*)$, $\boldsymbol{u}^* \in \mathcal{R}_k(\boldsymbol{u}_0)$ or

   ii) $\boldsymbol{u}^* = \boldsymbol{u}_0$.

Since we prescribe the parameter increment $\Delta\tilde{p}$, we will miss these states in general. However, we can detect them by the corresponding characteristic velocity $\lambda_k(\boldsymbol{u})$ and shock speed $\sigma_k(\boldsymbol{u}_0, \boldsymbol{u})$, respectively. If we compute a state where the monotonicity of the characteristic velocity in case a) or the shock speed in case b) and c,i) is violated or we step over p_0 corresponding to $\boldsymbol{u}_0$ in case c,ii) then we have to determine the end points of the admissible branch of the elementary curve accurately. To this end, we can use bisection techniques. Alternatively, we apply the same algorithms as before but now we incorporate the additional equation and determine $\tilde{p}$ (see e.g. (4.48)). In the sequel, we present the algorithms for the elementary curves in some detail. The rarefaction curve is determined as the solution of an IVP. In case of the shock curve or the mixed curve, we can compute the curves by solving an IVP or a nonlinear algebraic problem, alternatively.

Rarefaction Curve

Choosing the pressure p as parameter, i.e., $\beta = p$, the rarefaction curve is determined according to (4.6) by the IVP

$$\frac{d\overline{\boldsymbol{u}}(p)}{dp} = \boldsymbol{g}^r(p, \overline{\boldsymbol{u}}(p)), \qquad \overline{\boldsymbol{u}}(p_0) = \overline{\boldsymbol{u}}^{(0)} \tag{4.40}$$

with

$$\overline{\boldsymbol{u}}(p) = \begin{pmatrix} v(p) \\ u(p) \\ E(p) \end{pmatrix}, \quad \boldsymbol{g}^r(p, \overline{\boldsymbol{u}}) = \frac{1}{\overline{\lambda}_k^2(\overline{\boldsymbol{u}})} \overline{\boldsymbol{r}}_k(\overline{\boldsymbol{u}}) = \frac{1}{\overline{\lambda}_k^2(\overline{\boldsymbol{u}})} \begin{pmatrix} -1 \\ \overline{\lambda}_k(\overline{\boldsymbol{u}}) \\ p + \overline{\lambda}_k(\overline{\boldsymbol{u}})\, u \end{pmatrix}, \quad \overline{\lambda}_k(\overline{\boldsymbol{u}}) = \varepsilon_k \frac{v}{c}.$$

In general, this system of ODEs can not be solved explicitly. Therefore, we determine the rarefaction curve $\mathcal{R}_k(\boldsymbol{u}_0)$ in our computations by discretizing these equations.

For this purpose, we perform one step with the classical Runge–Kutta scheme of 4th order, i.e.

$$\begin{aligned}
\boldsymbol{k}_1 &= \boldsymbol{g}^r\left(p^{(0)}, \overline{\boldsymbol{u}}^{(0)}\right), \\
\boldsymbol{k}_2 &= \boldsymbol{g}^r\left(p^{(0)} + 0.5\,\Delta\tilde{p}, \overline{\boldsymbol{u}}^{(0)} + 0.5\,\Delta\tilde{p}\,\boldsymbol{k}_1\right), \\
\boldsymbol{k}_3 &= \boldsymbol{g}^r\left(p^{(0)} + 0.5\,\Delta\tilde{p}, \overline{\boldsymbol{u}}^{(0)} + 0.5\,\Delta\tilde{p}\,\boldsymbol{k}_2\right), \\
\boldsymbol{k}_4 &= \boldsymbol{g}^r\left(p^{(0)} + \Delta\tilde{p} = \tilde{p}, \overline{\boldsymbol{u}}^{(0)} + \Delta\tilde{p}\,\boldsymbol{k}_3\right), \\
\overline{\boldsymbol{u}}^{(1)} &= \overline{\boldsymbol{u}}^{(0)} + \frac{\Delta\tilde{p}}{6}(\boldsymbol{k}_1 + \boldsymbol{k}_2 + \boldsymbol{k}_3 + \boldsymbol{k}_4).
\end{aligned}$$

Here $\overline{\boldsymbol{u}}^{(0)}$ denotes the initial value and $\Delta\tilde{p}$ is the step size. In our computations, this scheme rendered satisfying results.

Since the approximation error accumulates along the integration path a step control is useful. Besides standard techniques, we can alternatively control the step size by the error in the pressure difference, i.e., if $|p(v^{(1)}, e^{(1)}) - \tilde{p}| > \varepsilon$ than we twice repeat the Runge–Kutta scheme with step size $\Delta\tilde{p}/2$. This procedure can be recursively repeated until the error tolerance is met or a number of refinement steps is exceeded.

Shock Curve

Again we choose the pressure p as parameter, i.e., $\alpha = p$. Then the admissible branch of the shock curve is determined by the IVP

$$\frac{d\overline{\boldsymbol{u}}(p)}{dp} = \boldsymbol{g}^s(p, \overline{\boldsymbol{u}}(p)), \qquad \overline{\boldsymbol{u}}(p_0) = \overline{\boldsymbol{u}}^{(0)}$$

with $\overline{\boldsymbol{u}}(p) = (v(p), u(p), E(p))^T$ and the right hand side, according to (4.15), (4.19) and (4.17)

$$\boldsymbol{g}^s(p, \overline{\boldsymbol{u}}) = \frac{1}{\overline{\lambda}_k^2} \begin{pmatrix} -\frac{\gamma\, k_p}{k_v} \\ \frac{1}{2}\left(\overline{\lambda}_k^2 + \frac{\gamma\, k_p}{k_v}\overline{\sigma}_k^2\right)\frac{1}{\overline{\sigma}_k} \\ \frac{\gamma}{k_v}\left(pk_p - 0.5\,\left(v - v^{(0)}\right)\left(\overline{\lambda}_k^2 - \overline{\sigma}_k^2\right)\right) + \frac{1}{2}u\left(\overline{\lambda}_k^2 + \frac{\gamma\, k_p}{k_v}\overline{\sigma}_k^2\right)\frac{1}{\overline{\sigma}_k} \end{pmatrix}.$$

For completion, we summarize here the representation of the coefficients

$$\overline{\lambda}_k = \varepsilon_k \frac{v}{c}, \quad \overline{\sigma}_k = \varepsilon_k \left\{ -\frac{p - p^{(0)}}{v - v^{(0)}} \right\}^{1/2}, \quad k_v := \gamma - \frac{\Gamma}{2}\frac{p - p^{(0)}}{p}, \quad k_p := 1 + \frac{\Gamma}{2}\frac{v - v^{(0)}}{v}.$$

Since the discretization error accumulates when integrating along the trajectory, it is more convinient to determine the state on the shock curve directly from the Rankine–Hugoniot relations. Therefore we want to describe how to determine a state on the Hugoniot curve depending on the parameter $\tilde{p}$. The starting point are the equations

$$p(v, e) = \tilde{p}, \qquad e = e_0 - 0.5(p(v, e) + p_0)(v - v_0).$$

Substituting p by $p(v, e)$ in e, these reduce to a scalar equation for the volume v

$$f(v) := p(v, e) - \tilde{p} \qquad \text{with} \qquad e(v) := e_0 - \frac{\tilde{p} + p_0}{2}(v - v_0). \tag{4.41}$$

Close to the initial state corresponding to p_0 this problem exhibits a unique solution, since

$$f'(v) = p_v(v, e) + p_e(v, e)e'(v) = -c^2/v^2 + 0.5(\tilde{p} - p_0)$$

holds. Obviously, the derivative is negative close to the initial state. Hence, we can iteratively solve (4.41) by the Newton scheme. The resulting scheme reads

$$v^{(i+1)} = v^{(i)} - \frac{p\left(v^{(i)}, e^{(i)}\right) - \tilde{p}}{p_v^{(i)} - p_e^{(i)}(p_0 + \tilde{p})/2} \tag{4.42}$$

with

$$e^{(i)} = e_0 - \frac{p_0 + \tilde{p}}{2}\left(v^{(i)} - v_0\right), \quad p_v^{(i)} = p_v\left(v^{(i)}, e^{(i)}\right), \quad p_e^{(i)} = p_e\left(v^{(i)}, e^{(i)}\right).$$

If the error tolerance (4.39) is met, we compute

$$\overline{\sigma}_k = \varepsilon_k \sqrt{-\frac{\tilde{p} - p_0}{v^{(i)} - v_0}}, \quad u = u_0 + \frac{\tilde{p} - p_0}{\overline{\sigma}_k}, \quad E = e^{(i)} + 0.5u^2.$$

Instead of solving (4.41), we alternatively could define e implicitly, i.e.,

$$e(v) = e_0 - \frac{p(v, e(v)) + p_0}{2}(v - v_0)$$

or rewrite (4.41) with respect to the two unknowns v and e, i.e.,

$$\begin{pmatrix} p(v,e) - \tilde{p} \\ e - e_0 + \frac{p(v,e)+p_0}{2}(v - v_0) \end{pmatrix} = \begin{pmatrix} 0 \\ 0 \end{pmatrix}.$$

These alternative formulations require more floating point operations, but they need the same iteration rate. Additionally, they differ from (4.41) in the fact that the iterates lie on the Hugoniot curve, whereas the iterates (4.42) do not.

Mixed Curve

We parametrize the admissible part of the mixed curve as well as the corresponding part of the rarefaction curve by the pressure, i.e., $\alpha = p$, $\beta = p_k$. Then we can determine the mixed curve by the IVP

$$\begin{aligned} \frac{d\overline{\boldsymbol{u}}(p)}{dp} &= \boldsymbol{g}^m(p, \overline{\boldsymbol{u}}(p), p_k(p)), \qquad \overline{\boldsymbol{u}}(p_0) = \overline{\boldsymbol{u}}^{(0)} = \hat{\boldsymbol{u}}, \\ \frac{dp_k(p)}{dp} &= f^m(p, \overline{\boldsymbol{u}}(p), p_k(p)), \qquad p_k(p_0) = p_0 = \hat{p} \end{aligned} \tag{4.43}$$

with $\overline{\boldsymbol{u}}(p) = (v(p), u(p), E(p))^T$ and the right–hand side

$$\boldsymbol{g}^m(p, \overline{\boldsymbol{u}}) = \frac{1}{\overline{\lambda}_k^2(p)} \begin{pmatrix} -\frac{\gamma\, k_p}{k_v} \\ \frac{1}{2}\left(\overline{\lambda}_k^2(p) + \frac{\gamma\, k_p}{k_v}\overline{\lambda}_k^2(p_k)\right)\frac{1}{\overline{\lambda}_k(p_k)} \\ \frac{\gamma}{k_v}\left(pk_p - 0.5\,\left(v - v^{(0)}\right)\left(\overline{\lambda}_k^2(p) - \overline{\lambda}_k^2(p_k)\right)\right) + \frac{u}{2}\left(\frac{\overline{\lambda}_k^2(p)}{\overline{\lambda}_k(p_k)} + \frac{\gamma\, k_p}{k_v}\overline{\lambda}_k(p_k)\right) \end{pmatrix}$$

according to (4.28), (4.31) and (4.34), (4.37), respectively. Here the characteristic velocities are calculated as functions of the states $\overline{\boldsymbol{u}}(p)$ on the mixed curve and $\overline{\boldsymbol{u}}_k(p_k)$ on the rarefaction curve

$$\overline{\lambda}_k(p) := \overline{\lambda}_k(\overline{\boldsymbol{u}}(p)), \qquad \overline{\lambda}_k(p_k) := \overline{\lambda}_k(\overline{\boldsymbol{u}}_k(p_k)) = \overline{\sigma}(\overline{\boldsymbol{u}}_k(p_k), \overline{\boldsymbol{u}}(p)).$$

In general, the rarefaction curve is not known explicitly but has to be determined by an IVP. Then we have to extend (4.43) by

$$\frac{d\overline{\boldsymbol{u}}_k(p)}{dp} = \boldsymbol{g}^r(\overline{\boldsymbol{u}}_k(p_k(p)), p_k(p)), \qquad \overline{\boldsymbol{u}}_k(p_0) = \overline{\boldsymbol{u}}_k^{(0)} = \hat{\boldsymbol{u}}.$$

Instead of discretizing the IVP, we compute the mixed curve by determining the zero p^* of

$$g(p^*) := p(v(p^*), e(p^*)) - \tilde{p} = 0 \tag{4.44}$$

with

$$v(p^*) := v_k(p^*) - \frac{\tilde{p} - p^*}{\overline{\lambda}_k^2(p^*)}, \quad e(p^*) := e_k(p^*) - \frac{1}{2}(\tilde{p} + p^*)(v(p^*) - v_k(p^*)). \tag{4.45}$$

In order to simplify notation we abbreviat here $\overline{\lambda}_k^2(p^*) := \overline{\lambda}_k^2(\overline{\boldsymbol{u}}(p^*))$ for the characteristic velocity on the rarefaction curve. This problem can be iteratively solved with the Newton scheme. To this end, we need the derivative g' which can be determined by (4.45) and (4.40). First of all, we calculate the variation of the Lagrangian wave speed

$$\overline{\lambda}_k'(p^*) = \frac{\mathcal{G}^*}{\overline{\lambda}_k(p^*) v_k(p^*)}$$

where $\mathcal{G}^*$ is evaluated at $\overline{\boldsymbol{u}}_k(p^*)$. From this we derive

$$v'(p^*) = \frac{2(\tilde{p} - p^*)\mathcal{G}^*}{\overline{\lambda}_k^4(p^*) v_k(p^*)}, \quad e'(p^*) = -\frac{(\tilde{p} + p^*)}{2} v'(p^*), \quad g'(p^*) = \frac{\tilde{p}\, k_v}{v} v'(p^*), \tag{4.46}$$

where k_v is defined accordingly to (4.14) with $\Delta p = \tilde{p} - p^*$. Obviously, g' vanishes if

$$\text{a)} \quad p^* = \tilde{p} \qquad \text{or} \qquad \text{b)} \quad \mathcal{G}^* = 0 \qquad \text{or} \qquad \text{c)} \quad \gamma - \frac{\Gamma}{2}\frac{\Delta p}{\tilde{p}} = 0.$$

Considering the state $\hat{\boldsymbol{u}} = \overline{\boldsymbol{u}}_k(\hat{p})$ on the rarefaction curve where the nonlinear field degenerates, i.e., $\hat{\mathcal{G}} = 0$, we conclude that a) and b), respectively, hold if and only if $\tilde{p} = p^* = \hat{p}$. Then $p^* = \tilde{p}$ is a root of (4.44). This parameter value corresponds to a point of primary bifurcation. Furthermore, condition c) can be rewritten as

$$\frac{\overline{\lambda}_k^2(\tilde{p})}{\overline{\lambda}_k^2(p^*)} + \frac{\Gamma}{2}\frac{v - v^*}{v} = 0$$

where we apply (4.24). This equation holds if $\tilde{p}$ corresponds to a point of secondary bifurcation (4.10) where the shock speed becomes sonic, i.e.,

$$\overline{\sigma}_k^2(\overline{\boldsymbol{u}}_k(p^*), \overline{\boldsymbol{u}}(\tilde{p})) = \overline{\lambda}_k^2(p^*) = \overline{\lambda}_k^2(\tilde{p}). \tag{4.47}$$

These states are excluded in our investigations, since we assume that (4.23) holds. We emphasize that (4.23) implies that k_v is positive, because k_v can be represented as $k_v = \gamma - \Gamma/2 + \Gamma p^*/\tilde{p}$. Hence, locally there exists a unique solution of (4.44) as long as $\tilde{p}$ does not correspond to a state of primary or secondary bifurcation. Except for bifurcation points the roots can be computed by applying the Newton scheme.

Finally, we want to remark that the admissible part of the mixed curve is terminated by two different kinds of states (i) the zeros of $dp^*/d\tilde{p}$ which coincide with sonic shocks and (ii) p^* is approaching p_0. The latter state can be analogously calculated by determining the zero of (4.44) where we fix $p^* = p_0$ and search for $\tilde{p} = \tilde{p}(p_0)$ instead, i.e.,

$$g_0(\tilde{p}) := p(v(\tilde{p}), e(\tilde{p})) - \tilde{p} = 0 \tag{4.48}$$

with

$$v(\tilde{p}) := v_0 - \frac{\tilde{p} - p_0}{\overline{\lambda}_k^2(p_0)}, \quad e(\tilde{p}) := e_0 - \frac{1}{2}(\tilde{p} + p_0)(v(p_0) - v_0).$$

The derivatives are given by

$$v'(\tilde{p}) = -\frac{1}{\overline{\lambda}_k(p_0)}, \quad e'(\tilde{p}) = \frac{\tilde{p}}{\overline{\lambda}_k(p_0)}, \quad g_0'(\tilde{p}) = \frac{\overline{\lambda}_k(\tilde{p})}{\overline{\lambda}_k(p_0)} - 1.$$

Once more, g_0' does not vanish except for points of secondary bifurcation.

For computing a state of the mixed curve $\mathcal{C}(\mathcal{R}_k, \boldsymbol{u}_0)$ we apply the Newton scheme to (4.44) in order to determine $p^* = p^*(\tilde{p})$. The algorithm reads

$$p^{(i+1)} = p^{(i)} - g\left(p^{(i)}\right)/g'\left(p^{(i)}\right)$$

where g and g' are defined by (4.44), (4.45) and (4.46). For this purpose, we need the states of the Hugoniot curve $\mathcal{H}_k\left(\boldsymbol{u}_k\left(p^{(i)}\right)\right)$

$$v^{(i)} = v_k\left(p^{(i)}\right) - \frac{\tilde{p} - p^{(i)}}{\overline{\lambda}_k^2\left(p^{(i)}\right)}, \quad e^{(i)} = e_k\left(p^{(i)}\right) - \frac{1}{2}\left(\tilde{p} + p^{(i)}\right)\left(v^{(i)} - v_k\left(p^{(i)}\right)\right)$$

which originate from $\boldsymbol{u}_k(p^{(i)})$ of the rarefaction curve $\mathcal{R}_k(\boldsymbol{u}_0)$. From this we compute

$$g\left(p^{(i)}\right) = p\left(v^{(i)}, e^{(i)}\right) - \tilde{p}$$

and

$$g'\left(p^{(i)}\right) = -\frac{2\left(\tilde{p} - p^{(i)}\right)\mathcal{G}^{(i)}}{\overline{\lambda}_k^4\left(p^{(i)}\right)v_k\left(p^{(i)}\right)}\left(\overline{\lambda}_k^2(p) - \frac{1}{2}\left(\tilde{p} + p^{(i)}\right)p_e\left(v^{(i)}, e^{(i)}\right)\right),$$

where

$$\overline{\lambda}_k^2\left(p^{(i)}\right) = \frac{c_k^2\left(p^{(i)}\right)}{v_k^2\left(p^{(i)}\right)}, \quad \overline{\lambda}_k^2(p) = \frac{c^2\left(\tilde{p}\right)}{v^2\left(\tilde{p}\right)},$$

denote the characteristic velocities with respect to the states $\boldsymbol{u}_k(p^{(i)})$ of the rarefaction curve and the state $\boldsymbol{u}^{(i)}$ of the mixed curve, respectively.

If the error tolerance (4.39) is met, we put $p^* = p^{(i)}$ and compute

$$\overline{\sigma}_k = \overline{\lambda}_k\left(p^*\right), \quad v(\tilde{p}) = v_k\left(p^*\right) - \frac{\tilde{p} - p^*}{\overline{\lambda}_k^2\left(p^*\right)}, \quad e(\tilde{p}) = e_k\left(p^*\right) - \frac{\tilde{p} + p^*}{2}\left(v(\tilde{p}) - v_k\left(p^*\right)\right),$$

and

$$u(\tilde{p}) = u_k\left(p^*\right) + \frac{\tilde{p} - p^*}{\overline{\sigma}_k}, \quad E(\tilde{p}) = e(\tilde{p}) + \frac{1}{2}u^2(\tilde{p}).$$

Since we compute the mixed curve starting at the state where the nonlinear field degenerates, i.e., $p_0 = \hat{p}$ with $\hat{\mathcal{G}} = 0$, we may encounter problems. Here Lemma 4.2 is helpful. It states that proceeding forward on the mixed curve implies that we locally move backward on the rarefaction curve half as fast. By this relation it is possible to determine an appropriate initial guess for the Newton scheme on the rarefaction curve.

In the end, we emphasize that it is more convenient to determine the mixed curve by (4.48) instead of realizing Liu's geometric definition in Section 3.2.3. Here we prescribe the parameter of the mixed curve and search for the corresponding state on the rarefaction curve. The geometric construction principle is the other way around, i.e., it starts from a state on the rarefaction curve and moves along the corresponding Hugoniot curve until a state is arrived where (3.25) is satisfied. Since the rarefaction curve is approximately determined by an ODE solver, the approximation error accumulates which might have a strong influence on the approximation of the mixed curve.

4.5.2 Determining the Curve Construction

For each initial state $\boldsymbol{u}_l$ and $\boldsymbol{u}_r$, respectively, we have to determine the k–curves, $k = 1, 3$. They can be determined by the same procedures. We proceed *forward* on the 1–curve and *backward* on the 3–curve. This means that we search for states which can be connected to $\boldsymbol{u}_l$ by a 1–curve. Otherwise we determine states such that $\boldsymbol{u}_r$ is connected to this state by a 3–curve. In $\boldsymbol{u}_l$ and $\boldsymbol{u}_r$ the curves are split into two branches that correspond to increasing or decreasing pressure. Since we assume u to be monotone with respect to p we do not have to compute all of the four branches when determining the intersection point. Here we distinguish three cases. Obviously, there is nothing to do for $\boldsymbol{u}_l = \boldsymbol{u}_r$. If either $p_l = p_r$ or $u_l = u_r$, then we have to compute only one branch for each of the two curves. The four possible configurations are sketched in Fig. 13. The most expensive case occurs,

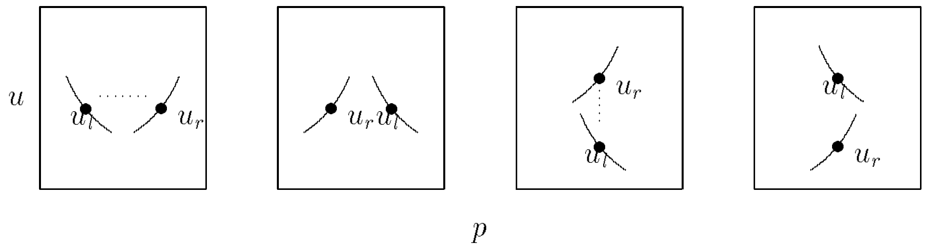

Figure 13: Three branches

if $p_l \neq p_r$ as well as $u_l \neq u_r$. Then one branch may have an intersection point with either of the two branches of the other curve. This makes it necessary to determine three of four branches. Again, the four different configurations are presented in Fig. 14.

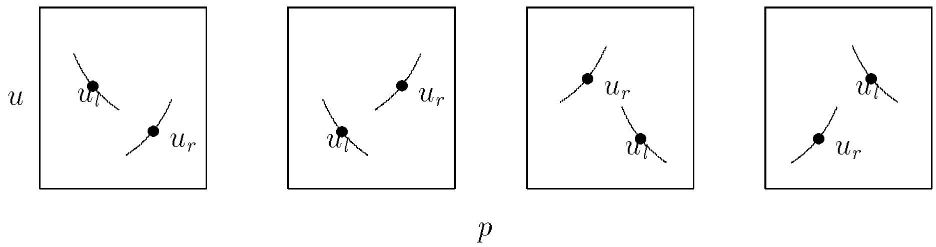

Figure 14: Two branches

Except for the trivial initial configuration, there are $k_{num} \in \{2, 3\}$ branches to be computed. Here k_{num} can be directly determined from the initial values. For each of the branches we have to store the following information:

- the parameter value p is *increasing* or *decreasing*, i.e., sign $\Delta p = \pm 1$;
- the *type* of the elementary curve ($\mathcal{H}$, $\mathcal{R}$, $\mathcal{C}$) that is actually computed and whether the current state is *admissible*;
- the *states* of the branch which already have been determined;

- the *parameter pressure* $\overline{p}$ for which we will compute the corresponding state $\overline{\boldsymbol{u}}$ of the branch;
- the *origin* $(u_o,\ p_o)$ of the elementary curve (here: only shock and rarefaction curve), that is actually computed.

As long as there is no intersection between the branches of the different curves we proceed with computing the next state of the branch. Here we distinguish between three cases depending on the type of the elementary curve.

Type = Shock

- compute the state $\overline{\boldsymbol{u}}$ of the shock curve $\mathcal{H}_k(\boldsymbol{u}_o)$ corresponding to the parameter $\overline{p}$;
- if the shock speed is still monotone, then add $\overline{\boldsymbol{u}}$ to the computed values of the current branch;
- else compute the state $\boldsymbol{u}_s$ and the pressure p_s, respectively, where the shock speed is sonic and add $(\boldsymbol{u}_s, p_s)$ to the list of already computed values of the current branch. For preparation of the next step we set type = rarefaction and $\boldsymbol{u}_o = \boldsymbol{u}_s$.

Type = Rarefaction

- compute the state $\overline{\boldsymbol{u}}$ of the rarefaction curve $\mathcal{R}_k(\boldsymbol{u}_o)$ corresponding to the parameter $\overline{p}$;
- if the characteristic velocity is still monotone, then add $\overline{\boldsymbol{u}}$ to the computed values of the current branch;
- else compute the state $\boldsymbol{u}_g$ and the pressure p_g, respectively, where the nonlinear fields degenerates, i.e., $\mathcal{G} = 0$ and add $(\boldsymbol{u}_g, p_g)$ to the list of already computed values of the current branch. For preparation of the next step we set type = mixed and $\boldsymbol{u}_o = \boldsymbol{u}_g$.

Type = Mixed

- compute the state $\overline{\boldsymbol{u}}$ of the mixed curve $\mathcal{C}(\mathcal{R}_k, \boldsymbol{u}_o)$ corresponding to the parameter $\overline{p}$; p^* denotes the pressure value of the corresponding state $\boldsymbol{u}^*$ of the rarefaction curve $\mathcal{R}_k(\boldsymbol{u}_o)$;
- if $p^* \notin (\min(p_o, p_g), \max(p_o, p_g))$, then compute the state $\boldsymbol{u}_R \in \mathcal{C}(\mathcal{R}_k, \boldsymbol{u}_o)$ such that the corresponding state $\boldsymbol{u}^*$ of the rarefaction curve $\mathcal{R}_k(\boldsymbol{u}_o)$ coincides with the origin $\boldsymbol{u}_o$ of the rarefaction curve and add $(\boldsymbol{u}_R, p_R)$ to the list of already computed values of the current branch. For preparation of the next step we set type = shock and $\boldsymbol{u}_o = \boldsymbol{u}_R$;
- if $p^* \in (\min(p_o, p_g), \max(p_o, p_g))$ but the monotonicity of the shock speed $\overline{\sigma}_k(\boldsymbol{u}^*, \overline{\boldsymbol{u}})$ is changing in the calculated state, then determine the state $\boldsymbol{u}_s$ where the shock speed becomes sonic and add $(\boldsymbol{u}_s, p_s)$ to the list of already computed values of the current branch. For preparation of the next step we set type = rarefaction and $\boldsymbol{u}_o = \boldsymbol{u}_s$.
- else if $p^* \in (\min(p_o, p_g), \max(p_o, p_g))$, then add $\overline{\boldsymbol{u}}$ to the computed values of the current branch;

4.5.3 Determining the Initial Curve Type

In the previous section, we have described how to proceed on one branch. To this end, we need to know the current type of the elementary curve. For the initial states $\boldsymbol{u}_0 \in \{\boldsymbol{u}_l, \boldsymbol{u}_r\}$ this type has to be determined for the branch of interest that is to start at this state. The starting point is the eigenvector decomposition in Lagrangian coordinates (cf. Prop. 3.2 b))

$$\overline{\boldsymbol{u}} - \overline{\boldsymbol{u}}_0 = \frac{1}{\overline{\sigma}_k}\left(\overline{\boldsymbol{f}}(\overline{\boldsymbol{u}}) - \overline{\boldsymbol{f}}(\overline{\boldsymbol{u}}_0)\right) = a_1\overline{\boldsymbol{r}}_1(\boldsymbol{u}) + a_2\overline{\boldsymbol{r}}_2(\boldsymbol{u}) + a_3\overline{\boldsymbol{r}}_3(\boldsymbol{u})$$

where the coefficients are determined by

$$a_1 = \Delta p\,\frac{\overline{\sigma}_k|\overline{\lambda}_k| + p_v - p_0 p_e}{2\overline{\sigma}_k^2|\overline{\lambda}_k|}, \quad a_1 = -\left(\frac{\Delta p}{\overline{\sigma}_k|\overline{\lambda}_k|}\right), \quad a_3 = \Delta p\,\frac{\overline{\sigma}_k|\overline{\lambda}_k| - p_v + p_0 p_e}{2\overline{\sigma}_k^2|\overline{\lambda}_k|}$$

with $\Delta p = p - p_0$. Provided that (2.21) and (2.22), respectively, hold then we conclude

$$\operatorname{sign} a_1 = -\operatorname{sign}\Delta p, \quad \operatorname{sign} a_3 = \operatorname{sign}\Delta p.$$

According to Liu, the shock curve $\mathcal{H}_k(\boldsymbol{u}_0)$ can be split into two separate branches by the sign of a_k. From this observation we derive the following classification of the admissible branches depending on Δp:

- $k = 1$:

  a) $\Delta p > 0$: $\boldsymbol{u} \in \mathcal{H}_k^-(\boldsymbol{u}_0) \Leftrightarrow \overline{\sigma}_k' > 0 \Leftrightarrow \mathcal{G}_0 > 0$;

  b) $\Delta p < 0$: $\boldsymbol{u} \in \mathcal{H}_k^+(\boldsymbol{u}_0) \Leftrightarrow \overline{\sigma}_k' < 0 \Leftrightarrow \mathcal{G}_0 < 0$;

- $k = 3$:

  a) $\Delta p > 0$: $\boldsymbol{u} \in \mathcal{H}_k^+(\boldsymbol{u}_0) \Leftrightarrow \overline{\sigma}_k' > 0 \Leftrightarrow \mathcal{G}_0 < 0$;

  b) $\Delta p < 0$: $\boldsymbol{u} \in \mathcal{H}_k^-(\boldsymbol{u}_0) \Leftrightarrow \overline{\sigma}_k' < 0 \Leftrightarrow \mathcal{G}_0 > 0$.

We emphasize that the 3–curve is determined in backward parameter direction, since we start in the end point $\boldsymbol{u}_r$ and not in the intersection point. Hence Δp has to substituted by $-\Delta p$ for the computation.

4.5.4 Computation of Intersection Points

Up to now, we have described how to determine the branches that might intersect and how to proceed on these branches. We finally have to explain the computation of the intersection point itself. For this purpose we introduce the *support* of pressure values corresponding to that part of the branch which has been already computed. If the supports of the two curves do not overlap, then no intersection is possible (see Fig. 15). An intersection may only happen if the supports overlap. For each end point of the currently computed branches we introduce *pointers*. These point at already computed states of the other curve such that the new state lies in their support. This situation is shown in Fig. 16. If the corresponding u values overlap, then we compute the possibly existing intersection point by determining the intersection of two straight lines. In the other case, we update the pointers such that the last state always knows where to look for an intersection. For instance, we consider the configuration plotted in Fig. 17. Suppose that in the previous step the curve end lies between the state P_2 and P_3. In the next step this curve end may

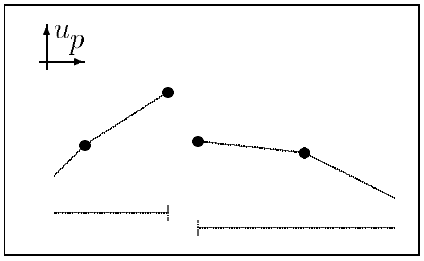

Figure 15: Supports

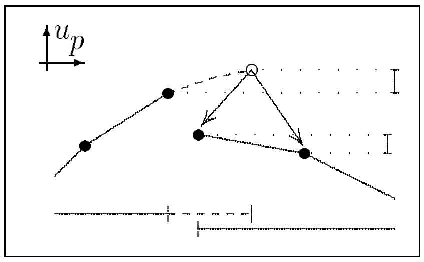

Figure 16: Non–overlapping supports

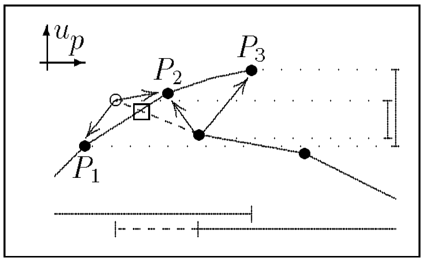

Figure 17: Overlapping supports

be between the states P_1 and P_2. Then we compare the range of values between the states P_1 and P_3 as well as the new and old value of the curve. If these ranges overlap, then we test for an intersection otherwise we continue.

This procedure seems to be rather complicated. But the update of the pointers only requires one or two values to be compared. Since we consider the curves as sorted lists of states, the effort for searching the corresponding states for the first time increases logarithmically. The most expensive part is the computation of the intersection of two straight lines. But this is only performed in the neighborhood of the intersection point itself and in the case of overlapping p and u supports. This, however, only marginally affects the overall complexity.

5 Comparison between an Ideal Gas and a Real Gas

In order to investigate the quantitative influence of the non–convex EOS on the solution of the Riemann problem, we compare an ideal gas and a real gas. For this purpose we modify the ideal EOS for a perfect gas

$$p_c(v,e) = (\gamma - 1)\, e\, v^{-1}, \quad \gamma = 1.4 \tag{5.1}$$

by a non–convex perturbation

$$p_{nc}(v,e) = e(-0.0024\, v^5 + 0.0469\, v^4 - 0.3444\, v^3 + 1.1760\, v^2 - 1.8942\, v + 1.4182) \tag{5.2}$$

in such a way that the resulting real gas EOS

$$p_\alpha(v,e) = \begin{cases} \alpha\, p_{nc} + (1-\alpha)\, p_c \;, & v \in [1.0, 5.5]; \\ p_c & , \text{ elsewhere }; \end{cases} \tag{5.3}$$

exhibits a non–convex region in the p–v plane for $v \in [1, 5.5]$. Here the degree of non–convexity can be varied by the parameter $\alpha \in [0,1]$. The coefficients in (5.2) are chosen such that p_α is twice differentiable and, in addition, $p_v(v,e) < 0$ for all states $v, e > 0$. In Fig. 18 the isoenergetic lines to $e = 5 = const$ are presented in the p–v plane for the convex case ($\alpha = 0$) and the non–convex case ($\alpha = 1$). Within the range $v \in [1.0, 5.5]$ the modified pressure p_α is concave, and elsewhere it coincides with the ideal gas law p_c. The corresponding isentropes can be computed by (2.19) which are shown in Fig. 19. We notice that they do not necessarily coincide outside $v \notin [1.0, 5.5]$.

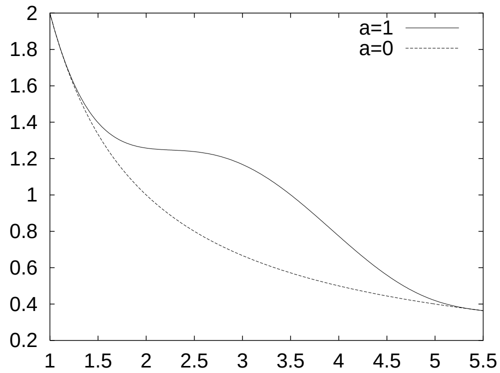

Figure 18: Isoenergetic lines

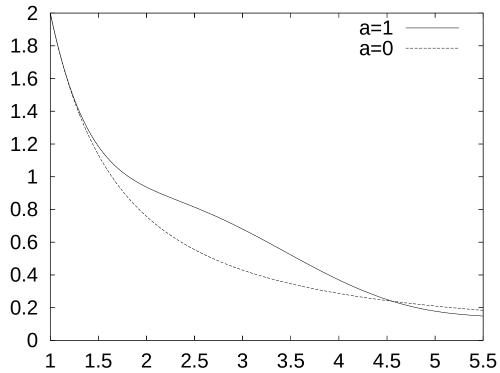

Figure 19: Isentropes

We now consider the Riemann problem given by the initial values

$$\begin{pmatrix} v_l \\ u_l \\ E_l \end{pmatrix} = \begin{pmatrix} 1 \\ -1.5 \\ 6.125 \end{pmatrix}, \qquad \begin{pmatrix} v_r \\ u_r \\ E_r \end{pmatrix} = \begin{pmatrix} 5.5 \\ 1.5 \\ 6.125 \end{pmatrix}$$

where the corresponding pressures are $p_l = p_\alpha(v_l, e_l) = 2$ and $p_r = p_\alpha(v_r, e_r) = 0.\overline{36}$, $\alpha = 1$. This problem is solved applying the perfect gas (5.1) and the real gas (5.3), respectively. In Fig. 20 the 1–curves and 3–curves originating from $\boldsymbol{u}_l$ and $\boldsymbol{u}_r$ are presented for the cases $\alpha = 0$ and $\alpha = 1$. There is a significant difference between the two different EOSs along the curves. But for the test configuration at hand the intersection points are close to each

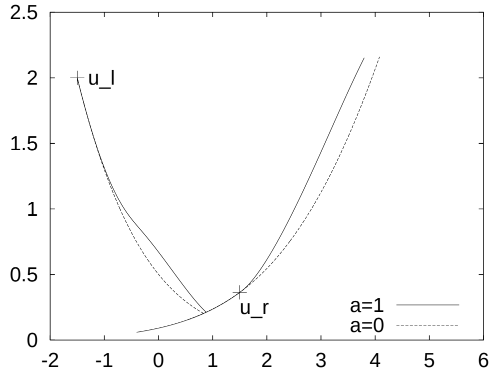

Figure 20: Intersection of curves p–u plane

other since the 3–curves almost coincide along the connection path, whereas the remaining part of the path differs essentially. This is also reflected in the wave propagation in the t–x plane (here: $t = 0.2$), see Fig. 21 – 24. Since there occur two states where the 1–field degenerates, the 1–wave is composed of a shock wave which is continued by a rarefaction wave when the shock speed becomes sonic and finally we proceed with a mixed curve.

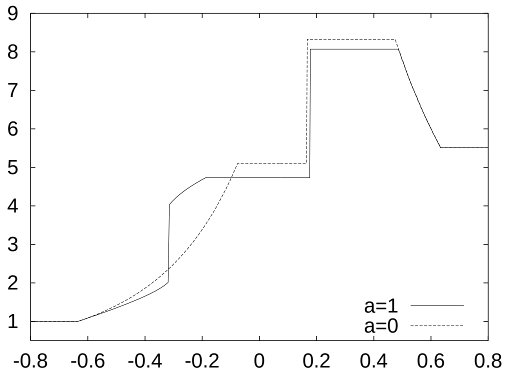

Figure 21: specific volume

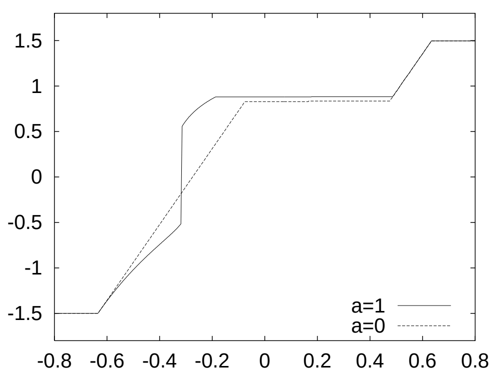

Figure 22: velocity

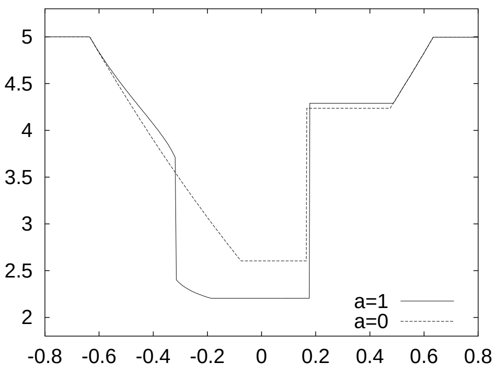

Figure 23: specific internal energy

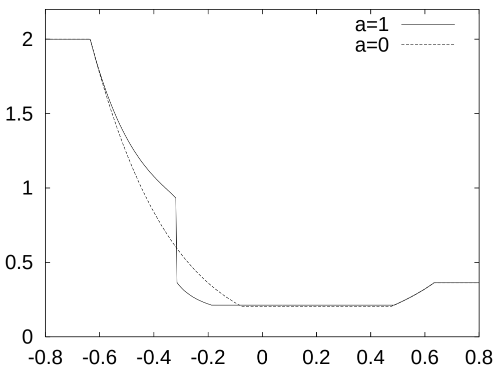

Figure 24: pressure

6 Conclusion and Outlook

An extended Riemann solver for the Euler equations has been derived where the EOS is not supposed to be strictly convex. This solver is meant to be a helpful tool in the following context

- performing parameter studies in order to investigate the influence of the non–convexity of the EOS
- design of shock tube experiments,
- derivation of appropriate initial states for test configurations,
- validation of numerical schemes applied to flow simulations in materials exhibiting a region where the isentropes are not convex, e.g. retrograde fluids.

In a forthcoming work, we want to investigate the influence of anomalous wave structures caused by the non–convexity of the isentropes on the numerical scheme. For instance, the *approximate* Riemann solver originally introduced by Roe in [Roe81] is frequently applied in many finite volume methods. The Roe solver is known to exhibit non–physical expansion shocks in the presence of sonic points which can be suppressed by an entropy fix (see e.g. [LeV90]). However, expansion shocks are physically admissible in fluids with non–convex EOS and may not be suppressed by the numerical scheme.

Finally, we emphasize that the analysis of the mixed curve has not been completed yet. For the two by two case of hyperbolic equations Liu verified the Conjecture (3.1) (see [Liu74]). For the Euler equations its validity is supported by our numerical investigations.

Acknowledgement

The authors feel very grateful to Wolfgang Dahmen for many fruitful and inspiring discussions. He had a strong influence on the structure of the present work.

7 Appendix

7.1 Some Remarks on Hyperbolic Systems of Conservation Laws

In the analysis of (3.1) it is sometimes convenient to switch to an equivalent system by performing a coordinate transformation

$$t = t(\tilde{t}, \tilde{x}), \quad x = x(\tilde{t}, \tilde{x})$$

and to change the variables

$$\boldsymbol{u} = \boldsymbol{g}(\boldsymbol{w}). \tag{7.1}$$

In view of a invertible transformation, the Jacobians

$$\boldsymbol{G}(\boldsymbol{w}) := \partial \boldsymbol{g}(\boldsymbol{w})/\partial \boldsymbol{w} \quad \text{and} \quad \boldsymbol{D}(t, x) := \partial(\tilde{t}, \tilde{x})/\partial(t, x)$$

have to be regular. Then the system (3.1) can be equivalently transformed to the *quasi–conservative form*

$$\boldsymbol{w}_t + \tilde{\boldsymbol{A}}(\boldsymbol{w})\boldsymbol{w}_x = \boldsymbol{0} \tag{7.2}$$

with

$$\tilde{\boldsymbol{A}}(\boldsymbol{w}) := (\boldsymbol{H}(\boldsymbol{w}))^{-1}(\tilde{x}_t \boldsymbol{I} + \tilde{x}_x \boldsymbol{B}(\boldsymbol{w})), \quad \boldsymbol{B}(\boldsymbol{w}) := (\boldsymbol{G}(\boldsymbol{w}))^{-1}\boldsymbol{A}(\boldsymbol{u})\boldsymbol{G}(\boldsymbol{w})$$

whenever

$$\boldsymbol{H}(\boldsymbol{w}) := \tilde{t}_t \boldsymbol{I} + \tilde{t}_x \boldsymbol{B}(\boldsymbol{w})$$

is regular.

Analogously to $\boldsymbol{A}(\boldsymbol{u})$, there exists a complete set of eigenvalues $\tilde{\lambda}_k(\boldsymbol{w})$ of the matrix $\tilde{\boldsymbol{A}}(\boldsymbol{w})$ corresponding to the right eigenvectors $\tilde{\boldsymbol{r}}_k(\boldsymbol{w})$ and the left eigenvectors $\tilde{\boldsymbol{l}}_k(\boldsymbol{w})$. These are related to those of $\boldsymbol{A}(\boldsymbol{u})$ by

$$\boldsymbol{\Lambda}(\boldsymbol{u}) = (\tilde{t}_t \tilde{\boldsymbol{\Lambda}}(\boldsymbol{w}) - \tilde{x}_t \boldsymbol{I})(\tilde{x}_x \boldsymbol{I} - \tilde{t}_x \tilde{\boldsymbol{\Lambda}}(\boldsymbol{w}))^{-1},\ \boldsymbol{R}(\boldsymbol{u}) = \boldsymbol{G}(\boldsymbol{w})\tilde{\boldsymbol{R}}(\boldsymbol{w}),\ \boldsymbol{L}(\boldsymbol{u}) = \tilde{\boldsymbol{L}}(\boldsymbol{w})(\boldsymbol{G}(\boldsymbol{w}))^{-1}$$

such that

$$\tilde{\boldsymbol{\Lambda}}(\boldsymbol{w}) = \tilde{\boldsymbol{L}}(\boldsymbol{w})\tilde{\boldsymbol{A}}(\boldsymbol{w})\tilde{\boldsymbol{R}}(\boldsymbol{w}), \quad \tilde{\boldsymbol{L}}(\boldsymbol{w})\tilde{\boldsymbol{R}}(\boldsymbol{w}) = \boldsymbol{I}. \tag{7.3}$$

Since $\boldsymbol{H}$ and $\boldsymbol{D}$ are supposed to be regular, we easily verify

$$\tilde{x}_x - \tilde{t}_x \tilde{\lambda}_k(\boldsymbol{w}) \neq 0 \quad \forall\, \boldsymbol{w} \in \mathcal{D}, \quad 1 \le k, j \le n.$$

This means that the matrix $\tilde{x}_x \boldsymbol{I} - \tilde{t}_x \tilde{\boldsymbol{\Lambda}}(\boldsymbol{w})$ is also regular. Furthermore, the characteristic fields can be written in terms of the eigenvalues and right eigenvectors of $\tilde{\boldsymbol{A}}$, in particular,

$$\alpha_k(\boldsymbol{u}) := \nabla_{\boldsymbol{u}} \lambda_k(\boldsymbol{u})\, \boldsymbol{r}_k(\boldsymbol{u}) = \sigma_k \nabla_{\boldsymbol{w}} \tilde{\lambda}_k(\boldsymbol{w})\, \tilde{\boldsymbol{r}}_k(\boldsymbol{w}) =: \sigma_k \tilde{\alpha}_k(\boldsymbol{w})$$

with

$$\sigma_k := \frac{\det\ \boldsymbol{D}}{(\tilde{x}_x - \tilde{t}_x \tilde{\lambda}_k(\boldsymbol{w}))^2} \neq 0.$$

We emphasize that the structure of the k–wave characterized by the nonlinearity factor α_k remains unchanged under an invertible transformation.

Furthermore, we need to know how the second derivative of the characteristic field in the direction of the eigenvector $\boldsymbol{r}_k$ behaves under a transformation. A similar calculation as in the case of α_k yields

$$\begin{aligned}\beta_k(\boldsymbol{u}) := \nabla_{\boldsymbol{u}}\alpha_k(\boldsymbol{u})\,\boldsymbol{r}_k(\boldsymbol{u}) &= \sigma_k\left(\frac{-2\,\tilde{t}_x\,\tilde{\alpha}_k(\boldsymbol{w})}{\tilde{t}_x\tilde{\lambda}_k(\boldsymbol{w})-\tilde{x}_x}\sigma_k\nabla_{\boldsymbol{w}}\tilde{\lambda}_k(\boldsymbol{w})\,\tilde{\boldsymbol{r}}_k(\boldsymbol{w})+\nabla_{\boldsymbol{w}}\tilde{\alpha}_k(\boldsymbol{w})\,\tilde{\boldsymbol{r}}_k(\boldsymbol{w})\right)\\ &= \sigma_k\left(\frac{-2\,\tilde{t}_x}{\tilde{t}_x\tilde{\lambda}_k(\boldsymbol{w})-\tilde{x}_x}\tilde{\alpha}_k^2(\boldsymbol{w})+\tilde{\beta}_k(\boldsymbol{w})\right).\end{aligned}$$

Whenever the nonlinear field degenerates, i.e., $\alpha_k(\boldsymbol{u}) = \tilde{\alpha}_k(\boldsymbol{w}) = 0$, we conclude that $\beta_k(\boldsymbol{u}) = 0$ if and only if $\tilde{\beta}_k(\boldsymbol{w}) = 0$. This means that the type of degeneration is invariant under a transformation.

There are two kind of transformations which are of special interest, namely a variable transformation of the form (7.1) without changing the underlying coordinate system, i.e., $t = \tilde{t},\ x = \tilde{x}$ and a coordinate transformation in space only, i.e., $t = \tilde{t},\ x = x(\tilde{t},\tilde{x})$, respectively. When performing a pure variable transformations, then the matrices reduce to

$$\tilde{\boldsymbol{A}}(\boldsymbol{w}) = \boldsymbol{B}(\boldsymbol{w}),\ \ \boldsymbol{D} = \boldsymbol{I},\ \ \sigma_k = 1$$

in the other case they are given by

$$\tilde{\boldsymbol{A}}(\boldsymbol{w}) = \tilde{x}_x\boldsymbol{B}(\boldsymbol{w}),\ \ \boldsymbol{D} = \operatorname{diag}(1,\tilde{x}_x),\ \ \sigma_k = 1/\tilde{x}_x \neq 0.$$

In the following we will consider two transformations for the Euler equations, namely the transformation to primitive variables and the Lagrangian equations. The first transformation is preferable in the context of analyzing rarefaction waves whereas the Lagrangian representation is helpful in the analysis of shock waves.

Example 1: Primitive Variables

As long as the solution of the Euler equations is smooth it is more convenient to transform the system (3.1) of the conservative quantities to the quasi–conservative form (7.2) of the primitive variables (v, u, e), i.e.,

$$\boldsymbol{u} = \boldsymbol{g}(\boldsymbol{w}) := \left(1/v, u/v, (e+u^2/2)/v\right)^T,$$

whereas the coordinate system remains unchanged, i.e.,

$$t = \tilde{t}, \quad x = \tilde{x}.$$

Then the Jacobian and its inverse are given by

$$\boldsymbol{G} = \begin{pmatrix} -v^{-2} & 0 & 0\\ -uv^{-2} & v^{-1} & 0\\ -(e+u^2/2)v^{-2} & uv^{-1} & v^{-1}\end{pmatrix}, \quad \boldsymbol{G}^{-1} = \begin{pmatrix} -v^2 & 0 & 0\\ uv & -v & 0\\ -(E+u^2)v & uv & v\end{pmatrix}$$

since $\det \boldsymbol{G}(\boldsymbol{w}) = -v^{-4} < 0$. The matrices $\boldsymbol{H}$ and $\boldsymbol{D}$ reduce to the identity matrix. Hence, the quasi–conservative system (7.2) is characterized by the matrix

$$\tilde{\boldsymbol{A}}(\boldsymbol{w}) = \boldsymbol{B}(\boldsymbol{w}) = \begin{pmatrix} u & -v & 0\\ vp_v & u & vp_e\\ 0 & vp & u\end{pmatrix}$$

where p is the equilibrium pressure specified by an incomplete EOS $p = p(v, e)$. The eigenvalues of $\tilde{\boldsymbol{A}}$ are given by

$$\tilde{\lambda}_k(\boldsymbol{w}) = u + \varepsilon_k c, \qquad k = 1, 2, 3$$

and corresponding left and right eigenvectors satisfying (3.3)

$$\begin{aligned} \tilde{\boldsymbol{r}}_k(\boldsymbol{w}) &= p\left((1-\varepsilon_k^2)p_e - \varepsilon_k^2/p, \varepsilon_k c/(vp), \varepsilon_k^2 - (1-\varepsilon_k^2)p_v\right)^T \\ \tilde{\boldsymbol{l}}_k(\boldsymbol{w}) &= \frac{v^2}{(1+\varepsilon_k^2)c^2}\left(1-\varepsilon_k^2 + p_v\varepsilon_k^2, \varepsilon_k c/v, \varepsilon_k^2 p_e + (1-\varepsilon_k^2)/p\right)^T. \end{aligned}$$

Here, the sound speed is supposed to be strictly positive. Then the characteristic fields are essentially characterized by the fundamental derivative of gas dynamics $\mathcal{G}$ since the nonlinearity factor turns out to be

$$\tilde{\alpha}_k(\boldsymbol{w}) = \nabla_{\boldsymbol{w}} \lambda_k(\boldsymbol{w})\, \boldsymbol{r}_k(\boldsymbol{w}) = \varepsilon_k \mathcal{G} c/v, \qquad k = 1, 2, 3.$$

Furthermore, the coefficient $\tilde{\beta}_k$ is determined by

$$\tilde{\beta}_k(\boldsymbol{w}) = \nabla_{\boldsymbol{w}} \tilde{\alpha}_k(\boldsymbol{w})\, \boldsymbol{r}_k(\boldsymbol{w}) = -\varepsilon_k \left(\varepsilon_k \mathcal{G} + \frac{v^2}{2\,c} p_{vvv}(v, s)\right), \qquad k = 1, 2, 3.$$

Instead of e we also might have used p or s as a new variable which is frequently done in the literature. However, in the latter case we have to impose some constraints on the sign of $p_v(v, e)$ and $p_e(v, e)$ in view of a reversible transformation. This is not necessary when choosing e as primitive variable.

Example 2: Lagrangian Representation

An alternative representation of the fluid equations is based on the trajectories of the particles in a flow field. This can be derived from the Eulerian representation by the Lagrange transformation

$$\tilde{t} = t, \ \tilde{x} = \int_0^{x(t)} \rho(t, y)dy, \ x'(t) = u(t, x(t))$$

where we might have used any positive quantity in the definition of $\tilde{x}$ in order to ensure the existence of the inverse as can be concluded from the Jacobian

$$\frac{\partial(t, x)}{\partial(\tilde{t}, \tilde{x})} = \begin{pmatrix} t_{\tilde{t}} & t_{\tilde{x}} \\ x_{\tilde{t}} & x_{\tilde{x}} \end{pmatrix} = \begin{pmatrix} 1 & 0 \\ u & v \end{pmatrix}, \quad \frac{\partial(\tilde{t}, \tilde{x})}{\partial(t, x)} = \frac{\partial(t, x)}{\partial(\tilde{t}, \tilde{x})}^{-1} = \begin{pmatrix} 1 & 0 \\ -\rho u & \rho \end{pmatrix}, \tag{7.4}$$

since $\det \boldsymbol{D} = \rho > 0$. Additionally performing the variable transformation

$$\boldsymbol{u} = \boldsymbol{g}(\boldsymbol{w}) = (1/v, u/v, E/v)^T, \quad \boldsymbol{w} := \overline{\boldsymbol{u}}$$

the fluid equations are transformed to another system of conservation laws, the so called Lagrange equations

$$\overline{\boldsymbol{u}}_t + \left(\overline{\boldsymbol{f}}(\overline{\boldsymbol{u}})\right)_{\tilde{x}} = \boldsymbol{0}$$

with the flux $\overline{\boldsymbol{f}}\,(-u, p(v, e), u\, p(v, e)))^T$. The Jacobian of $\overline{\boldsymbol{f}}$ is given by

$$\overline{\boldsymbol{A}}(\overline{\boldsymbol{u}}) = \partial\, \boldsymbol{f}(\overline{\boldsymbol{u}})/\partial\, \overline{\boldsymbol{u}} = \begin{pmatrix} 0 & -1 & 0 \\ p_v & -up_e & p_e \\ up_v & p - u^2 p_e & up_e \end{pmatrix}.$$

Here the eigenvalues are just

$$\overline{\lambda}_k(\overline{\boldsymbol{u}}) = \varepsilon_k c/v, \quad k = 1, 2, 3.$$

A set of corresponding left and right eigenvectors which are bi–orthonormal are

$$\begin{aligned} \overline{\boldsymbol{r}}_k(\overline{\boldsymbol{u}}) &= \left((\varepsilon_k^2 - 1)p_e - \varepsilon_k^2, \overline{\lambda}_k, (1-\varepsilon_k^2)p_v + \varepsilon_k^2 p + \overline{\lambda}_k u\right)^T, & (7.5)\\ \overline{\boldsymbol{l}}_k(\overline{\boldsymbol{u}}) &= \frac{v^2}{(1+\varepsilon_k^2)c^2}\left((\varepsilon_k^2-1)p + \varepsilon_k^2 p_v, (1-\varepsilon_k^2)u - \varepsilon_k^2 u p_e, \varepsilon_k^2 - 1 + \varepsilon_k^2 p_e\right)^T. & (7.6) \end{aligned}$$

Hence the nonlinearity factor is just

$$\overline{\alpha}_k(\overline{\boldsymbol{u}}) = \nabla_{\overline{\boldsymbol{u}}}\overline{\lambda}_k\,\overline{\boldsymbol{r}}_k = \mathcal{G}\overline{\lambda}_k/v = \varepsilon_k\mathcal{G}c/v^2$$

and the coefficient $\overline{\beta}_k$ is determined by

$$\overline{\beta}_k(\overline{\boldsymbol{u}}) = \nabla_{\overline{\boldsymbol{u}}}\overline{\alpha}_k(\overline{\boldsymbol{u}})\,\overline{\boldsymbol{r}}_k(\overline{\boldsymbol{u}}) = -\frac{1}{2\,\overline{\lambda}_k(\overline{\boldsymbol{u}})}\left(2\,\overline{\alpha}_k^2(\overline{\boldsymbol{u}}) + p_{vvv}(v,s)\right), \quad k = 1, 3.$$

7.2 Representation of Curves and Waves corresponding to a Nonlinear k–Field

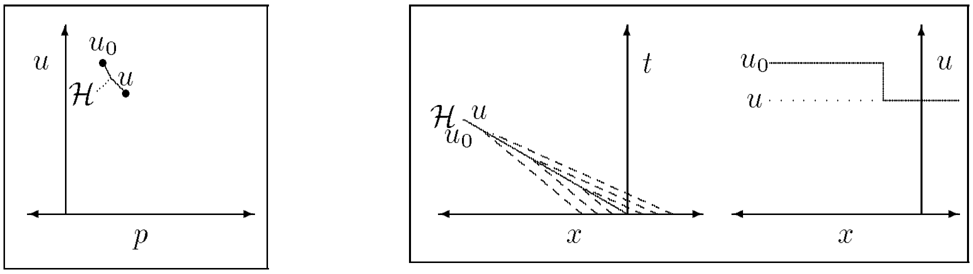

Figure 25: Single Shock

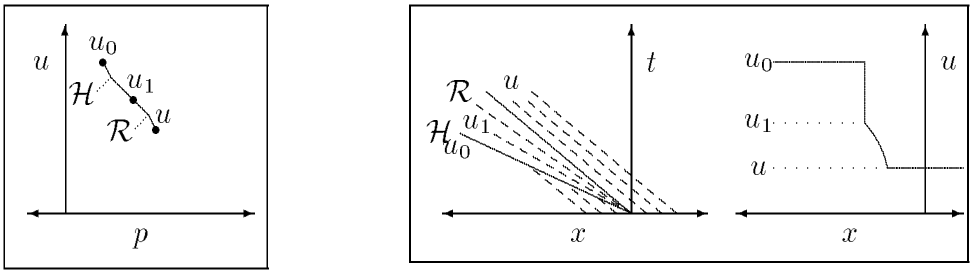

Figure 26: Sonic Shock – Rarefaction

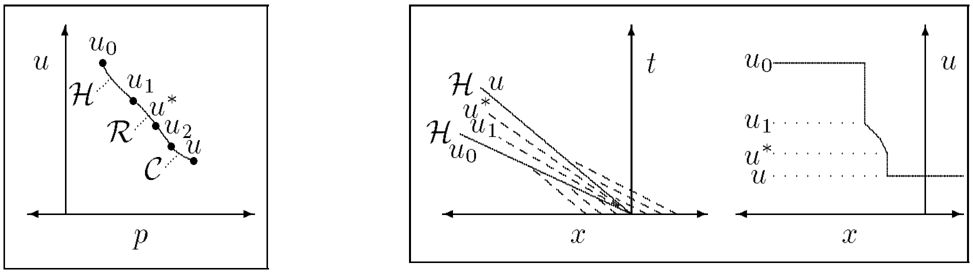

Figure 27: Sonic Shock – Rarefaction – Mixed

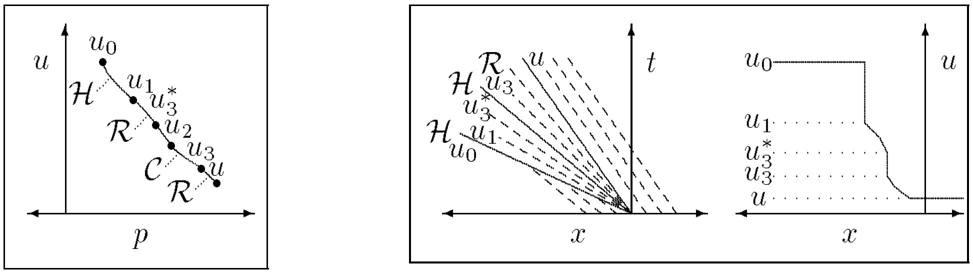

Figure 28: Sonic Shock – Rarefaction – End Mixed – Rarefaction

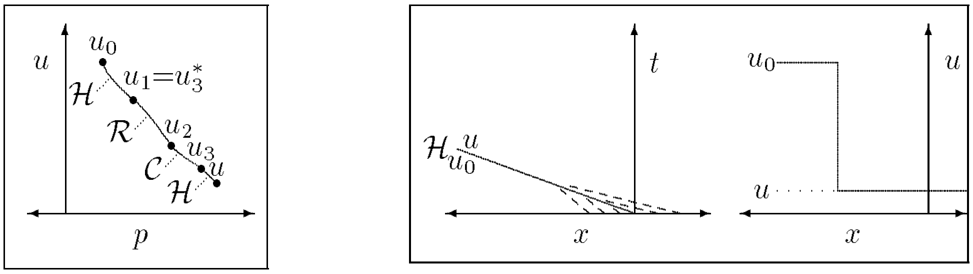

Figure 29: Sonic Shock – Rarefaction – End Mixed – Shock

References

[Bet42] H. Bethe. The Theory of Shock Waves for an Arbitrary Equation of State. Report PB-32189, Clearinghouse for Federal Scientific and Technical Information, U.S. Department of Commerce, Washington D.C., 1942.

[CF48] R. Courant and K.O. Friedrichs. *Supersonic Flow and Shock Waves.* Pure and Applied Mathematics. Interscience Publishers, New York, 1948.

[CG85] Ph. Colella and H.M. Glaz. Efficient solution algorithms for the Riemann problem for real gases. *J. Comp. Phys.*, 59:264–289, 1985.

[Dav85] W. Davis. Equation of state for detonation products. In J. Short, editor, *Proc. Eigth International Detonation Symposium*, page 785 ff, 1985. Naval Surface Weapons Center, White Oak, Silver Springs, MD.

[Ess91] B. Esser. *Die Zustandsgrößen im Stoßwellenkanal als Ergebnisse eines exakten Riemannlösers.* PhD thesis, RWTH Aachen, 1991.

[FFMV] H. Freistühler, Ch. Friess, S. Müller, and A. Voß. Investigations of rarefaction curves and mixed curves at degeneration points. Technical report, RWTH Aachen. in preparation.

[Gel59] I. Gelfand. Some problems in the theory of quasilinear equations. *Usp. Math. Nauk*, 14:87 ff, 1959. Am. Math. Soc. Transl., Ser. 2, 29 (1963), 295 ff.

[Gil51] D. Gilbarg. The existence and limit behavior of the one–dimensional shock layer. *Am. J. Math.*, 73:256 ff, 1951.

[God59] S.K. Godunov. A finite difference method for the numerical computation and discontinuous solutions of the equations of fluid dynamics. *Math. Sb*, 47:271–295, 1959.

[Lax57] P.D. Lax. Hyperbolic systems of conservation laws, II. *Comm. Pure Appl. Math.*, 10:537–566, 1957.

[Lax71] P.D. Lax. A concept of entropy. In E. Zaratonello, editor, *Proc. Wisconsin Conference*, 1971.

[LeV90] R. LeVeque. *Numerical Methods for Conservation Laws.* Birkhäuser, 1990.

[Liu74] T.-P. Liu. The Riemann problem for general systems 2×2 conservation laws. *Am. Math. Soc.*, 199:89–112, 1974.

[Liu75] T.-P. Liu. The Riemann problem for general systems of conservation laws. *J. Diff. Eqns.*, 18:218–234, 1975.

[Liu76a] T.-P. Liu. Shock waves in the nonisentropic gas flow. *J. Diff. Eqns.*, 22:442–452, 1976.

[Liu76b] T.-P. Liu. The entropy condition and the admissibility of shocks. *J. Math. Anal. Appl.*, 53:78–88, 1976.

[LL59] L. Landau and E. Lifshitz. *Fluid Mechanics.* Addison Wesley, 1959.

[MP89] R. Menikoff and B.J. Plohr. The Riemann problem for fluid flow of real materials. *Rev. Mod. Physics*, 61:75–130, 1989.

[Ole59] O. Oleinik. Uniqueness and stability of the generalized solution of the Cauchy problem for a quasi–linear equation. *Usp. Mat. Nauk.*, 14:165 ff, 1959. Am. Math. Soc. Transl., Ser. 2, 33 (1964), 285 ff.

[Peg86] R. Pego. Nonexistence of a shock layer in gas dynamics with a nonconvex equation of state. *Arch. Rat. Mech. Anal.*, 94:165 ff, 1986.

[Rie53] B. Riemann. Über die Fortpflanzung ebener Luftwellen von endlicher Schwingungsweite, 1860. In H. Weber, editor, *Collected Works of Bernhard Riemann*, 1953.

[Roe81] P. Roe. Approximate Riemann solvers, parameter vectors, and difference schemes. *J. Comp. Phys.*, 43:357–372, 1981.

[Smo82] J. Smoller. *Shock Waves and Reaction–Diffusion Equations.* Springer, 1982.

[Tho72] P. Thompson. *Compressible Fluid Dynamics.* Rosewood Press, Troy, New York, 1972.

[Wen72a] B. Wendroff. The Riemann problem for materials with nonconvex equations of state, I: Isentropic flow. *J. Math. Anal. Appl.*, 38:454–466, 1972.

[Wen72b] B. Wendroff. The Riemann problem for materials with nonconvex equations of state, II: General flow. *J. Math. Anal. Appl.*, 38:640–658, 1972.

[Wey49] H. Weyl. Shock waves in arbitrary fluids. *Comm. Pure Appl. Math.*, 2:103 ff, 1949.